POLITECNICO DI MILANO

Facoltà di Ingegneria Industriale e dell'Informazione

Corso di Laurea in
Ingegneria Aeronautica

COLD WIRE THERMOMETRY FOR TURBINE MEASUREMENTS

Relatore: Prof. Carlo Osnaghi

Co-relatore: Dr. Sergio Lavagnoli

Tesi di Laurea di:

Guido LATORRE Matr. 799309

Anno Accademico 2014-2015

Acknowledgements

Contents

List of Figures

List of tables

Nomenclature

Roman Symbols

A_c	convection heat transfer area	[m^2]
A_R	radiation heat transfer area	[m^2]
C	absolute velocity of fluid	[m/s]
C_p	heat capacity at constant pressure	[J/(kgK)]
C_p	heat capacity of prong	[J/(kgK)]
C_w	heat capacity of wire	[J/(kgK)]
C_θ	tangential component of absolute velocity	[m/s]
d_p	diameter of the prong	[m]
dP	dynamic pressure , Ptot-Ps	[Pa]
d_w	diameter of the wire	[m]
F	view factor	[-]
$f_{cut\text{-}off}$	cut-off frequency	[Hz]
h	convective heat transfer coefficient	[W/(m^2K)]
I_0	current	[A]
k_g	conductivity of the gas	[W/(mK)]
k_p	conductivity of the prong	[W/(mK)]
k_w	conductivity of the wire	[W/(mK)]
l_w	length of the wire	[m]
l_p	length of the prong	[m]
M	Mach number	[-]
Nu	Nusselt number	[-]

P_s	static pressure	[Pa]
P_{tot}	total pressure	[Pa]
Q	heat flux	[W]
R	resistance	[Ω]
R	radius	[m]
S_{wire}	surface of the wire	[m^2]
T_{hot}	temperature of the gas	[K]
$T_{junction}$	temperature of the junction (thermocouple)	[K]
T_0	total temperature	[K]
T_{ref}	reference temperature	[K]
T_w	wall temperature	[K]
v_g	velocity of the gas	[m/s]
V_w	volume of the wire	[m^3]

Greek Symbols

α	$k_w/\rho_w c_w$	[W/m^2]
α	thermal diffusivity	[m^2/s]
α_w	sensitivity to temperature	[1/K]
ε_{wall}	emissivity	[-]
Λ^2	$4h/k_w d_w$	[$1/m^2$]
ρ_p	density of the prong	[kg/m^3]
ρ_w	density of the wire	[kg/m^3]
γ	specific heat ratio	[-]
σ	Stefan-Boltzmann constant	[$W/(m^2K^4)$]
σ^{-1}	resistivity	[Ω/m]

ω	angular velocity	[rad/s]
τ	time constant	[s]
μ_g	viscosity of gas	[kg/(ms)]

Abstract

The aim of this work is the characterization of the dynamic behaviour of a cold wire. The probe has been first calibrated in static conditions in two different ways (oven and heated jet); the dynamic calibration has been realized with temperature step tests. In these tests a shield has been used to isolate the cold wire from an air-heated jet of a certain temperature and Mach number: the shield has been removed abruptly with a finite velocity thus exposing the transducer to the jet. In this way it has been realized a 'step' of temperature. This experimental test has been compared to the theoretical step and it was possible to get the transfer function describing the dynamic behaviour of the cold wire at low frequencies. The obtained transfer function has been modified adding the contribution of the tungsten wire in order to take into account the high frequencies: the wire behaves like a first order system whose transfer function can be obtained analytically. The compensation has been obtained using the inverse of the transfer function. Finally the cold wire has been tested in a turbine running at 2200 rpm in vacuum-ambient pressure transient conditions in order to see the effects of compensation

Key words: cold wire, unsteady conditions, transfer function, conduction effects, compensation, turbine.

Chapter 1

Introduction

1.1 Research and instrumentation for turbine measurements

The aerospace sector has always been one of the leader in the research investigation and the opening of this industry to the global business has subjected it to an extreme rivalry. In particular, the commercial and civil branch of the aerospace industry has been focused on the reduction of fuel consumption, being the first source of cost for airline companies [1]. The main efforts in research have been addressed to the efficiency of engines, in particular the turbine and compressor stages, Fig.1.1. The numerous unknown mechanisms of fluid dynamic occurring inside aero-engines have become an important challenge in the last years and new measurement techniques have been adopted in order to better describe these phenomena. The main problem of internal fluid dynamics is the per se unsteady behaviour of the flow: due to potential and viscous flow effects, the working fluid experiences rapid periodic changes of total and static pressure, Mach number and flow angle which has to be sensed by innovative technologies.

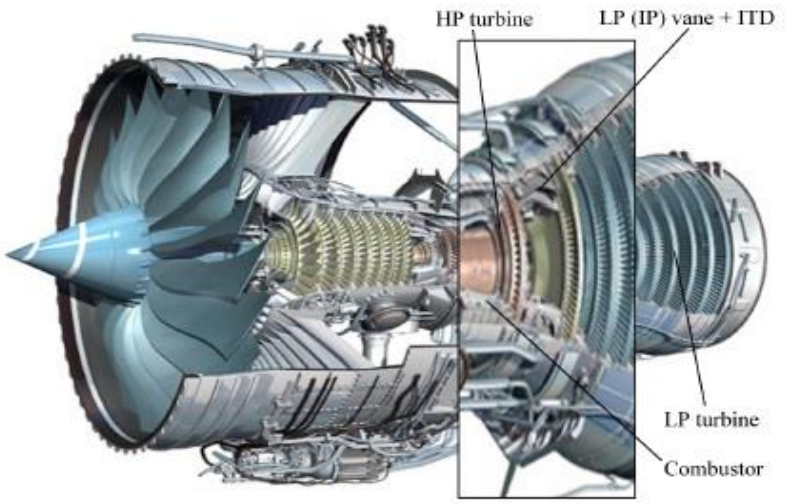

Figure 1.1: *Section view of the Rolls-Royce Trent 1000 (Copyright Rolls Royce)*

Nowadays, in spite of the efforts done, we do not dispose of enough information about unsteady flows in air-breathing engines: research has been focused on computational and experimental activities. The computational studies have the advantage to forecast rather accurately fluid dynamics models with a relatively low cost. Nevertheless they do not represent reality but they are an useful tool to estimate physical phenomena: the validation of these numerical works comes from the experimental activity. The experimental investigation of aerothermodynamics phenomena requires a thorough study and a long and expensive effort in order to obtain convincing results: the importance of the measurement techniques adopted become fundamental.

The analysis of flow inside an aero-engines has to take into account complicate aspects of mass and heat transfer and the current technology on the measurement investigation offers a wide choice on instrumentations: pressure transducers (variable capacitance, variable resistance, variable inductance, piezoelectric probes), anemometers (how wire, hot film sensors), thermometry (thermocouples, cold wires, infrared thermography) and optical measurements. The transducers adopted in fluid dynamic research have a wide range of applications and, depending on their accuracy and velocity response, variable costs. The analysis of flow in aero-engine conditions is one of the most complicate due to the extreme rapidity of the phenomena: suitable instrumentations with a high frequency response have to be used to achieve a good scientific survey.

The thermometry and related instrumentation play a fundamental role in the turbomachinery. The analysis of temperature inside the engine is an important parameter to register and study in order to preserve the integrity of the engine itself. The turbine is the component of the engine which is subjected to the most extreme conditions: the rotor has to withstand temperatures around 850-1700°C (depending on the stage of the turbine) and a linear rotation speed that can reach 500 m/s. The current recommendations about the expected engine lifetime cycle states that the engines has to work for 6 years (14 hours/day) before overhaul or replacement and it becomes fundamental a map of the temperature and stress of the components.

Furthermore, the temperatures reached in the different stages are strictly related to the power that the flow supplies to the turbine as the Euler's equation states:

$$\dot{m}c_p(T_{t2} - T_{t1}) = \omega(r_2 C_{2-\theta} - r_1 C_{1-\theta}) \qquad (1.1)$$

This is a power balance where the total temperature variation across the rotor is related to the mechanical power exchanged by the rotating apparatus (r_i is the

distance respect to the axis of the turbine, $C_{i-\theta}$ is the tangential component of the absolute velocity of the flow).

Another important motivation of accurate thermometry studies inside engines is associated with the possibility to evaluate the real efficiency of the engines and study new methods in order to increase this parameter.

The most suitable instrumentations for turbines measurements are thermocouples and cold wires. The mechanisms to sense temperature variations are different and also the performances change a lot. The thermocouples are robust and simple instruments used to register temperature variations as a result of a difference of voltage between the extremities of two different metallic wires joined together (Seebeck effect). The cold wire is made of tungsten and inserted inside a balanced Wheatstone bridge: the wire is supplied by a low electric current and its resistance changes with temperature variations. The cold wire is extremely accurate and can have a frequency response one order of magnitude bigger respect to the thermocouple. On the other hand, the cold wire is very fragile, expensive and needs an adequate instrumentations.

1.2 Objectives of the work

The original aim of this thesis was to investigate the behaviour of one-and-a-half turbine stage in similarity conditions with aero-engine. Due to the damage of a component of the facility where the turbine should have been tested, it has been decided to address on other aspects.

The study of this work is focused on the static and dynamic characterization of the cold wire and thermocouples. They have been calibrated with different techniques in static conditions (water-bath, oven, heated jet) and it was possible to extrapolate calibration curves relating temperature and voltage. The same instruments have been tested in dynamic conditions realizing step tests of temperature using a "shield" and a heated jet of a known Mach number and temperature. It was possible to analyse the effect of Mach number in the response of the probes.

In order to overcome the physical limits of the cold wire to reproduce fast temperature variations we obtained several transfer functions referred to tests at different Mach numbers. The signal has been compensated using the inverse of the transfer function thus obtaining an acceptable result of the original true step.

These transfer functions have been used to compensate the signal of the cold wire used inside the CT3 facility of the Von Karman Institute in a vacuum-ambient pressure test.

1.3 Thesis Outline

The thesis is composed of five chapters. It is described the work done at Von Karman Institute from October 2014 to March 2015.

Chapter 1 provides a general description of the new challenges in the research of aero engines and it is given an overview on the thermometry instrumentation. A short paragraph is reserved to the description of the experimental work.

Chapter 2 is dedicated to the description of the experimental apparatus used at VKI, starting from the CT3 facility to the instruments and tools used in the 'Heat and mass exchange laboratories'.

Chapter 3 gives an accurate description of the working principles and of the static calibration of the thermocouples and cold wires. The results are presented at the end of the chapter.

Chapter 4 offers an overview of the problem of signal filtering and signal compensation. It is described how to characterize analogue filters (i.e. find the Bode diagrams) and how a transfer function determines the dynamic behaviour of a transducer.

Chapter 5 reports the experimental activity. It is shown how the step tests have been realized and how it was possible to extrapolate the experimental transfer functions. The second part of the chapter is dedicated to the description of a test in CT3 and the results registered by the cold wire with the related conclusions.

Chapter 2

Experimental apparatus

The Von Karman Institute for fluid dynamics is a renewed research centre specialized in the application of fluid dynamics in several fields, including environmental engineering, aerospace and turbomachinery. It was founded in 1956 with the aim of Theodore Von Karman, physicist and aerospace engineer, to create an institution specialized in training young engineers in the aerodynamics. Today is one of the most important centres in the word in the research of fluid dynamics and in the related technologies. It is located in Sint-Genesius-Rode, in Belgium. It is arranged in the three departments, each equipped with sophisticated laboratories and powerful computational machines.

2.1 The turbine test rig

The turbine test rig, also called CT3, is a short-duration wind tunnel used to test engine-size annular rotating turbine stages in aero-engines similarity. The technical name for this rig is "Isentropic Light Piston Compression Tube": it was designed for the first time at Oxford University in the 1970s and there are only three machines like this in the world. The one in VKI is the largest isentropic light piston compression tube: it was designed and constructed at Von Karman Institute starting in 1989. The CT3 is depicted in Fig. 2.1 and Fig. 2.2. It consists basically in a compression tube used to compress air, a test section where the turbine is mounted and a dump tank.

Inside the compression tube, which is 8 meter long, there is a free-moving light piston whose diameter is 1.6 meter long. Before starting the compression, the free-moving piston is in the rear part of the compression tube at atmospheric pressure. Cold high-pressure air is blown through some sonic throats in the back of the cylinder slowly increasing the pressure on one side. The difference of pressure created between the two chambers (separated by the piston) causes the free-moving light piston to move.

***Figure 2.1**: The turbine test rig of Von Karman Institute*

The machine has been designed in order to produce an isentropic compression so that the final temperature can be easily computed with the formula of isentropic processes:

$$T_2 = T_1 \left(\frac{P_2}{P_1}\right)^{\frac{\gamma-1}{\gamma}} \tag{2.1}$$

As the desired pressure and temperature are reached inside the compression tube, the shutter-valve that separates the piston chamber from the test section is open (~70ms). The turbine is at ambient temperature and rotates at a certain velocity: the hot gases with a high enthalpy content pass through the turbine stage causing the rotor to accelerate. Since the rotor is not connected to any break device that can absorb net power, the acceleration of the rotor has to be controlled and kept below a certain value: the turbine is linked to an inertia wheel which increases the rotating total inertia halving the maximum acceleration.

The hot gases flow through a sonic throat that regulates the turbine pressure ratio and then they are expelled into the vacuum tank, which is about at 30mbar absolute pressure before starting the experiment. The opening of the sonic valve is set in such a way that the volumetric flow rate entering at the back of the compression tube matches the volumetric flow rate through the test section. This condition ensures that the aero-thermal parameters are maintained constant during the blow-down. As the throttle valve become unchocked due to the filling of the dump tank the test can be considered ended since there are no more constant flow conditions.

In the ending phase of the test, the rotor starts decelerating due to ventilation losses and to the activation of the aero-break.

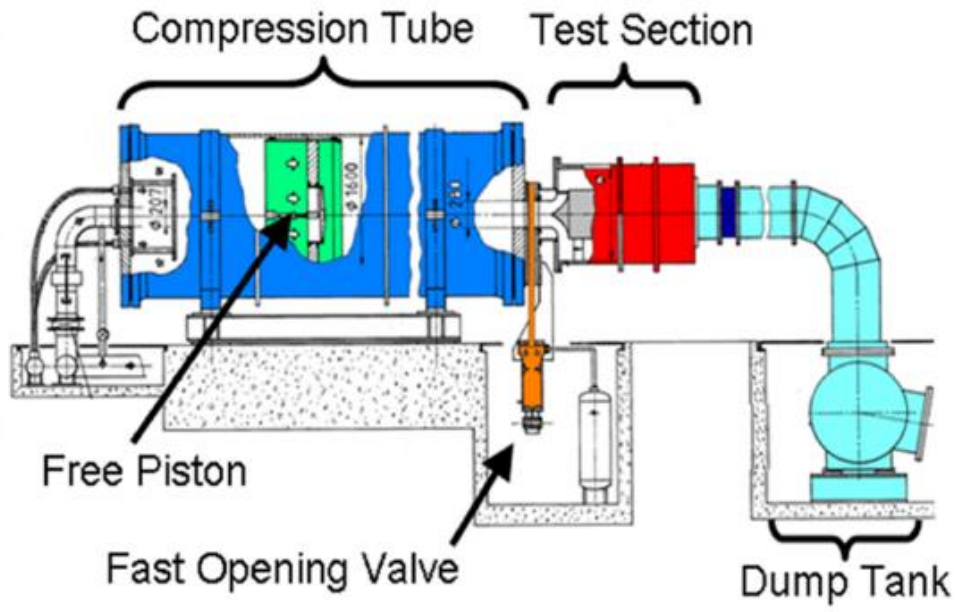

Figure 2.2: *A schematic representations of the CT3*

2.2 Setup for calibration of cold wires

The cold wires have been calibrated inside the heat exchange laboratory of the Von Karman Institute.

The static calibration has been done testing the probe in steady conditions inside an oven and in a heated jet. The laboratory has an oven realised in such a way to limit heat dispersion and keep the desired temperature to a constant value; an internal ventilation allows to obtain a spatial uniform temperature inside the oven. The probes have been placed inside and they have been tested recording the electrical output at different temperatures; the probes were tested with natural convection conditions.

The static calibration in heated jet was done to test the steady behaviour of the probe also in the case of forced convection. The cold wire has been mounted on a variable-height support, depicted in Fig. 2.3 (the metallic-grey tool), used to set the position of the probe respect to the nozzle and test it inside and outside the flow. The heated jet was blown from a nozzle realized in such a way to have the outgoing flow as much uniform as possible. The nozzle has been connected with a pipe to a heat exchanger: the cold wire has been tested at different Mach numbers and different temperatures.

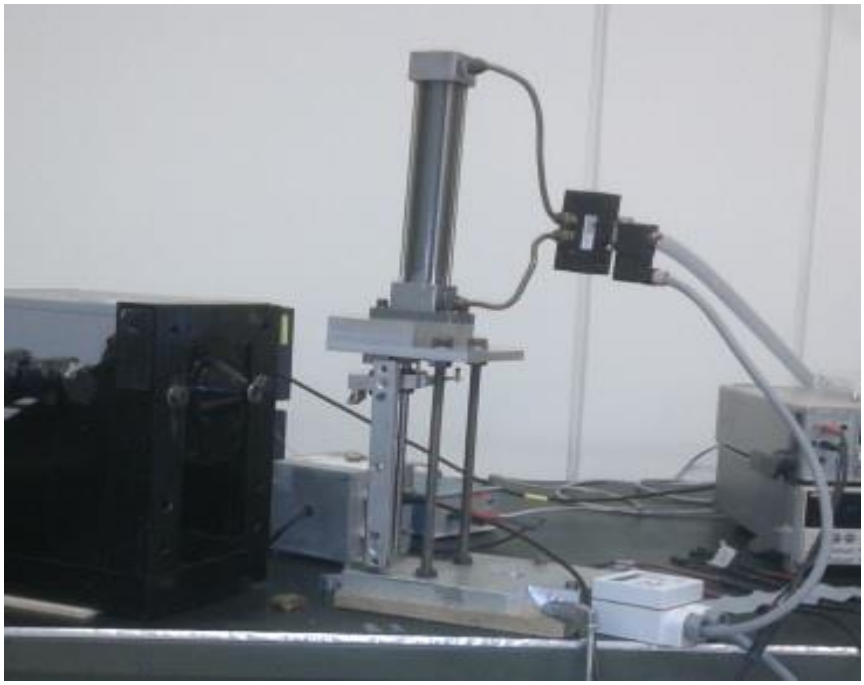

Figure 2.3: *The static and dynamic calibration of the cold wire have been done using a nozzle (to blow hot air at the desired Mach number) and a support used to mount the probe and set its positions.*

The cold wire has been calibrated dynamically with step tests using the same setup.

2.3 Support to set height and angle of probes

The probes have to be inserted in metallic supports (Fig 2.4), which in turn are inserted in the suitable holes of the CT3 facility. These probes have to be set to a desired depth of the turbine channel and to a certain angle respect to the expected direction of the flow. In order to make easier the operation of setting height and angle of the transducer it has been designed on CATIA a metallic support, called generically 'metallic tool' (Fig 2.5).

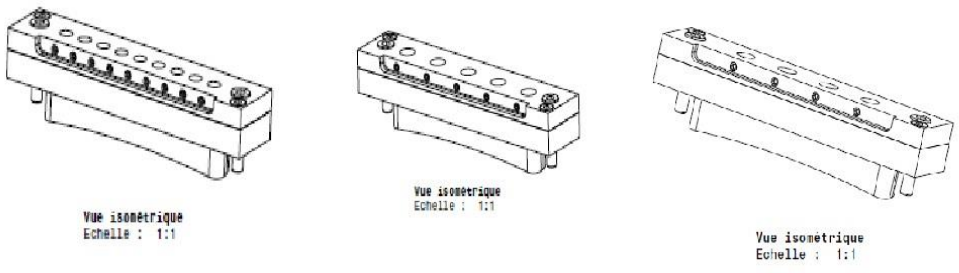

Figure 2.4: *Metallic supports: the probes tested in the CT3 were firstly inserted in the desired hole and fixed; then the support was mounted in the facility.*

This 'metallic tool' is realised in such a way to easily mount the supports for the probes and enough tall to insert the 'variable height instrument' already available in laboratory, depicted in Fig 2.5, in the bottom. The idea is to set the desired depth of the head of the transducer simply setting a correct value of height of the 'variable height instrument': the probe slides inside the hole of the metallic support as far as it touches the surface of the 'variable height instrument'. In this stable position the probe is already set to the desired depth (some geometrical computations have been done) and it is possible to set the angle and fasten it. The probe can be mounted with extreme accuracy and without running the risk of breaking it (some probes are very fragile).

First of all, the measures of the probes, of the 'variable height support' and the 'metallic tool' have been taken. These data have been inserted in a code written in Excel. Through this code it is possible to set the desired depth of the probe (defined as a percentage of the total length of the turbine channel), the angle α of the head of the probe respect to the flow direction and the position of the probe inside the metallic supports (they have different holes which are inclined of an

angle β). The outputs are the height the 'variable height tool' and a parameter which inform us if the probe is inserted in "critical" position respect to the case where it is placed.

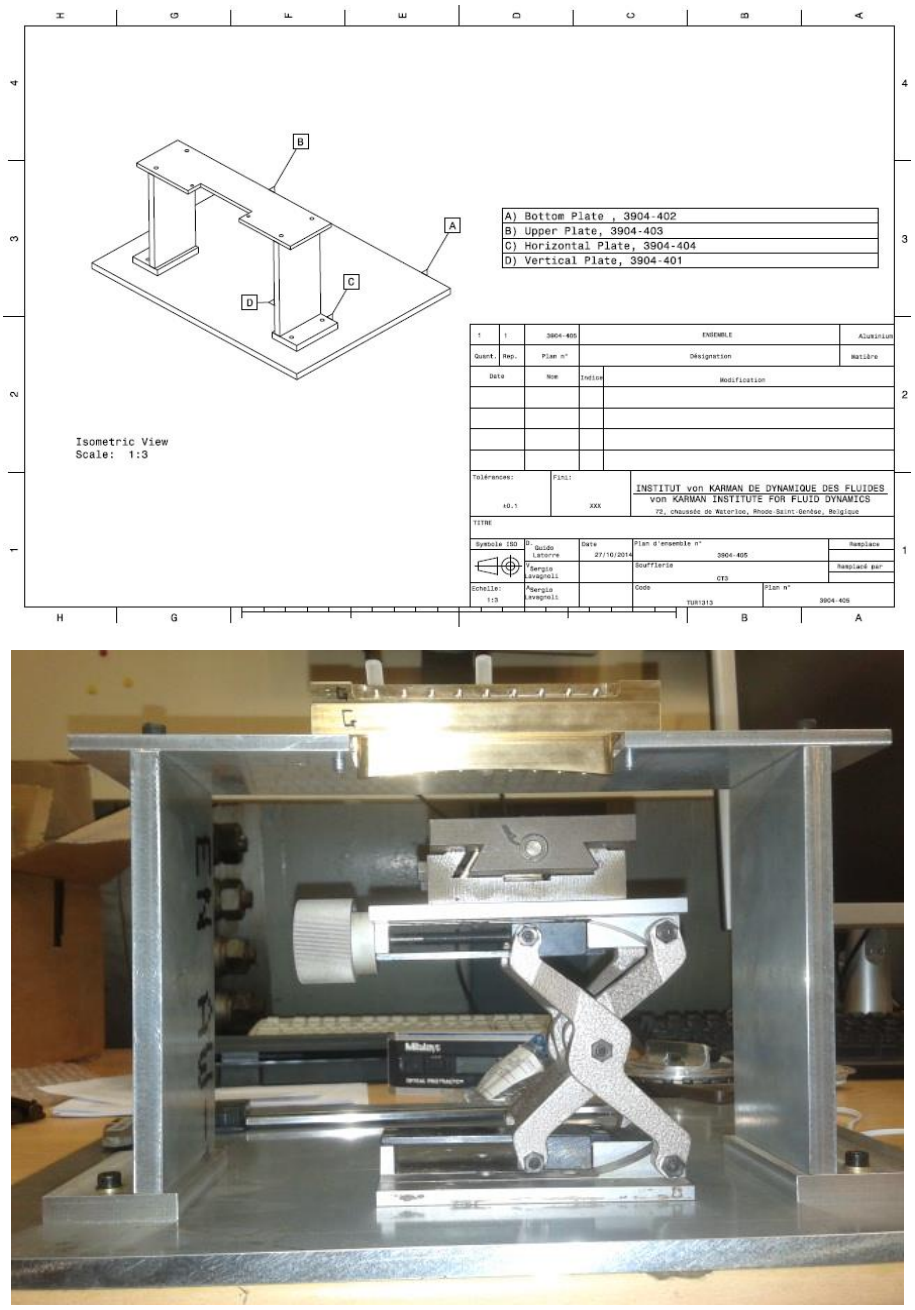

Figure 2.5: *The metallic tool designed in CATIA; in the bottom a picture of the setup used to set the correct position and angle of the probe.*

Chapter 3

Probes: working principle and calibration processes

The tests in the turbine rig have to be done using suitable probes able to perceive fluctuations of the measured quantities. The choice of a given probe is the result of a careful analysis of the characteristics required for the experiment. Indeed, for each probe it has been done a study to get some preliminary data about the quantities to be registered. Once the probe has been chosen, it has been calibrated in order to get the conversion value between the voltage and the desired measured quantity. The calibration tests have concerned thermocouples and cold wires of different geometrical and physical characteristics.

3.1 Thermocouples

Thermocouples are instruments used to senses temperature variations playing on the 'Seebeck' effect: two different metallic wires joined between themselves produce a voltage difference when a temperature difference occurs at their extremities. The voltage difference can be detected by a suitable instrument and, knowing the conversion value after a calibration process, it is possible to go back to the related value of delta temperature.

The thermocouples are instruments used by now since many years. They are reliable instruments used to senses small temperature variations in steady and unsteady conditions and their use in experimental activities is preferred to other instruments being low cost, robust and simple (Fig. 3.1). Depending on electrical or physical requirements, it is possible to use several combinations of metals for the wire. Some technical details are given in "Measurement techniques in fluid dynamics, an introduction" [2] and a table extracted from that work is here reported (see Table 3.1).

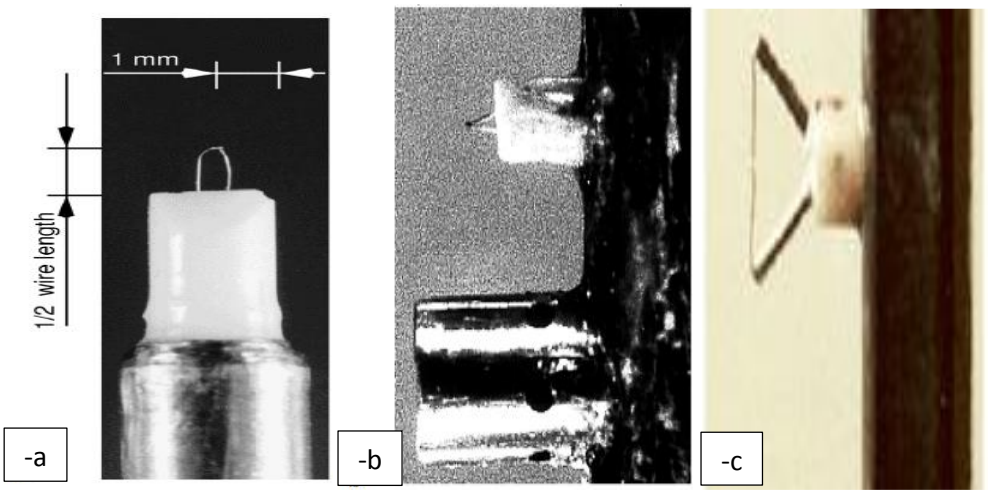

Figure 3.1: *a) Bare thermocouple; b) bare and shielded thermocouples; c) thermocouple suspended between two tubes.*

Combination	Maximum Temperature (°C)	Sensibility (μV/°C)
Chromel-Alumel (type K)	1250	40
Chromel-Constantan (type E)	870	60
Iron-Constantan (type J)	750	50
Copper-Constantan (type T)	370	40
0.6 Rhodium + 0.4 Iridium Tridium	2100	5

Table 3.1: *Electrical and physical properties of couples-wires*

Each metal has its own electrical features and it has its typical behaviour when heated up. Dealing with thermocouples it is common to plot the EMF (electric polarity) in function of temperature as shown in figure Fig. 3.2. In the figure it is shown the variation of the electromagnetic field (EMF or E(T), expressed in millivolts) in function of the temperature for several combinations of metals. It can be noticed that each combination has a different slope and produce a different EMF at a given temperature.

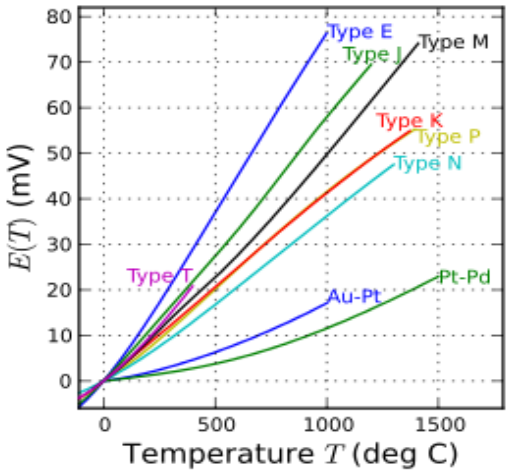

Figure 3.2: *Electric polarity of metals function of temperature*

When two different metallic wires are joined at the extremities (as in the case of thermocouples) the temperature variation registered at the edges produces a ΔEMF. This is shown in a graphic as depicted in Fig. 3.3.

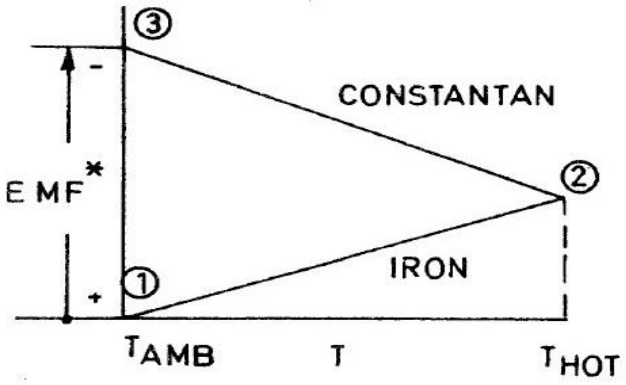

Figure 3.3: *Characteristic curve of a thermocouple without a reference zone box*

A standard thermocouple is able to read a temperature difference ΔT between the two extremities but none of the two values of temperatures is known. In order to obtain the absolute value of temperature in one extremity (T_{HOT}) the other edge has to be at a known temperature (T_{REF}) which can be an ice point or triple point (Fig. 3.4). Alternatively, the other edge of the wire can be equipped by another thermocouple able to read the reference temperature (Fig. 3.5).

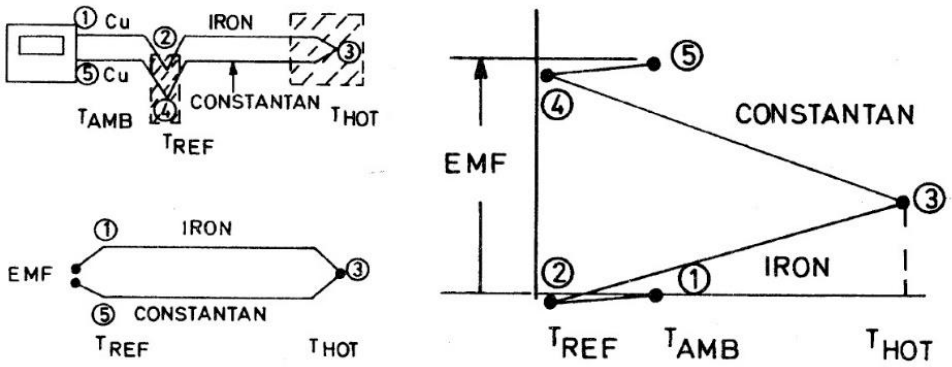

***Figure 3.4**: Thermocouple measurement with a reference zone box.*

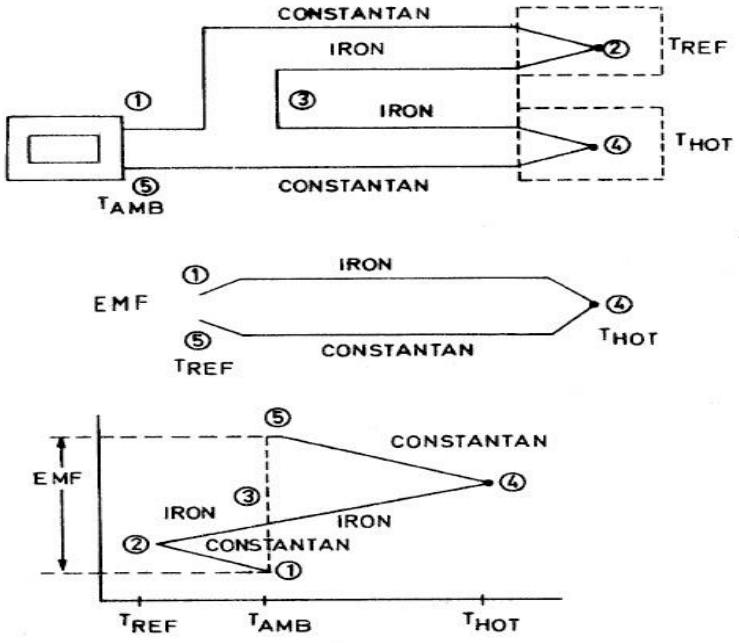

***Figure 3.5:** Measurements with a reference zone box- second configuration*

Numerous studies have been done trying to increase the performances of these instruments. All these improvements started from considerations on fluid dynamic. The wire of the thermocouple has been tested changing its direction in the flow (parallel or perpendicular) and protecting it with a shield able to reduce gas velocity near it (see Fig. 3.1.b shielded thermocouple; Fig. 3.1.a bare thermocouple).Anyway it doesn't exist a thermocouple that fits for every experimental test. Depending on the working conditions a kind of thermocouple is preferred to others for a particular feature and a careful study has to be done before deciding which is the most suitable.

Even the most reliable and accurate instrument can give erroneous results if it is not correctly used. It is fundamental to know which kind of errors can be done during the measurements. Depending on the kind of measurement effectuated, different errors can occur: referring to [3], Steady and Transient errors have been identified. Steady errors occurs in long duration tests measurements where a steady value can be detected. The sources of these errors stems from unsteady conduction, radiation and velocity phenomena. They are described in detail in [3]. Transient errors appears when temperature fluctuations occurs during the test.

3.1.1 Errors and corrections

3.1.1.1 Steady error: Radiation

Considering only convective and radiation phenomena the thermal equilibrium can be written as follow:

$$T_0 - T_{junction} = \frac{\in_{wall-junction} F\, \sigma\, A_r\, (T_{junction}{}^4 - T_{wall}{}^4)}{A_c\, h_c} \qquad (3.1)$$

Being $\in_{wall-junction}$ the emissivity, A_r the radiation area, A_c the convective area, T_0 the temperature of the gas, $T_{junction}$ the temperature in the connection point of the wires. With reasonable assumptions (low T_0 values) it can be demonstrated that the ΔT between gas and junction temperature is a small value and the radiation steady error can be neglected in most of the cases.

3.1.1.2 Steady error: Conduction

The wire is bounded to a ceramic base support which is a non-conductive material. Despite that, the conductive phenomena between wire and support are not negligible and the temperature registered in the wire is always smaller than the temperature of the flowing gas because of conduction. In certain cases the ceramic support have been heated up to the temperature of the wire thus eliminating heat losses: this is an expensive compensation technique. Usually starting from a physic description of the phenomenon it is possible to achieve approximate results obtaining a reasonable value of the conductive steady error.

Considering a wire of length l_w and diameter d_w bended and bounded to the ceramic support as depicted in Fig. 3.6 it is possible to treat the conduction steady

errors starting from the thermal equilibrium between conduction(ceramic support-wire) and convection (gas flow–wire) heat fluxes obtaining a differential equation with the related boundary conditions:

$$k_w \frac{\partial^2 T_w}{\partial x^2} \mathrm{dx}\pi \frac{{d_w}^2}{4} = h_c(T_w - T_0) dx \pi d_w \tag{3.2}$$

$$T_w = T_{base} \tag{3.3}$$

$$\left(\frac{\partial T_w}{\partial x}\right)_{\mathrm{x=l/2}} = 0 \tag{3.4}$$

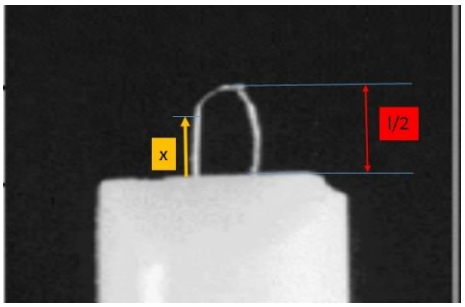

Figure 3.6: *Reference system for thermocouple steady errors*

According to the results showed in [3] the steady conductive errors gets smaller when the wire is perpendicular to the flow and when the l_w/d_w ratio is higher.

3.1.1.3 Steady error: Velocity error

Another source of steady errors is due to the incomplete conversion of the kinetic energy into thermal enthalpy because of viscous effects and heat transfer inside the boundary layer generated nearby the wire. The consequence is that the temperature registered in the wire is lower than the expected total temperature ($T_0 = T_s + v^2/(2Cp)$). This loss phenomenon is described with a recovery factor, r:

$$\mathrm{r} = 1 - \frac{T_0 - T_{junction}}{\frac{v^2}{2\,C_p}} \tag{3.5}$$

A total conversion of kinetic energy into thermal enthalpy corresponds to a recovery factor of 1. This factor is evaluated experimentally in a free jet calibration setup. The results show the recovery factor of a wire considering a bare and a shielded wire at different Mach numbers. Once the results of r have been obtained for a certain amount of Mach numbers, it is possible to get the value of the junction temperature:

$$T_{\text{junction}} = T_0 - (1 - \text{r}) \frac{(\gamma - 1)M^2}{2 + (\gamma - 1)M^2} \qquad (3.6)$$

The results obtained on steady error analysis say that the recovery factor increases considering a shielded thermocouple and a wire directed in parallel respect to the flow: the error between the temperature of the junction and the gas temperature decreases. Increasing the flow velocity the recovery factor rises and the velocity steady error gets smaller.

3.1.1.4 Transient errors

The treatise of the transient errors is rather complicate and some mentions are here provided. For further explanations is recommended the lecture of "Thermocouple probes for accurate temperature measurements in short duration facilities" [3].

The mathematical description of transient phenomena has to be done with reasonable approximations. Considering negligible radial conduction in the wire and minor radiation phenomena, the response of a thermocouple can be described using a first order differential equation:

$$T_0 - T_w = \tau \frac{\delta T_w}{\delta t} \qquad (3.7)$$

Being τ a time constant telling how quick the output system reaches a stable value. Better results have been obtained considering a linear combination of first order differential equation in order to describe transient phenomena in thermocouples.

In short duration tests the main source of errors stems from transient errors. It is required a high response probe able to sense fast fluctuations of temperature: the thermocouple must have a small time constant. At the same time, a suitable design should take into account also mechanical problems. Indeed a wire with a high l_w/d_w ratio can give good results in terms of recovery factor and have small conduction effects but can be extremely fragile and bend easily when exposed to high velocity flow. As mentioned at the beginning of the chapter the choice of a probe will result after a careful analysis of the working conditions expected in the test: in this way it is possible to choose the thermocouple that satisfies the desired requirements.

3.1.2 Thermocouples calibration process

For this experimental work two thermocouples have been calibrated. In the current chapter will be described the setup used to calibrate the thermocouples and the procedure to obtain the calibration curves.

3.1.2.1 Calibration oil-bath

The thermocouples have been calibrated using an oil-bath. For the calibration tests relative to thermocouples 4R and Ttube it has been used the Julabo 12b oil-bath represented in Fig. 3.7. It is a rectangular case realized with non-conductive material walls: this oil-bath is filled by a liquid (oil and water) that is warmed up by an internal heating system.

It is possible to select the desired temperature for the working fluid using a potentiometer: the heating system produces the correct amount of heat flux able to warm the fluid. The homogeneity of temperature inside the working fluid is granted by convective fluxes.

***Figure 3.7**: Julabo 12-b oil-bath*

3.1.2.2 Calibration Process

The thermocouples 2R and Ttube have been calibrated in the Julabo 12B oil-bath. Using a metallic support equipped by hooks it was possible to mount a mercury thermometer and the two thermocouples. The three instruments have been placed close each others in order to get a temperature reading as similar as possible. The heads of the transducers were submerged into the liquid of the oil-bath.

The output of thermocouples is an electric signal of small intensity: each thermocouple has been linked to an amplifier (4R linked to Black Tcbox 02, Ttube linked to Ampli TU5) in such a way to read a significant value. The outputs of the two amplifiers has been linked to two multimeters (KEITHLEY 1571351) to display the voltage output in digital format. For these calibrations it has been chosen a temperature range from T_{amb} to 70°C, obtaining 10 target temperatures equi-spaced by 5 °C.

After having taken data at ambient temperature from thermometer, 4R and Ttube, the Julabo 12B oil-bath has been switched on selecting the desired temperature by the potentiometer. The data from the multimeter have been monitored every 5 minutes to have an idea of the time required to have a stable value of temperature. These data have been plotted using Excel obtaining graphics similar to the one depicted in Fig. 3.8.

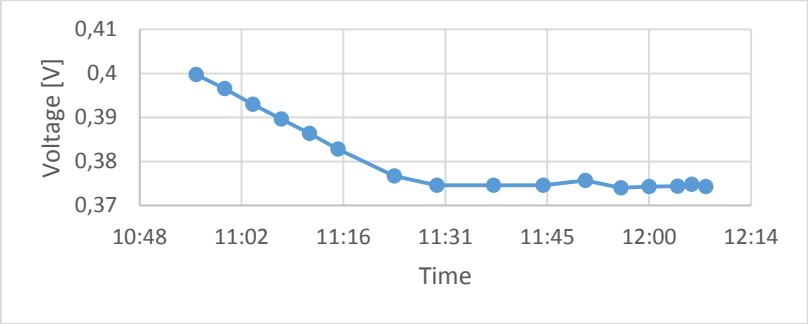

***Figure 3.8**: Stabilization of temperature of cold wires.*

The time required to obtain a stable value of temperature inside the calibration bath was about 40 minutes (in the graphic above it was necessary more than 20 minutes). Before selecting the new temperature, time, thermostate temperature, thermometer temperature and Voltage were saved in a table in Excel. All the temperatures they have been reported in a table in Excel as shown in Fig. 3.9.

Point no.	Measured temperature (4R)						Time of measurement
	Potentiometer [ºC]	Thermostate [ºC]	Thermometer [ºC]	Thermometer [K]	Voltemeter [V]	Ambient [ºC]	Time
0	*Off*	*Off*	20,40	293,55	0,193800	22,00	09:59:00
1	30,00	30,10	30,00	303,15	0,2938		10:58:00
2	35,00	35,10	34,90	308,05	0,3434		11:58:00
3	40,00	40,00	39,30	312,45	0,3927		13:04:00
4	45,00	45,70	45,1	318,25	0,4485		13:54:00
5	50,00	50,20	49,60	322,75	0,4936		14:47:00
6	55,00	55,20	54,50	327,65	0,5427		16:05:00
7	60,00	60,00	59,30	332,45	0,5899		17:30:00
8	65,00	65,20	64,40	337,55	0,6451		18:44:00
9	70,00	70,40	69,60	342,75	0,6972		19:45:00
10	75,00	74,90	not readable		0,7435		20:40:00

***Figure 3.9**: Table with values of thermometer and the two thermocouples in the range from 20 to 70°C*

3.1.2.3 Results and analysis

The two thermocouples have been calibrated twice since the first results were not enough accurate. The objective of the calibration is to obtain a relation of the measured quantity (temperature) with the electrical output expressed in V.

$$T = m*V + q \tag{3.8}$$

It is necessary to obtain a relation as much linear as possible thus obtaining the slope and the intercept of the line.

Plotting (t,V) values we obtain a graphic as the one shown in Fig. 3.10.

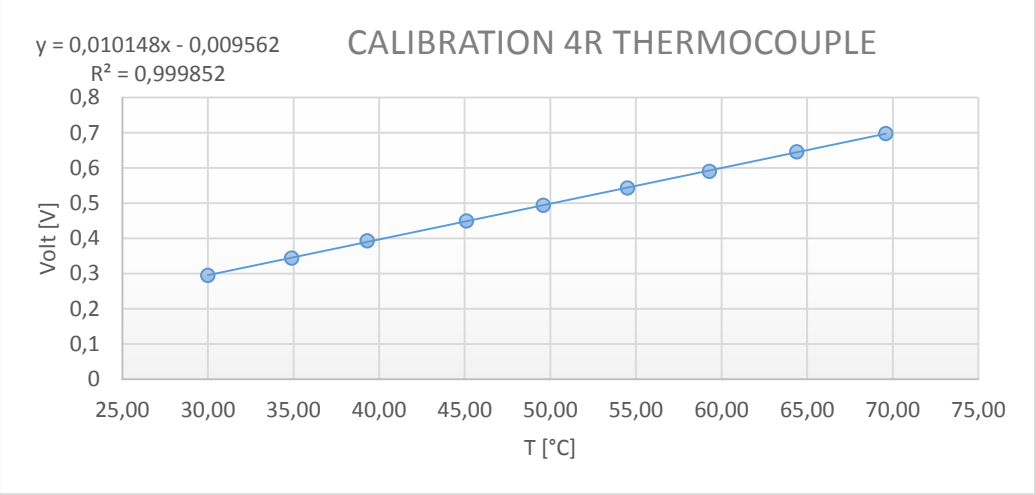

***Figure 3.10**: Calibration curve of 4R thermocouple*

The points have been related among them with a linear trendline (the blue straight line in the picture above). The accuracy of the calibration process (i.e. the linearity of curve) is expressed by the R^2 index: a value equal to 1 is referred to a straight line. The output of this calibration test are the slope (m) and the intercept (q) of this trendline (represented on the top-left of the graphic).Considering R^2 as index of accuracy of the calibration process it has been chosen the results of the first test showing a higher R^2 value.

T = m*V + q	4R	Ttube
Slope (m)	98.5260326	97.787811
Intercept (q)	274.0994312	273.43602
R^2	0.999852126	0.9996848

Table 3.2: Results of the calibration of the thermocouples 4R and Ttube

3.2 Cold wires

The limit of thermocouples is the relatively low frequency response which does not allow to discern temperature variations with frequencies higher than 100-500 Hz: cold wires are high performances instruments used for their fast frequency response.

Cold wires use the variation of resistance that occurs when the wire change its temperature from the reference value. The thin wire (d_w > 1µm) is inserted in a constant current Wheatstone bridge (Fig.3.11).

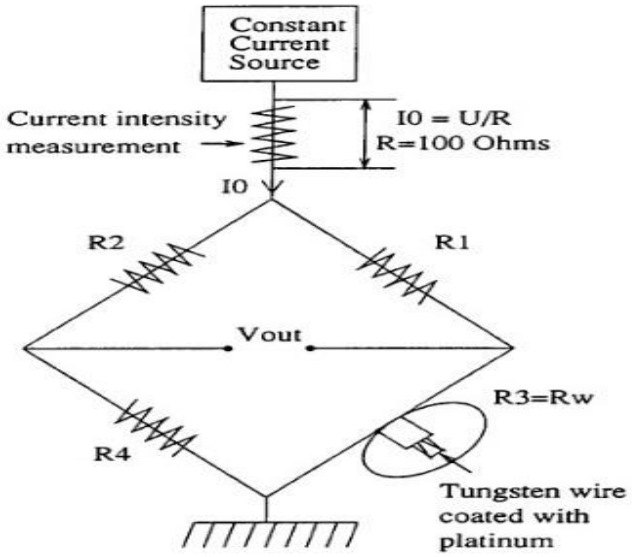

***Figure 3.11** : Principle of resistance thermometer*

Resistances R_2 and R_4 are usually far bigger than resistances R_1 and R_w so that current I_0 flows almost completely in the right branch of the bridge (through resistance R_1 and R_w). The wire used to senses temperature variations is usually

made by tungsten and coated with platinum in order to give a higher mechanical strength and an appreciable sensitivity to temperature α_w. The variation of resistance with temperature is expressed by:

$$R_w = R_0[1 + \alpha_w(T_w - T_0)] \qquad 3.9$$

$$R_0 = \frac{{\sigma_0}^{-1} l_w}{\frac{\pi \, {d_w}^2}{4}} \qquad 3.10$$

where ${\sigma_0}^{-1}$ is the resistivity of the wire and l_w the length of the wire. The output supplied by the bridge is a voltage expressed by:

$$V_0 = I_0 \frac{R_3(R_2 + R_4) - R_4(R_1 + R_3)}{R_1 + R_2 + R_3 + R_4} = I_0 \frac{R_3R_2 - R_4R_1}{R_1 + R_2 + R_3 + R_4} \qquad (3.11)$$

R_3 is the only resistance that changes with temperature, the other having a fixed value. Considering that $\Delta R_3 = (R_3 - R_{03})$ is far smaller than the other resistances, the denominator of the previous formula can be assumed constant and the electrical output is a linear relation proportional to ΔR_3 :

$$\Delta V = \Delta R_3 \, I_0 \, G \qquad (3.12)$$

The bridge must be set in equilibrium(V_0=0) changing R_2 so that:

$$R_2R_{03} = R_1R_4 \qquad (3.13)$$

The value of current I_0 must be enough high to get an appreciable value of ΔV (an amplifier can be used for this aim). Nevertheless, in order to have a good cold wire probe, this should be designed to be as much as possible insensitive to gas velocity: this means that the temperature of the wire must be low and that the current I_0 must be below a certain value in a way to consider Joule effect

negligible. The sensitivity of the probe respect to the gas velocity can be computed starting from a power balance between Joule effect and the power added to the wire by convective fluxes.

The probe has to register temperature variations occurring with conduction, convective and radiation phenomena. The physics behind a cold wire can be quite complicated and some assumptions have to be done in order to get satisfying results. A brief description of the dynamic model of a cold wire is here reported.

The unsteady behaviour of a cold wire can be described by a first order differential equation. Indeed the probe, having a certain thermal inertia, needs some time to respond to a temperature step. As a first approximation, it can be written that the temperature of the wire depends on its thermal inertia and its capacity to acquire heat from convective fluxes:

$$V_w \rho_w c_w \frac{\partial T_w}{\partial t} = -hS_w(T_w - T_g) \tag{3.14}$$

The equation can be rearranged in an easier way including a time constant τ:

$$\tau \frac{\partial T_w}{\partial t} + T_w = f(t) = T_g \tag{3.15}$$

$$\tau = \frac{V_w \rho_w c_w}{hS_w} = \frac{d_w \rho_w c_w}{4h} \tag{3.16}$$

This is a first order differential equation: from signal theory, first order equations have an analytical formula for transfer function and cut-off frequency. In order to compute these properties it is necessary to compute the time response constant which, in turns, requires the knowledge of the convective constant *h.* This value comes from Nusselt number expressed as a function of Reynolds number by an experimental equation:

$$Nu = A + B\, Re^n \tag{3.17}$$

$$Nu = \frac{h\, d_w}{k_g} \tag{3.18}$$

Where k_g is the conductivity of the gas. Substituting the equations below in the formula relative to the time constant we obtain the following equation whose constants A, B have to be found by experimental tests:

$$\tau = \frac{{d_w}^2 {\rho_w}^2 \, c_w}{4k_g \left[A + B \left(\frac{\rho_g v_g d_w}{\mu_g} \right)^n \right]} \tag{3.19}$$

The cut-off frequency, defined as the frequency at which the modulus of the signal is attenuated by $\sqrt{2}/2$ respect to the original value, can be easily found (for first order equations) as $f_{cut-off} = 1/2\pi\tau$. The results of the cut-off frequency versus the velocity of gas (v_g), taken from Dénos [4], are depicted in Fig. 3.12. It can be seen that, increasing the gas velocity the convection rises: the probe reacts quicker (low τ) and the cut-off frequency increases. In the same figure we can see that low diameter probes have a higher cut-off frequency.

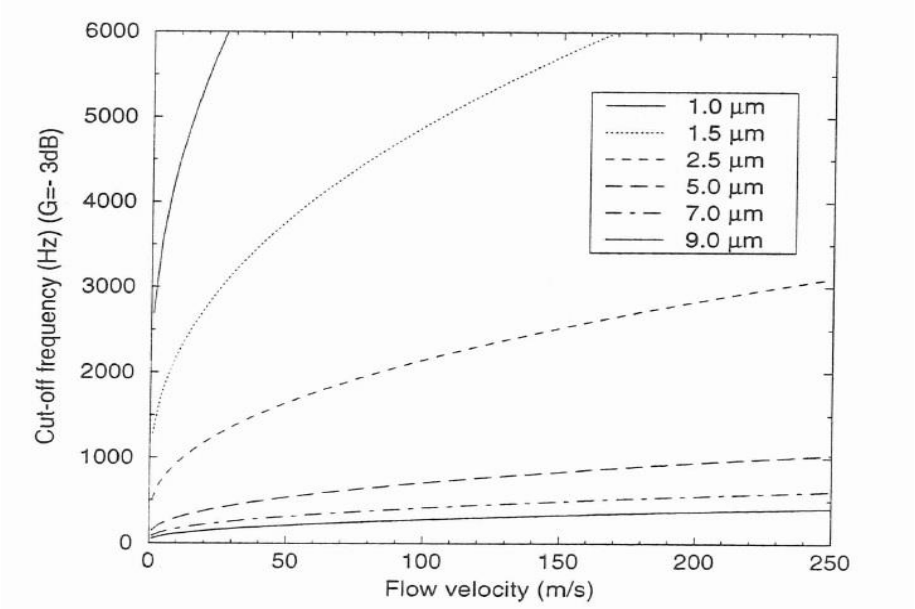

***Figure 3.12**: The effect of convection (velocity) on the cut-off frequency. A smaller wire has a higher frequency response, which results in a higher cut-off frequency.*

In the model described up to now an important phenomenon, source of significant errors, has not been considered: conduction of heat between wire and prongs. The wire is mounted between two stain prongs whose dimension are far bigger than those of the wire (Fig 3.13): conduction cannot be neglected.

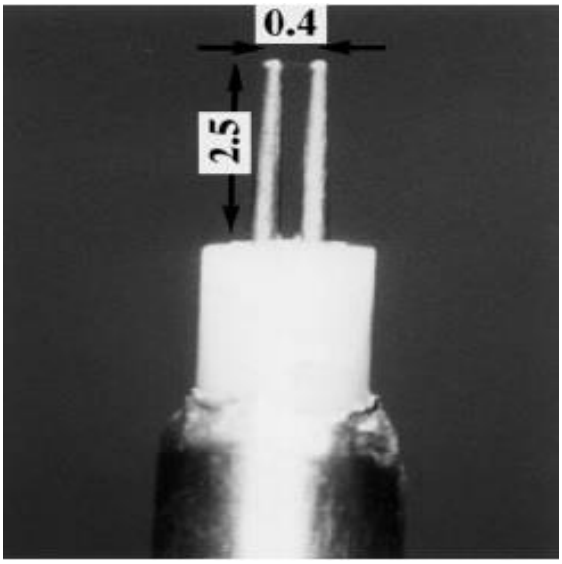

***Figure 3.13**: Particular of a cold wire: the wire is suspended between two stain prongs.*

The problem of conduction in *steady conditions* can be solved considering a symmetric problem (respect to the centre of the wire) described by the following equation contoured by two boundary conditions:

$$\frac{\partial^2 T_w}{\partial x^2} = \lambda^2 (T_w - T_g) \tag{3.20}$$

$$Q_{cond}\left(x = \frac{l}{2}\right) = 0 \tag{3.21}$$

$$T_w(x = 0) = T_p \tag{3.22}$$

Where $\lambda^2 = \frac{4h}{k_w\, d_w}$, T_g is the gas temperature and T_p is the temperature of the prong which has been considered at an imposed value (assumption of infinite thermal capacity of the prong); it has been considered a reference system centred to one edge of the wire, being the problem symmetric . The steady problem stems from

a heat balance between conductive and convective fluxes (unsteady phenomena and Joule effects have been neglected). The results of this equation computed by Dénos are reported in Fig. 3.14. It has been defined the ratio $\frac{T_w - T_p}{T_a - T_p}$, being T_a the temperature of the gas and T_p the temperature of the prong: this is an index of the disturbance of conduction phenomena between wire and prong. When this ratio is equal to 1 there is no interference between wire and prong and the wire has (at least theoretically) the same temperature of the gas. The parameter l/d , length over diameter of the wire, is a non-dimensional number describing its geometry. A high l/d value refers to a thin wire developing in length.

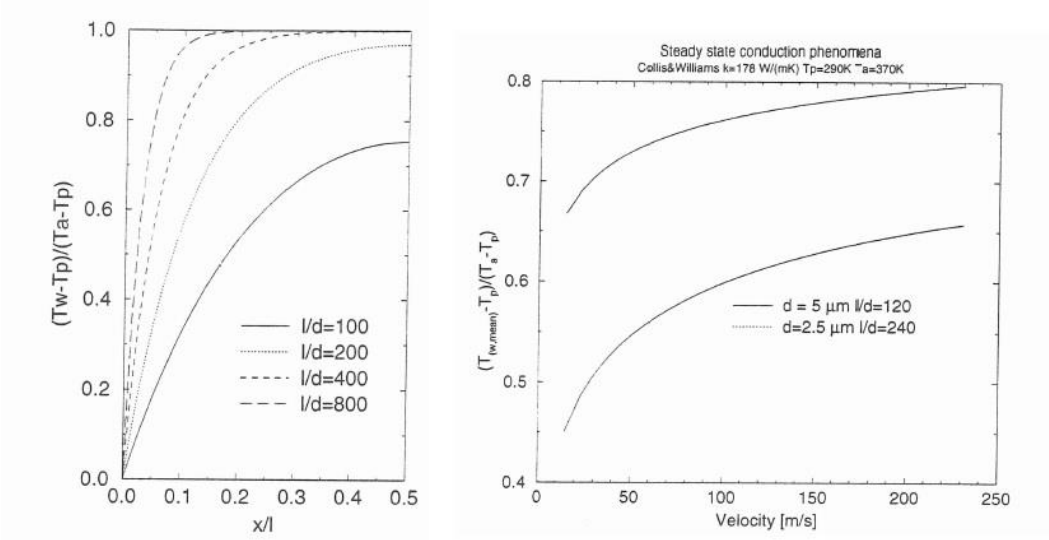

Figure 3.14*: The effect of conduction of the prongs: the temperature of the wire is closer to the temperature of the gas in the centre of the wire (less conduction effect); the conduction error decreases considering wire with a high l/d ratio. Velocity has an important dependence on the mean wire temperature: higher velocity are associated to higher convection and a reduced conduction error.*

It can be noticed that conduction effects are smaller when we refer to the temperature at the centre of the wire ($x/l = 0.5$). When *l/d* rises, the conduction errors affect only the edges of the wire. The figure on the right (always referring to Fig 3.14) shows the favourable effects of a higher gas velocity: higher convection (h, coming from a higher gas velocity) reduces the conduction effects between wire and prongs and the mean temperature of the wire approaches the temperature of the gas.

The description of *unsteady conduction* between wire and prongs requires a more complicated physical description. Referring always to [4] only a short resume will

be given. The unsteady conduction phenomena is described by the following differential equation contoured by boundary conditions (temperature of the prongs) and initial conditions:

$$\frac{\partial T_w}{\partial t} = \alpha \frac{\partial^2 T_w}{\partial x^2} - \frac{1}{\tau}\left(T_w - T_g\right) \tag{3.23}$$

Where $= \frac{k_w}{\rho_w c_w}$, $\tau = \frac{d_w \rho_w c_w}{4h}$. This equation can be solved using as numerical solution the implicit Crank-Nicholson scheme. The equation have been discretized in the time and space domain obtaining the following equation:

$$\frac{{T_i}^{n+1} - {T_i}^n}{\Delta T} = \alpha \frac{[\eta({T_{i+1}}^{n+1} - 2{T_i}^{n+1} + {T_{i-1}}^{n+1}) + (1-\eta)({T_{i+1}}^n - 2{T_i}^n + {T_{i-1}}^n)]}{\Delta x^2} - \frac{1}{\tau}\left[\left(\eta {T_i}^{n+1} + (1-\eta){T_i}^n\right) - {T_g}^n\right] \tag{3.23.1}$$

The numerical system has been tested with an input signal. A sine wave signal of gas temperature has been used as input for a prong-wire system in order to test its response. This sine signal has been tested at different frequencies (100Hz, 1000Hz) and several values of gain have been obtained. These results are shown in Fig 3.15. It can be noticed that, at low frequency, both prong and wire follow the sine input because the gain is 0 dB; at higher frequencies the prong is not able to follow the input signal. In the picture representing the transfer function we can observe a plateau region. At further higher frequencies neither the tungsten wire can reproduce the gas temperature signal: the gain decreases abruptly. Other results relative to the influence of the prong time constant on the frequency response can be found in the paper written by Dénos [4].

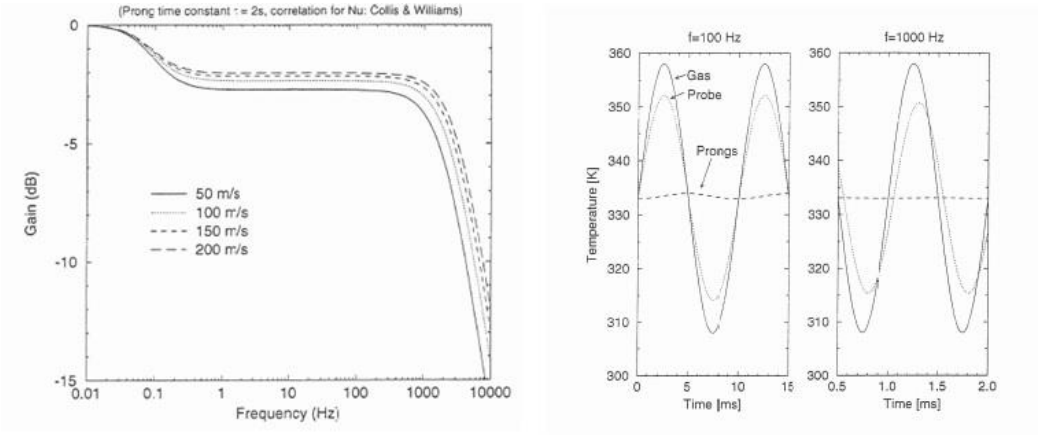

***Figure 3.15**: (left) Transfer function of the wire-prong system: it is possible to see the effects of velocity. (right): The numerical system represented in equation 3.23.1 has been tested with a sinusoidal input for different frequencies. The prong is not able to follow the input at high frequency.*

Another resolution for the unsteady conduction problem can be found considering the first order system as a discrete system described by the following equation:

$$\frac{{T_w}^{n+1} - {T_w}^{n}}{\Delta t} = -\frac{1}{\tau}\left({T_w}^{n} - {T_g}^{n}\right) \tag{3.24}$$

Better results can be achieved considering combinations of discrete first order systems. The probe output (T) can be written as a linear combination of the responses of wire and prongs: this will discussed in detail in chapter 4 and chapter 5.

3.2.1 Cold wire static calibration (oven)

The cold wires have been calibrated with static tests: they have been tested in steady conditions, i.e. neglecting dynamic effects, using the oven and the heated jet.

The static calibration in the oven and heated jet has been done for two cold wires: DAO121A (identified with letter B) and DAO123A (identified with letter A). The two probes are represented in Fig 3.16.

Each probe has two transducers: the first one placed in the middle and indicated with number 2; the second one placed at the edge and indicated with number 1.

The wire is made of tungsten and has a length (l_w) of 1 mm and a diameter (d_w) of 2.5µm; it is held by two prongs 2 mm long.

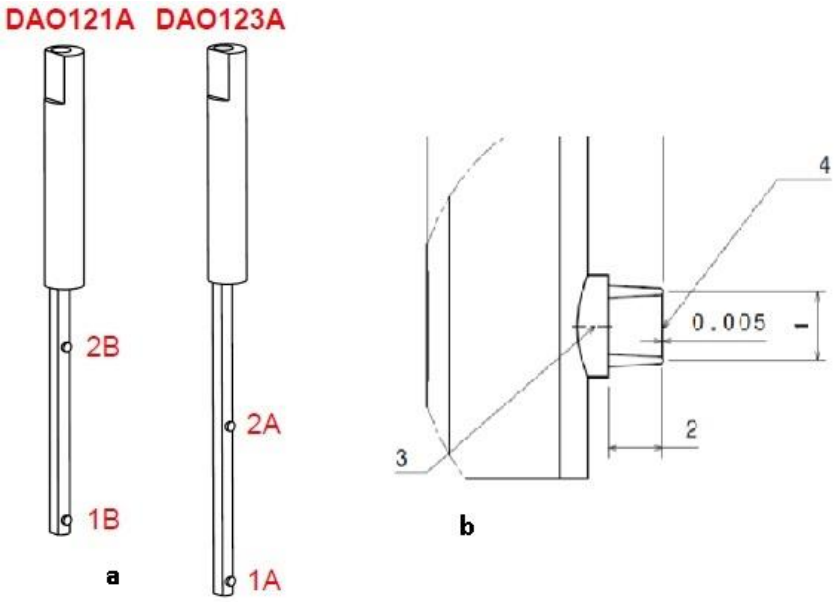

***Figure 3.16**: Cold wires DAO121A, DAO123A*

3.2.1.1 Calibration Process

The calibration in still air has been done in steady conditions: the cold wire and a thermocouple have been placed inside a metallic box which, in turn, have been put inside an oven (Fig. 3.17(a), Fig.17(b)). The electric cables of the probes come out of the oven through a hole which have been closed with red plasticine in order not to have heat dispersion (see Fig. 3.17(c)).

DAO121A has been tested with 4R thermocouple; DAO123A has been tested with 2R thermocouple. The thermocouples have been linked to an amplifier in order to obtain significant values as output (in detail: thermocouple 4R was linked with TC amplifier TU4, thermocouple 2R was linked with TC amplifier TU7).

For the calibration of these probes two cold wire boxes have been used: the black one (TUCW3) and the white one (TUCW2). These boxes basically consist in a Wheatstone bridge in which one of the four resistances is the cold wire, linked to the box by its input entries (Fig. 3.18).

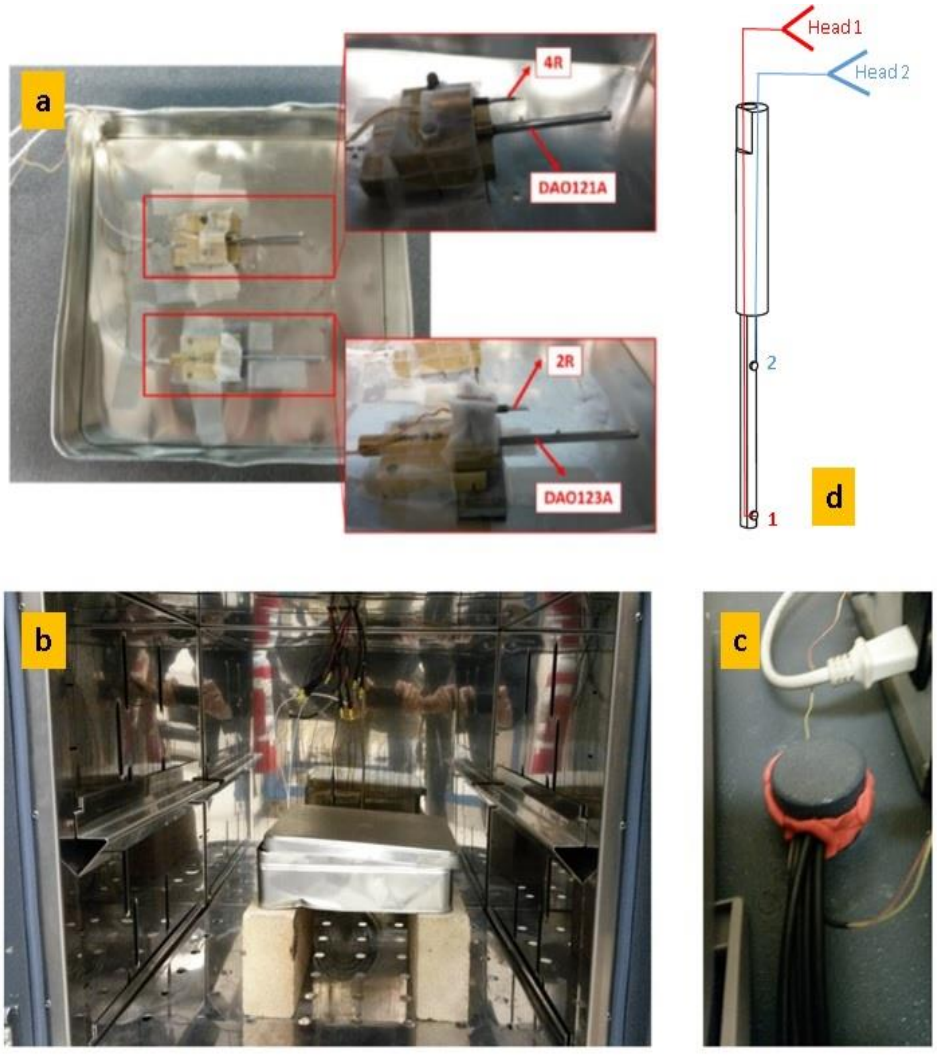

***Figure 3.17**: Setup for the static calibration in the oven*

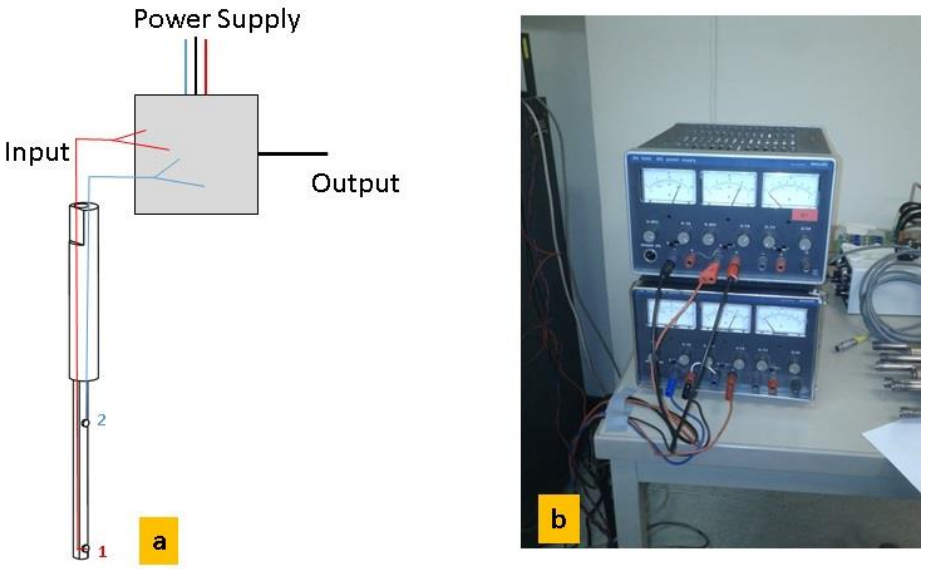

***Figure 3.18**: (a) Schematic representation of the wiring of a cold wire; (b) power supplier.*

The cold wire box is linked to a power supply (Fig. 3.18 (b)) which produces the desired value of voltage: for this test it has been set a value of ± 15V in order obtain a current inside the wire of around 0.2 mA. It's important to have an electric current of small intensity in order to have a negligible Joule Effect. Through some BNC cables it was possible to read the output of the box (voltage of the bridge and current inside the wire) displayed in a multimeter.

For the calibration of the cold wire it has been chosen to set the range of temperatures between 20 and 90 °C with a ΔT of 10°C between two points. Before starting the test, the stability of the electronic setup has been tested monitoring the values of the cold wire and current outputs in function of time at ambient temperature. This is shown in Fig. 3.19: these data are relative to the white box TUCW2 and it can be noticed that they drift a bit.

Once the data relative to the current, cold wire and thermocouples outputs have been taken at ambient temperature, the oven is heated up to the prefixed target temperature. To obtain a stable value it took 1h40 minutes. The data have been registered up to 90°C degrees and the calibration was brought to an end in two days. As done for the calibration of thermocouples, also for the cold wires these data have been related with a linear trendline: using Excel it was possible to obtain the slope, the intercept and the R^2 of the curve.

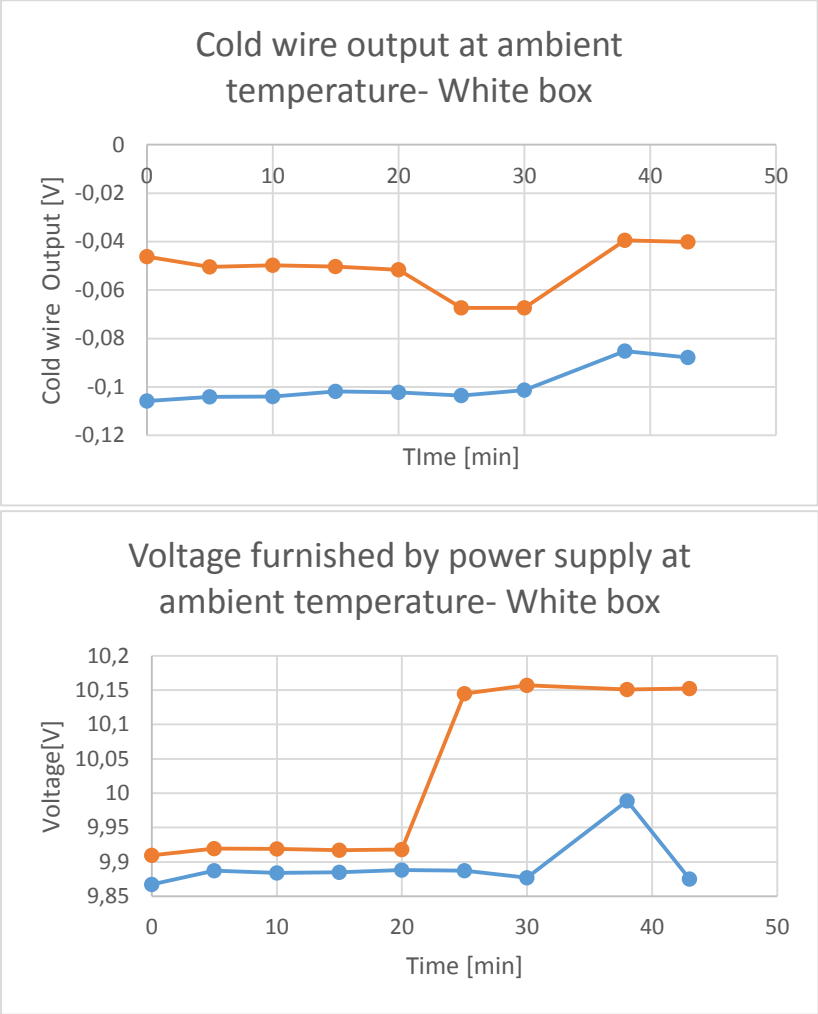

***Figure 3.19**: Stability of the white box TUCW2. The cold wire signal and the current supplied by the power generator have been monitored at ambient temperature to test the stability of the Wheatstone bridge.*

3.2.1.2 Wiring of the cold wires

Probe	Head	Electronics (input)
DAO123A	1A	Black Box CH1
	2A	White Box CH1
DAO121A	1B	Black Box CH2
	2B	White Box CH2

***Table 3.3** Wiring of the cold wire transducers with the Wheatstone bridge entries.*

3.2.1.3 Results

The following graphics (Fig. 3.20) are the calibration curves for the two probes.

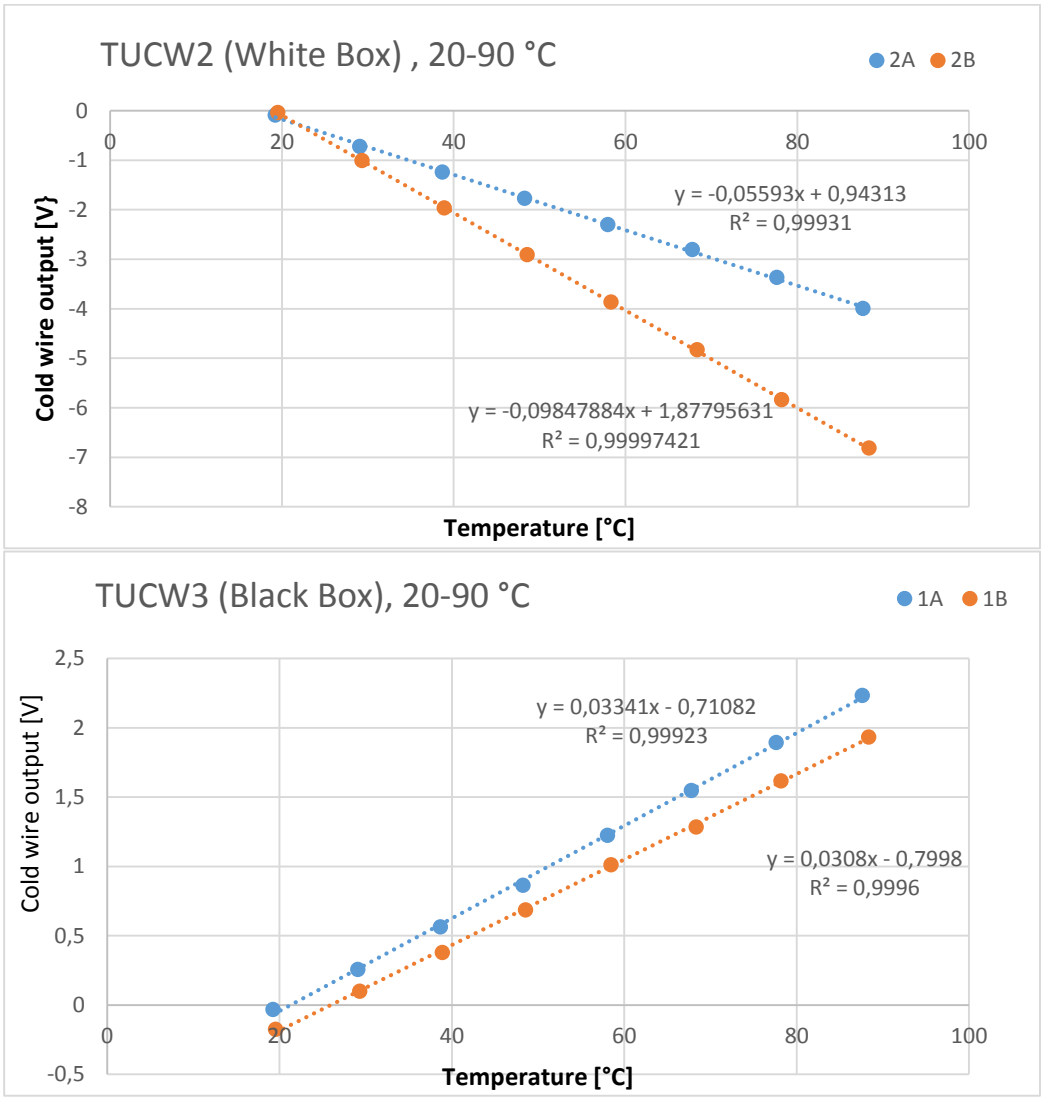

***Figure 3.20**: Results of the static calibration in the oven of the two cold wires DAO121A , DAO123A*

3.2.2 Cold wire static calibration (heated jet)

The calibration in heated jet has been done using a more complicated setup. The cold wire has been tested always in static conditions registering its outputs at different Mach and temperature of an air jet.

For these tests the cold wire has been mounted on variable height support in order to put manually the probe inside and outside the heated jet setting the height of the support (Fig. 3.21). This support has been placed near a facility that blows the jet of air through a nozzle: changing the height of the support the head of the transducer was submerged into the flow. The facility for the heated jet was linked with a pipe to a heating system that, in turn, was linked to the air pressurised reservoir of the Von Karman Institute. The head of the probe was tested only for few seconds into the flow to preserve the wire which is extremely fragile: after having taken the data the support was moved manually to remove the probe from the jet.

The test consisted in measuring the output of the cold wire when inserted into a flow with known temperature and Mach conditions. At the same time pressure and temperature variations were registered with other probes. Before starting the test, the pressurized air reservoir was opened to reach a sufficient ΔP to get the desired Mach number.

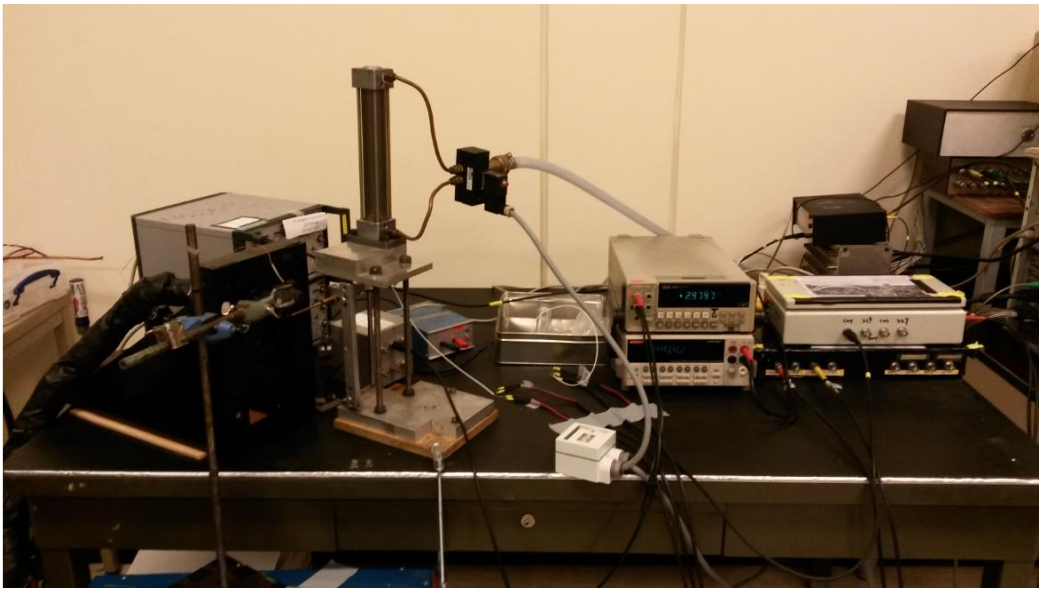

***Figure 3.21**: Experimental setup for the static calibration of the cold wire in the jet; it is visible the metallic support used to set the position of the cold wire.*

3.2.2.1 Experimental Setup

The cold wires have been linked to the Wheatstone bridge as done in the calibration in the oven: the tested transducer has been linked to the input of the box used as Wheatstone bridge (Fig. 3.22); this box, in turn, has been connected to a power supply and to a multimeter in order to read the output of the probe.

The pressurized air has been blown through a nozzle. Inside the nozzle it has been placed a differential pressure transducer (SENSYM) and a thermocouple (2R): the latter has been linked to an amplifier in order to obtain significant values.

Outside the nozzle, through some rigid supports it has been installed the second thermocouple (4R, connected to an amplifier) while the cold wire has been mounted on a variable height support, as mentioned before.

The connections of the heads of the probes with the Wheatstone bridge (black/white boxes) are the same used for the calibration in the oven.

***Figure 3.22**: The cold wire boxes (Wheatstone bridge)*

3.2.2.2 Pressure Readings

A differential pressure transducer (SENSYM, R4S4) has been inserted inside the nozzle in a way to get differential pressure readings. Before using the probe in the static test the transducer has been calibrated: one head of the probe has been connected inside the sealed case of the pressure calibrator through a thin plastic pipe while the other was kept to ambient pressure (Fig. 3.23). The transducer has been linked with a power supply through a connector: through a multimeter it was possible to read the electrical output of the probe.

***Figure 3.23**: Setup for the calibration of the SENSYM (differential pressure transducer)*

The pressure calibrator output was set initially to zero. Once the sealed chamber was closed it was possible to add or subtract pressure to one side of the transducer (the other side being at constant ambient pressure) with the handles of the instrument. As done for the calibration of thermocouples also in this case several points of pressure-voltage have been taken and have been inserted in Excel in order to get a linear trend with values of slope and intercept. As can be seen in the following graphic this instrument has a high R^2 (>0.99999).

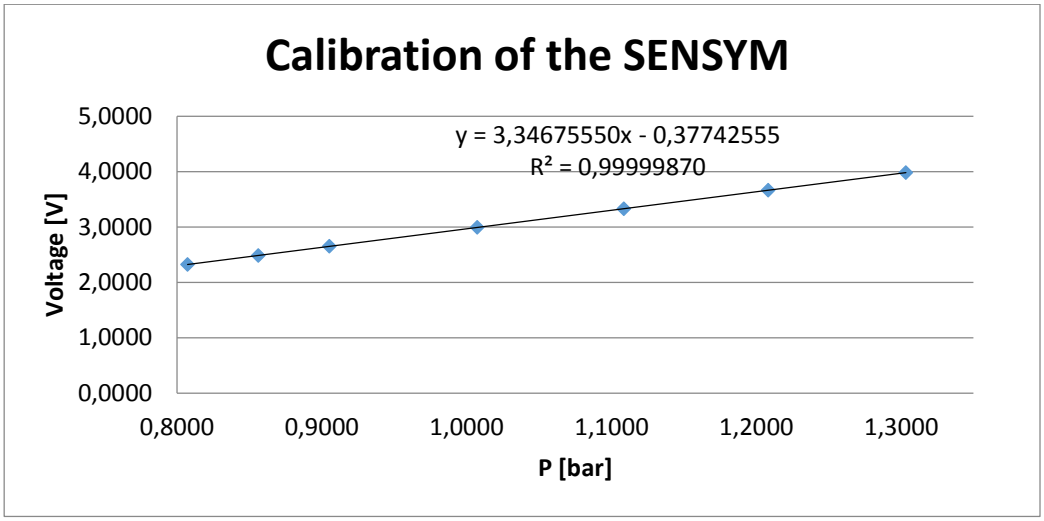

Figure 3.24: *Calibration curve of the SENSYM R4S4*

3.2.2.3 Temperature Readings

Two temperature probes have been installed in the facility to get more details on the evolution of temperature. The 2R thermocouple was mounted inside the nozzle and linked to the TC amplifier TU7; the 4R thermocouple was mounted with a rigid support right at the exit of the nozzle and linked to the TC amplifier TU4. In Fig. 3.25 we can see that the head of the thermocouple 4R is closely placed near one of the two heads of the cold wire.

Other two thermocouples have been installed inside the heating system (Fig. 3.26).

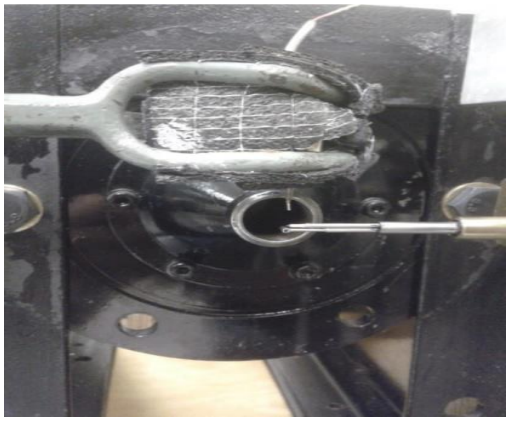

Figure 3.25: *Thermocouple 4R (up) and cold wire (put horizontally).*

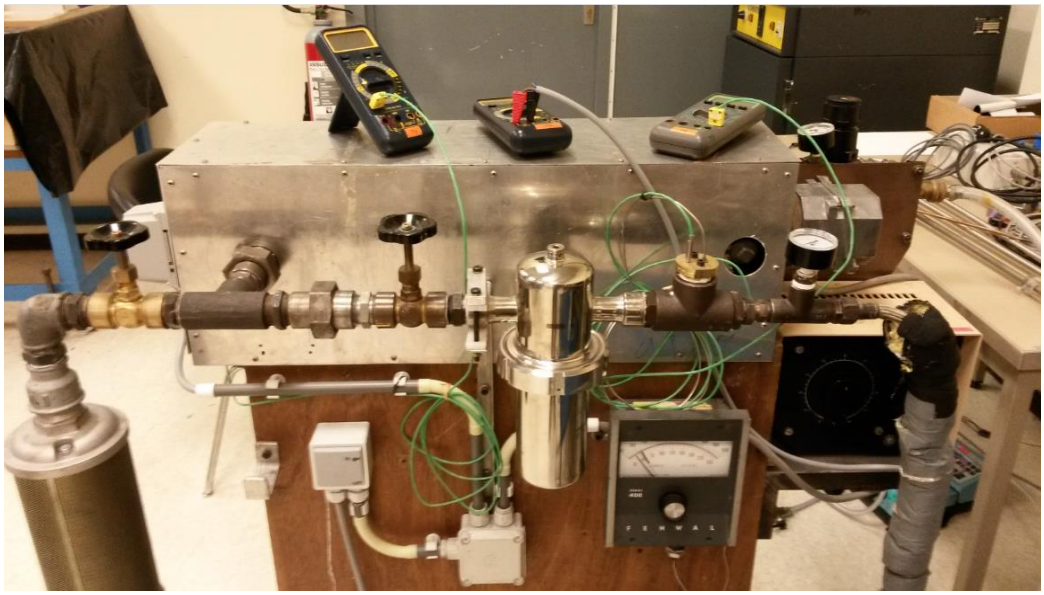

Figure 3.26: *The heating system for the air pressurized reservoir. It is provided with two thermocouples to monitor the temperature before the air reach the nozzle.*

3.2.2.4 Setting Mach number

The tests in the heated jet have been done using several Mach numbers. The desired value has been reached using air pressurized into a reservoir.

The data of ambient pressure came from the server of Von Karman Institute. Knowing the value of Mach number required for the test and the ambient pressure it was possible to obtain the required total pressure using equation (3.25)

$$\frac{P_{tot}}{P_s} = \left[1 + \left(\frac{\gamma - 1}{2}\right) M^2\right]^{\frac{\gamma}{\gamma - 1}} \tag{3.25}$$

Being P_s the ambient pressure and k the specific heat ratio of air. The air has been considered a perfect gas, having $\gamma = 1.4$, specific heat at constant pressure $C_p = 1.005 \frac{KJ}{Kg\ K}$ and specific constant $R = 287.05 \frac{J\ Kg}{K}$.

The dynamic pressure dP stems from the difference from the total and static pressure (P_{amb}) :

$$dP = P_{tot} - P_{amb} \tag{3.26}$$

The related value expressed in Volts in the multimeter is obtained using the values obtained with the calibration of the SENSYM (see Pressure Readings).

3.2.2.5 Setting temperature of the air

As mentioned before, the air coming from the pressurized reservoir has been heated up to a desired temperature. To obtain the required value air passed into the heat exchanger shown in Fig. 3.26. The temperature has been chosen using a handle while the rate of heating has been changed increasing the current inside the resistances in the heat exchanger thus increasing Joule effect.

3.2.2.6 Calibration Process

The two probes DAO121A and DAO123A have been calibrated in the heated jet: in each experiment the head of the transducer was tested at different Mach numbers and different temperatures. The values of Mach have been chosen at 0.05, 0.2 and 0.3; for each velocity (Mach number) the probe was tested at 10 different temperatures (from 20°C to 65-70°C).

The electronics of the bridge have been set up in order to get small current in the wire (values lower than 2mA); as done for the calibration in the oven the power supply was arranged to give 15V of voltage.

The first point of calibration curve has been taken at ambient temperature at Mach 0. After having opened the valve of the air pressurized reservoir and having chosen the correct value of total pressure to apply it was possible to start the calibration.

The first test has been done at Mach 0.05 and ambient temperature (~17°C). For each point the data of the two thermocouples, the cold wire and the pressure transducer have been monitored. The cold wire has been exposed to the air flux for few seconds in order to preserve it. After having taken the data, the temperature was raised to the target temperature using the handle of the heat exchanger.

The same procedure has been followed raising the Mach number to 0.2 and 0.3: before starting the calibration to a new Mach number starting from ambient temperature we had to wait for a while since the heat exchanger was still hot.

3.2.2.7 Results

During the investigations the head 2A (DAO123A) got broken when tested at Mach 0.3: the wire was repaired and tested again. The results obtained with the two wires (of head 2A) have been compared and discussed at the end of the paragraph. In the following graphs it have been shown the results of the output of the cold wire in function of the temperature inside the nozzle (temperature registered by the thermocouple 2R) and temperature in the jet (temperature registered by the thermocouple 4R). The subscript 1 refers to the CW-TC Jet Temp; the subscript 2 refers to the CW-Nozzle temp.

DAO123A- Head 1A

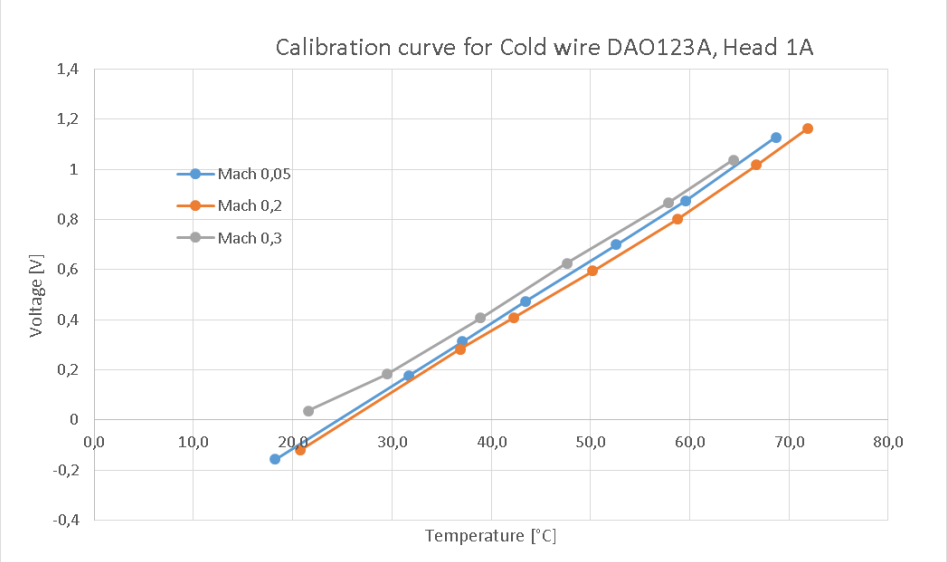

In this graphic are visible the effects of Reynolds causing the curve to change slope and intercept with the Mach number. The results relative to the calibration coefficients are reported in table 3.4. The electric output of the cold wire has been associated to the value of temperature registered by the thermocouple placed near the cold wire in the jet.

DAO123A- Head 2A

The probe got broken testing it at 70°C. It has been repaired and tested again

.

Mach 0.3 (second calibration, after reparation)

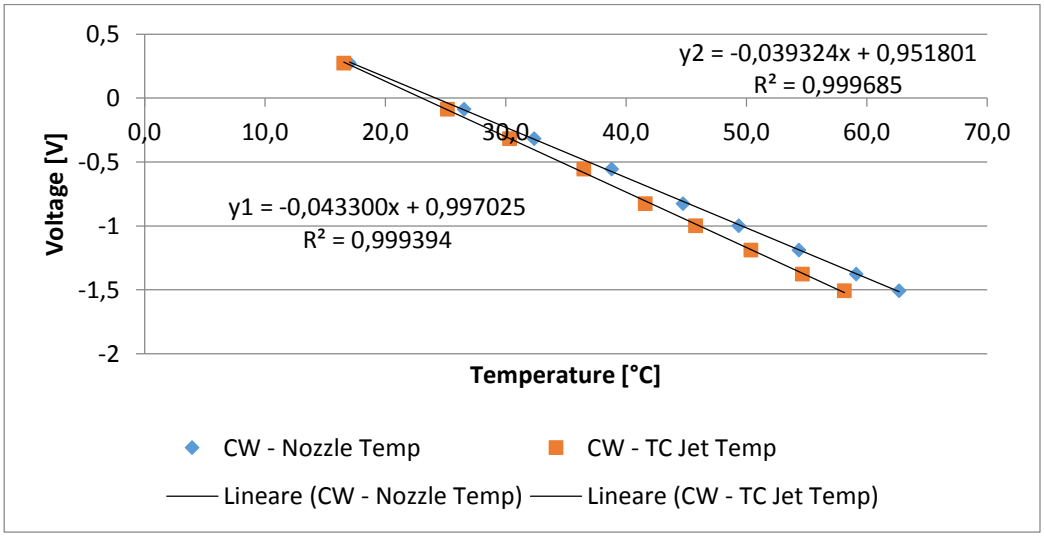

After the reparation the calibration curve of head 2A has changed: there's a small change in the slope of the curves (before and after reparation) of 3.34% but a significant change of the intercept that can be due to the variation of the overall resistances. The two curves are shown in the following picture. The head 1A which has been tested twice even if it hasn't been repaired keeps the same values of intercept and slope with insignificant variations.

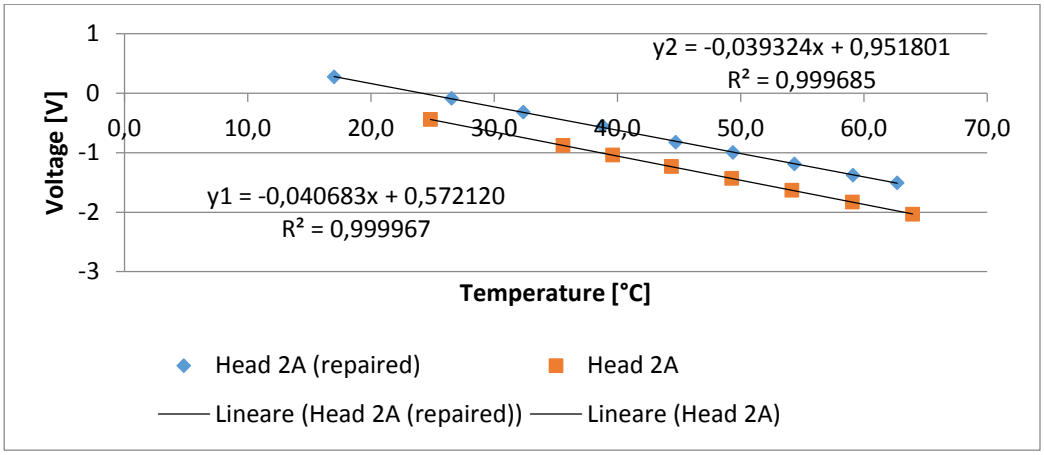

***Figure 3.27**: Comparison of head 2A before and after reparation. There is significant variation in the intercept due to the change of the overall resistance of the cold wire.*

3.2.2.7.3 DAO123A- Head 1B

Mach 0.3

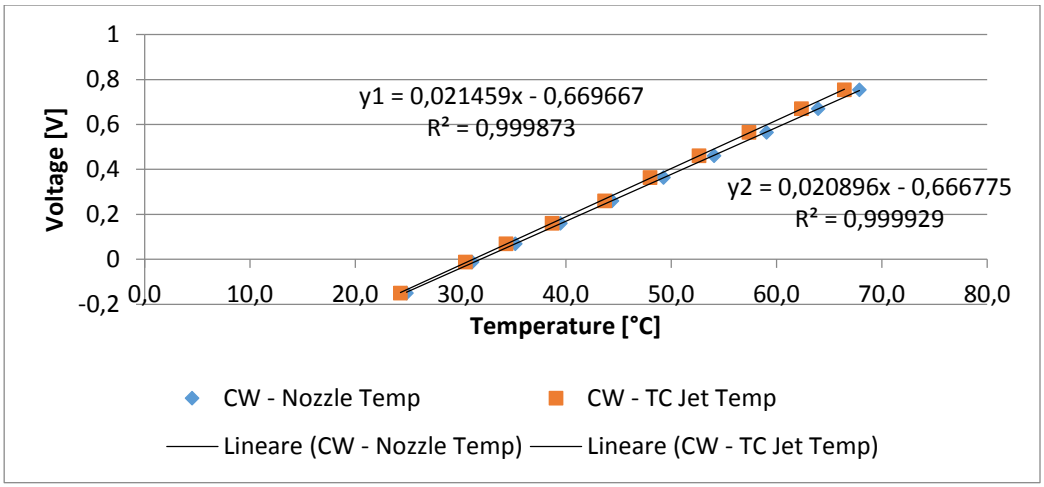

3.2.2.7.4 DAO123A- Head 2B

Mach 0.3

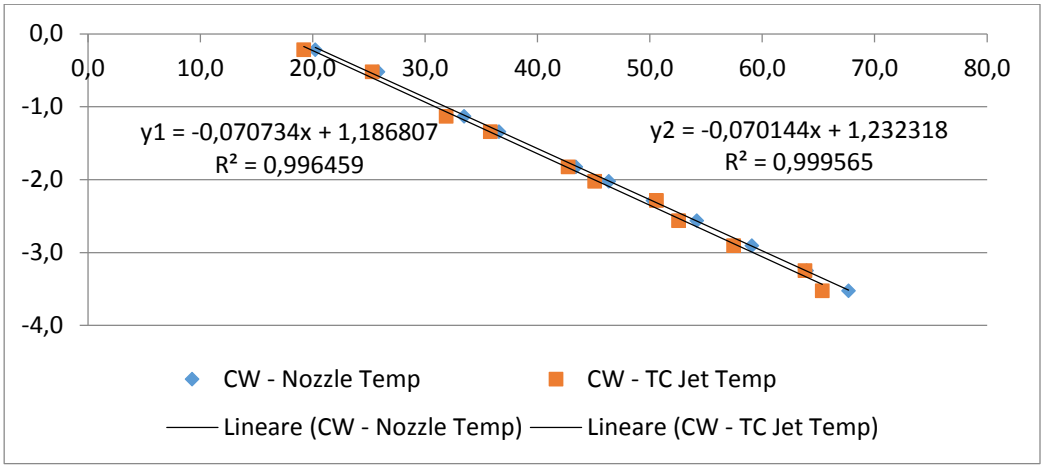

The probe DAO123A Head-2A has been tested at different Mach numbers: the slope changes without following a precise relation with the velocity. Changes of the slope are in the order of 5% and can be related to Reynolds effects.

Probe	Head	Mach	Reynolds	a	b	R^2
			T_{TOT}= 323 K	T = a*V + b (with T in °C)		
DAO123A	1A	0	-	29,92972	21,2746	0,999232
		0.05	2.49	43,16862	25,0399	0,999810
		0.2	10.04	41,66523	26,8696	0,999227
		0.3	15.25	43,58036	19,1749	0,999737
	2A	0	-	-17,8797	16,8628	0,999312
		0.3	15.25	-25,4295	24,2039	0,999685
DAO121A	1B	0	-	32,44697	25,95118	0,99955
		0.3	15.25	47,85493	31,90849	0,99993
	2B	0	-	-10,15446	19,06964	0,99997
		0.3	15.25	-14,25648	17,56851	0,99957

Table 3.4: *Results of the static calibration of cold wire*

Chapter 4

Numerical Filtering and Signal Compensation

The calibration process has been done in order to obtain a relation between the electrical output of the probes and the desired physical characteristic (i.e. temperature, pressure). The modern transducers have a high sensitivity to physical variations and it is possible to display these changes in digital multimeteres obtaining high accuracy measurements.

The main problem of electrical instruments is that they produce an internal noise associated with an unsteady distribution of electrical charge inside the instrument itself. This is known as thermal noise: the microscopic variations inside a conductive material turn into macroscopic variations (fluctuations) of the output (Voltage). This kind of fluctuations, described with probabilistic tools, depends on the material properties and is not possible to eliminate them: they superimpose on the original signal causing an alteration or distortion of the signal itself.

For this reason it becomes important to adopt some tools in order to obtain experimental results that can be easily interpreted: the signal is filtered and cleaned from unnecessary noise and disturbances. In this chapter will be described the numerical analysis done in order to obtain the amplitude and phase curves of analogue filters used for experiments in CT3.

On the other hand, this chapter deals with the problem of the theory on numerical compensation of signals. Transducer have physical limits that do not allow to get accurate results when the registered phenomena are extremely fast. The compensation allows reconstructing the real signal starting from the original one through the probe transfer function. It is possible to obtain it through experimental tests and compensate the signal through the inverse of the transfer function. This problem will be described in detail in the second part of this chapter; the experimental activity is presented in the last chapter.

4.1 Numerical filtering

In this paragraph it is shown the description of the experimental tests done in order to characterize the filter boxes and a quick description of the code developed on Matlab to process the obtained data.

4.1.1 Experimental Setup

4.1.1.1 Filter boxes

The filter boxes utilised for the experiments are those ones shown in Fig. 4.1. The one on the left, the bigger one, has 4 boards that, in turn, have 4 channels each. In every channel there are 4 entries relative to the Input, Raw Output, Low Pass Output, High Pass Output. Each channel is done in such a way that the Raw Output reproduces exactly the input signal while the Low Pass Output filters the input frequencies higher than 100 Hz and the High Pass Output filters those ones lower than 750 Hz. Before starting the data acquisition the electronic cards that powered the filter box have been set up as shown in Fig. 4.2.

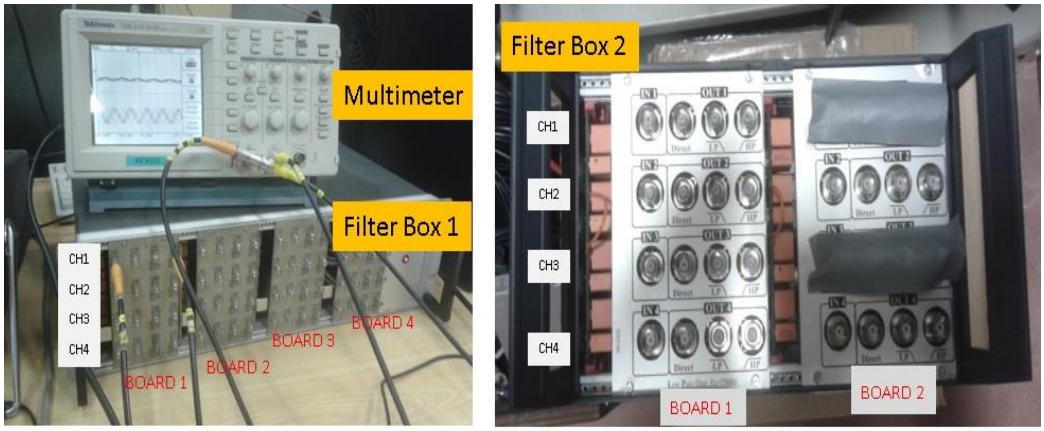

***Figure 4.1**: Filter boxes: each channel has a certain behaviour in the frequency domain. The aim of testing these boxes is getting the Bode diagrams of every channel.*

The filter box shown in Fig. 4.1 on the right has 2 boards with 4 channel each, which, in turn have the same four entries: Input, Raw Output, Low Pass Output, High Pass Output (same Low Pass, High pass frequencies as the first filter box). Channel 1 and channel 3 of the second board are not working.

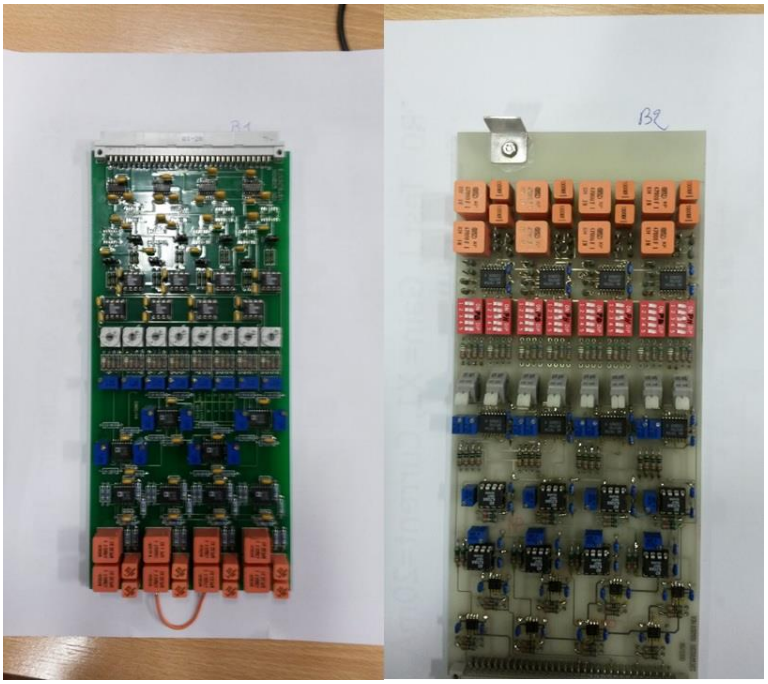

***Figure 4.2**: Electronic cards. The filter boxes are supplied by electronic cards.*

4.1.1.2 Frequency generator

The signal to be tested in the filter boxes has been generated by the frequency generator depicted in Fig. 4.3. With this instrument it is possible to generate electric input signals at the desired frequency and shape (triangular, sinusoidal, step-shaped). The frequency generator has been linked with a cable to the input entry of the chosen board-channel of the filter box. It has been decided to analyse a sinusoidal input signal of 0.7 0-to-peak amplitude (1.4 peak-to-peak amplitude) in a particular range of frequencies (0-200000 Hz, more detail later in the paragraph 4.1.1.4).

***Figure 4.3**: The frequency generator is used to produce signal of known shape and frequency*

4.1.1.3 Data acquisition system

The three output entries (Raw, Low-Pass, High-Pass) have been linked to GENESIS, a data acquisition system (DAS). This machine is used to acquire electric data at a high sampling rate from a continuous input signal. The three outputs of the filter have been linked to 3 of the 8 channels of a port (GENESIS has 8 ports). In Fig. 4.4 a representation of GENESIS. For the tests it has been chosen a sampling frequency of 1MHz. A computer interacts with the DAS through Perception, a software that allows to set some configurations of the data acquisition system and register easily the data in different formats. Having chosen the amplitude of the input signal equal to 0.7V, it has been set to 5V the span range for the Input, Raw Output, Low Pass Output and to 20V for the High Pass Output.

In the end of the paragraph it's sketched the whole setup used for this test (Fig. 4.5).

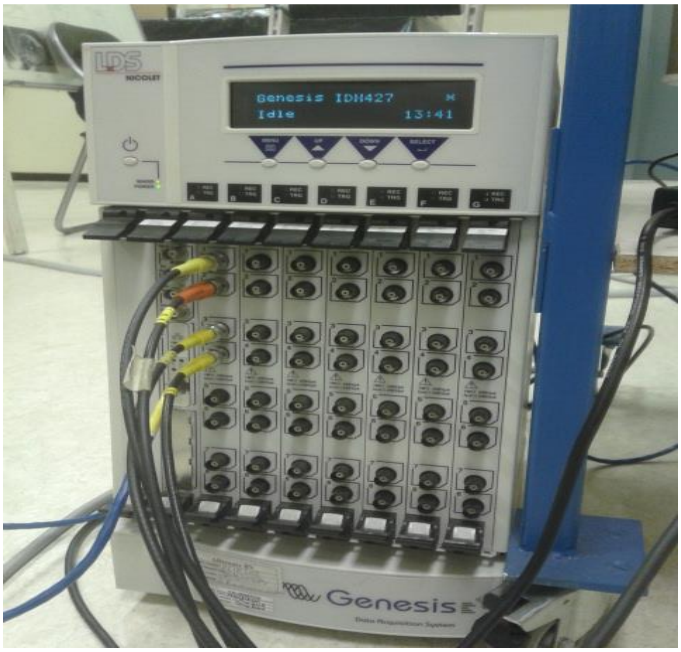

***Figure 4.4**: GENESIS data acquisition system. It has 8 ports, each provided with 8 channels*

4.1.1.4 Analysed frequencies

According to Nyquist theorem, the sampling frequency must be higher than twice the maximum frequency of the analysed signal. Having set the sampling frequency to 1MHz the range of the possible frequencies analysable is 0-500000Hz. For these test was sufficient to test the filter box in a range 5-200000Hz, along 20 points. The frequencies range to be analysed was chosen to be equi-spaced in the logarithmic scale. Being L=5 the lowest frequency, U=200000 the highest one and n = 20 the number of frequencies, it was found the factor k used to find all the equi-spaced frequencies in the logarithmic scale:

$$k = \left(\frac{U}{L}\right)^{\frac{1}{1-n}} \tag{4.1}$$

$$f(n) = f(n-1) * k \tag{4.2}$$

In this list of frequencies were added also values at 100 Hz, 600Hz, 900 (the cut-off frequencies of the filters) and the value at 0 Hz (actually in the test it has been

sent a square wave at 0,1 Hz). In the following table is reported also the File name which has been used to name the txt file later used in Matlab.

Approx. Frequency [Hz]	Periods [ms]	File name (number)
5	200	001
9	114.502	002
15	65.5545	003
27	37.53089	004
47	21.48697	005
81	12.30159	006
100	10	007
142	7.042	008
248	4.032127	009
433	2.30845	010
600	1.6666	011
757	1.32162	012
900	1.11111	013
1322	0.756646	014
2308	0.43319	015
4032	0.248008	016
7043	0.14198	017
12302	0.08129	018
21487	0.0465	019
37531	0.0266	020
65555	0.01525	021
114503	0.0087	022
200000	0.005	023
0.1(square wave)	-	024

***Table 4.1**: Range of frequencies analysed for the test of the filter boxes*

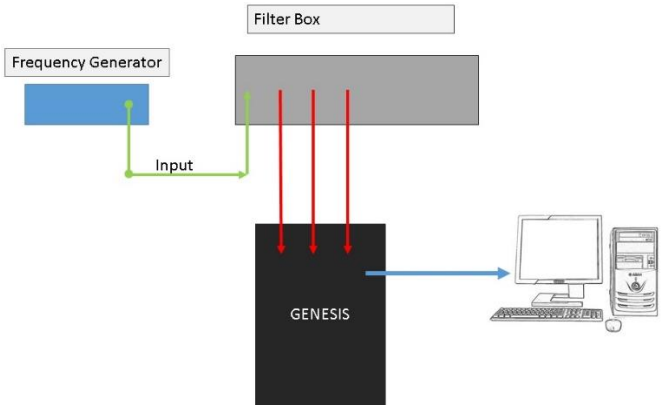

Figure 4.5: Experimental setup for filter boxes tests.

4.1.2 Experimental Procedure to test Filter Box

Once the experimental setup was settled it was possible to test the known input signals in the filter box. The frequency generator was set to the desired shape/frequency; the input and outputs responses of the filter box were displayed in Perception. Using a trigger it was possible to acquire data with the required options chosen in the software.

The data have been registered as .txt files like the one showed in the following image (Fig 4.6). The first column shows the vector of times; the other columns show respectively the values of the Input, Raw, Low-Pass and High-Pass outputs in each sampling instant. Each columns has one million points.

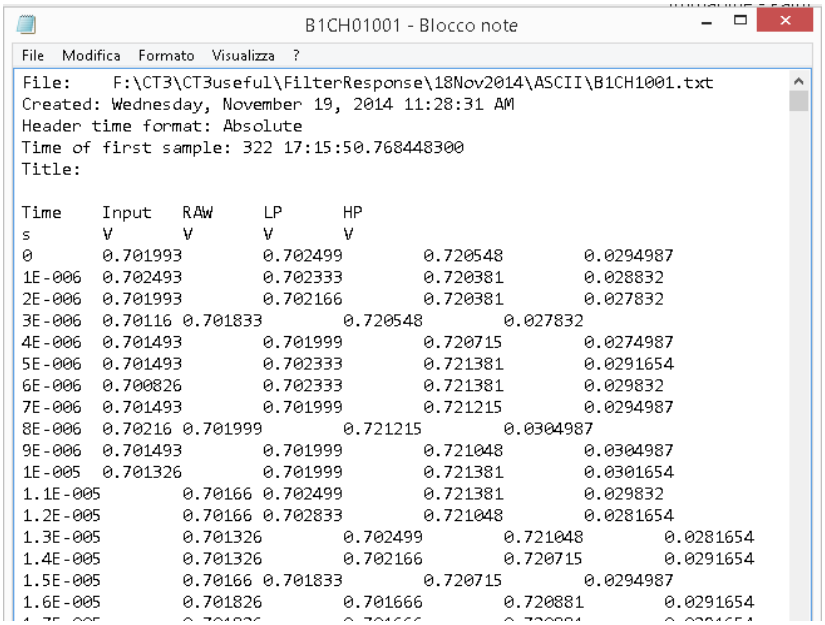

***Figure 4.6**: The output of the acquisition obtained with Perception. The first columns is the sampling time; the other 4 columns are referred to the channels of the filter box*

Each channel was tested for all the 24 frequencies (see Table 4.1); the same work was done for all the channels of both filter boxes. Each .txt file was named in the formula B(number)CH(number) number (example B1CH1001) in order to be read by the automatized Matlab code.

4.1.3 Post-processing of data

The aim of this test was to understand the behaviour of the analogue filters using some known inputs. Basically, for each frequency, the input signal was compared to the output and it was defined the Gain and the Phase at that frequency. The Gain is defined as the ratio of the amplitude of the output over the amplitude of the input A_{out}/A_{in}; it's quite common to express the Gain in dB and then plot the results on a logarithmic scale using this formula:

$$G(dB) = 20log\left(\frac{A_{out}}{A_{in}}\right) \tag{4.3}$$

The phase shift is defined as the delay of the output signal respect to the input one. It is usually expressed in seconds [s] or radians. It is possible to convert the unit using the following formula:

$$1\ [\text{rad}] = \frac{T}{2\pi}\ [\text{s}] \tag{4.4}$$

Being T the period of the signal. It is not complicated to find the gain and the phase shift of an analogue signal (for example a sinus): facing this problem with digital signals, as in our case, is much more complicate especially if this process has to be done in an automatized routine for generic input signals. In Fig. 4.7 is possible to see a digitalised sinusoidal signal. It is a vector of 1 million points: it looks like a normal analogue signal at first sight; but it's a signal affected by a certain level of noise as can be seen zooming on the image.

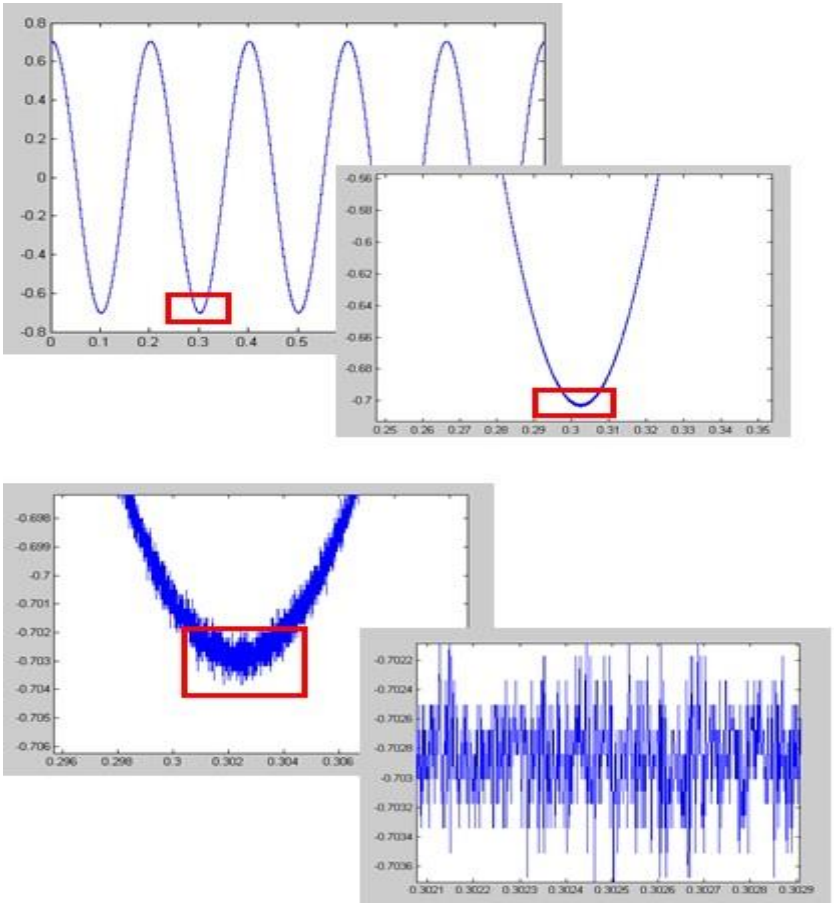

***Figure 4.7**: The acquired sinusoidal signal is affected by noise that has to be dealt correctle.*

For this reason it's necessary to write a code which is able to detect the absolute peaks in the signal or find the zero values in the time vector. In the next paragraphs are quickly shown two processes used to compute frequency, gain and phase shift of the signals.

4.1.3.1 Code 1

In order to find the frequency and the gain of the signal this code finds the zeros of the function and their position along the time axis. Knowing this last parameter it is possible to go back to the period of the signal and obtain the frequency. The position of zeros in time axis were easily find with a *for cycle* in the whole length of the signal checking the following condition:

$$f(k) * f(k+1) < 0 \tag{4.5}$$

being k the index of the for cycle. The problem is that the digitalised signal is composed by "clouds" of zeros as can be seen in Fig. 4.8. The code was developed in a way to find a mean value in every "zero-cloud" and then obtain the period of the signal as the mean of periods between two consecutively zeros.

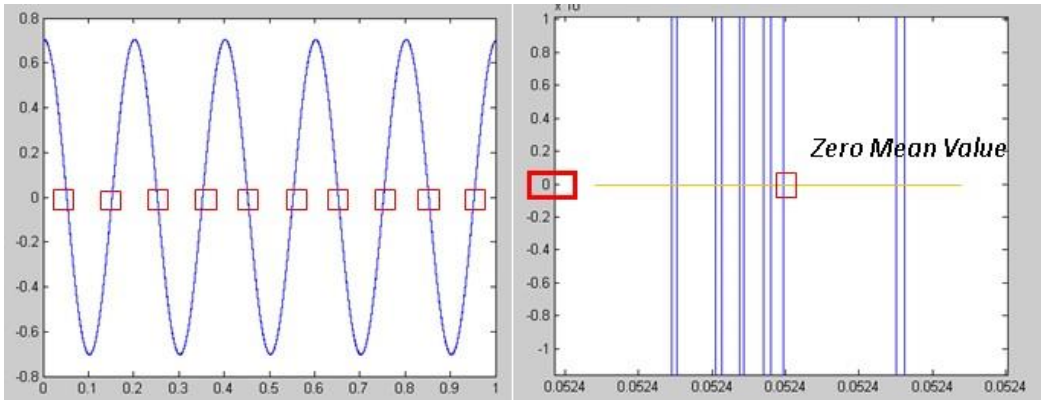

***Figure 4.8**: The sinusoidal signal crosses the zero several times generating a 'zero cloud'. It has been chosen to find the zero as the mean of these zero values.*

Once the zero positions were found, it was easy to apply the function *max(-)* in Matlab, find the mean maximum value and compare it with the mean maximum of the input signal thus obtaining the gain.

The phase shift was obtained using a mathematic tool, the cross correlation. The cross correlation is a measure of the similarity of two waveforms, f(t) and g(t), as a function of the time-lag τ applied to one of them:

$$(f * g)(\tau) = \int_{-\infty}^{\infty} f^*(t) g(t+\tau) dt \tag{4.6}$$

where *f** denotes the complex conjugate of *f*. In the code they were used the input and output vectors of the signal.

```
[r,lags] = xcorr(Input_s,Output_s);
```
(4.7)

The bigger is the value $(f * g)(\tau)$, `r` in the code, the more similar are the two functions. The biggest value of $(f * g)(\tau)$, `r(k)`, it's obtained when the two signals overlap. The phase shift between the two signal is obtained in this condition: this is equal to τ (or `lags(k)` in Matlab). In Fig. 4.9 an example of the cross-correlation between two signals.

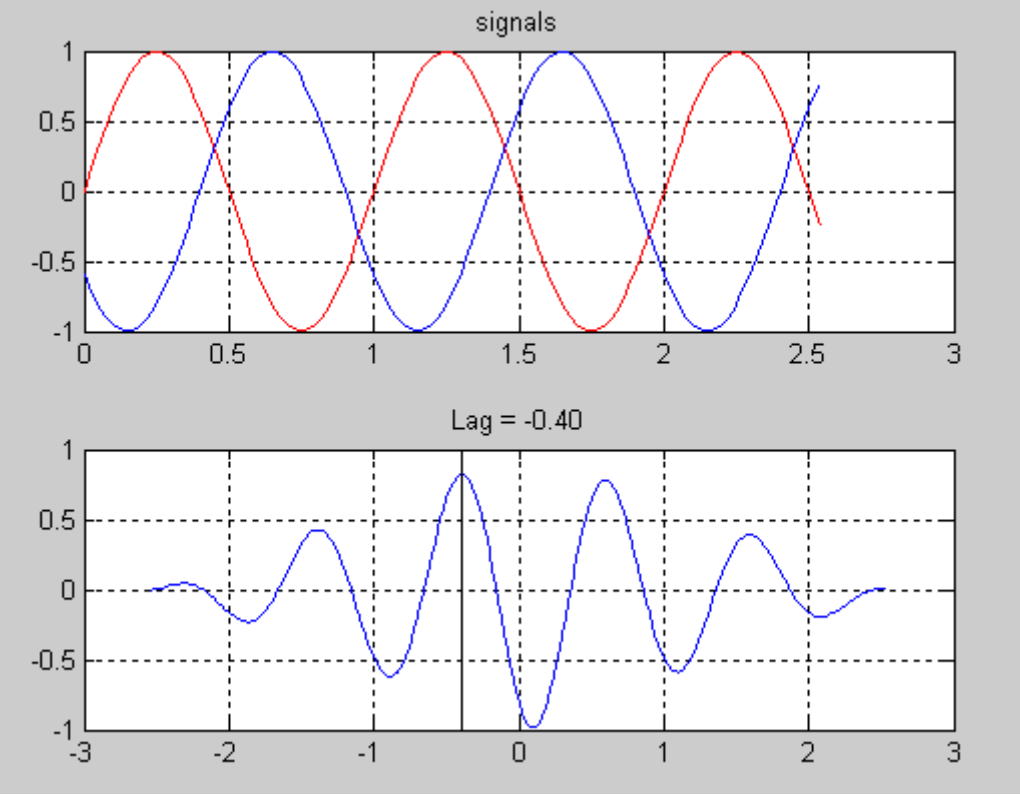

Figure 4.9: *An example of cross-correlation*

The code was working correctly for frequencies up to 65000 Hz. It was not possible to obtain frequency, gain and phase shift for the last two frequencies 114000 and 200000Hz because of the high computational cost.

4.1.3.2 Code 2

To get the results for all the frequencies the code was re-written using some other tools to simplify the computations. Before starting any computation the signal was filtered from the noise using the function 'smooth' in Matlab. The following picture shows how the signal appears after this filtering:

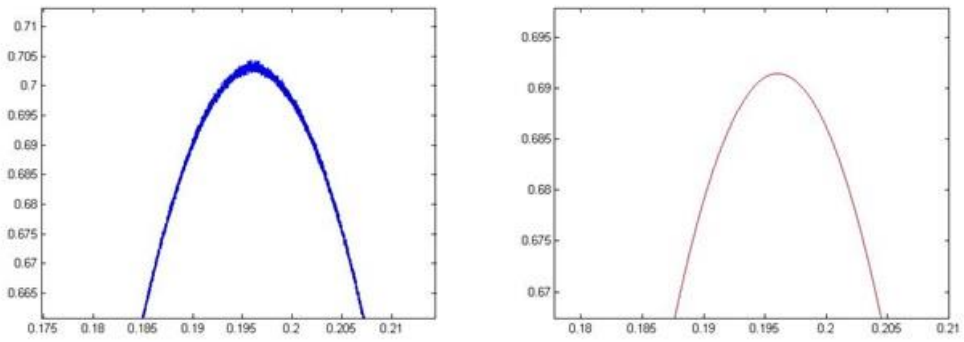

***Figure 4.10**: The signal before and after having used the 'smooth' function in Matlab*

The frequency was computed easily using the Fourier Fast Transform on the signal: the frequency was founds as the maximum of the modulus of this vector. The results of an FFT is shown in Fig. 4.11.

The Gain was easily computed using a function in Matlab called 'peakdet': it is possible to obtain the maxima and their positions in the input vector simply setting the input vector and a threshold value between two peaks as input of the function. Once obtained the value of the peaks, it was done the mean among them and this value was divided by the mean value of the peaks of the input signal.

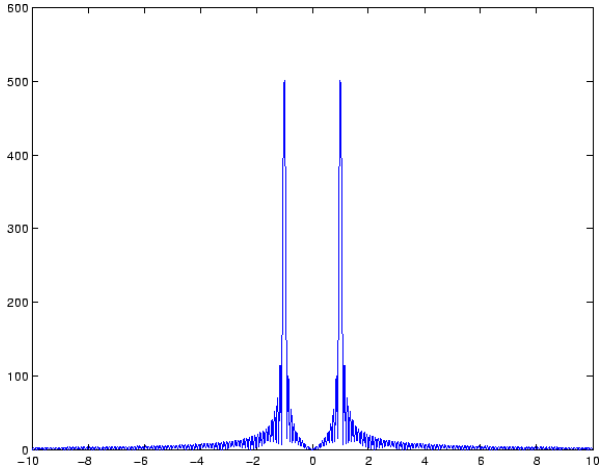

***Figure 4.11**: The Fast Fourier Transfrom of a signal allows to find the frequency content of a signal.*

The phase shift was computed “manually” subtracting the position values of maxima for the output and input signals and then taking a mean value. This second code was preferred to the other, having a lower computational cost and thus allowing to test the filter box at high frequencies (>100000Hz). In the next paragraph it will be shown the results obtained testing the two filter boxes with this code.

4.1.4 Results

Each channel was tested using this code and it took 15 minutes to compute gain, frequency and phase shift for all the selected range of frequencies (0-200000Hz). This code was preferred respect to the first one because faster and it allowed to compute the behaviour of the box also at high frequencies. The results have been grouped in different graphics: in the following pictures the channels will be indicated by the abbreviation F-B-C which stands for filter, board, channel followed by the number.

GAIN: High-Pass channel

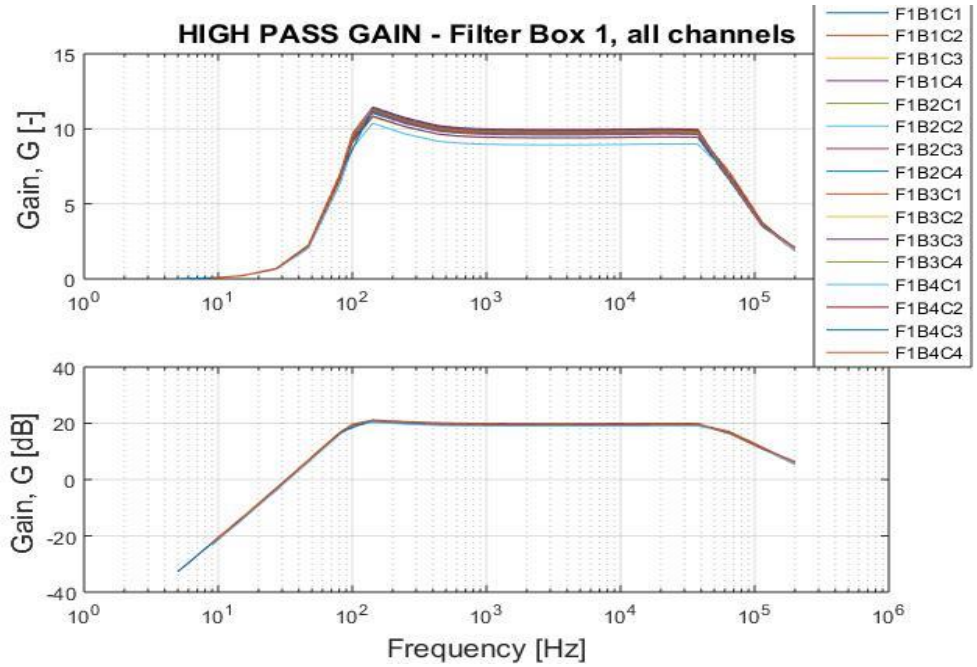

Figure 4.12

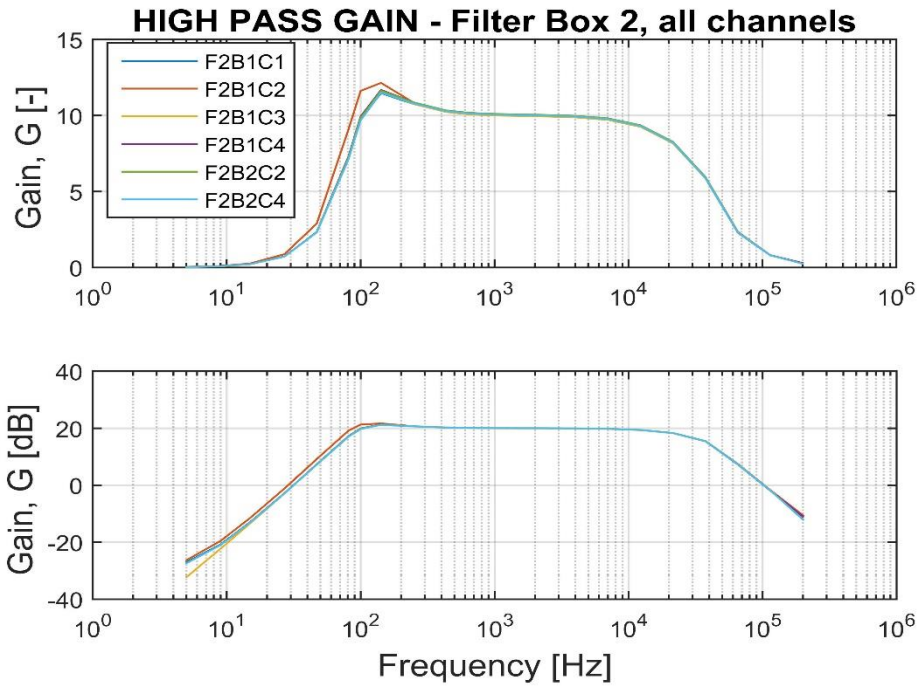

Figure 4.13

GAIN: Low-Pass channel

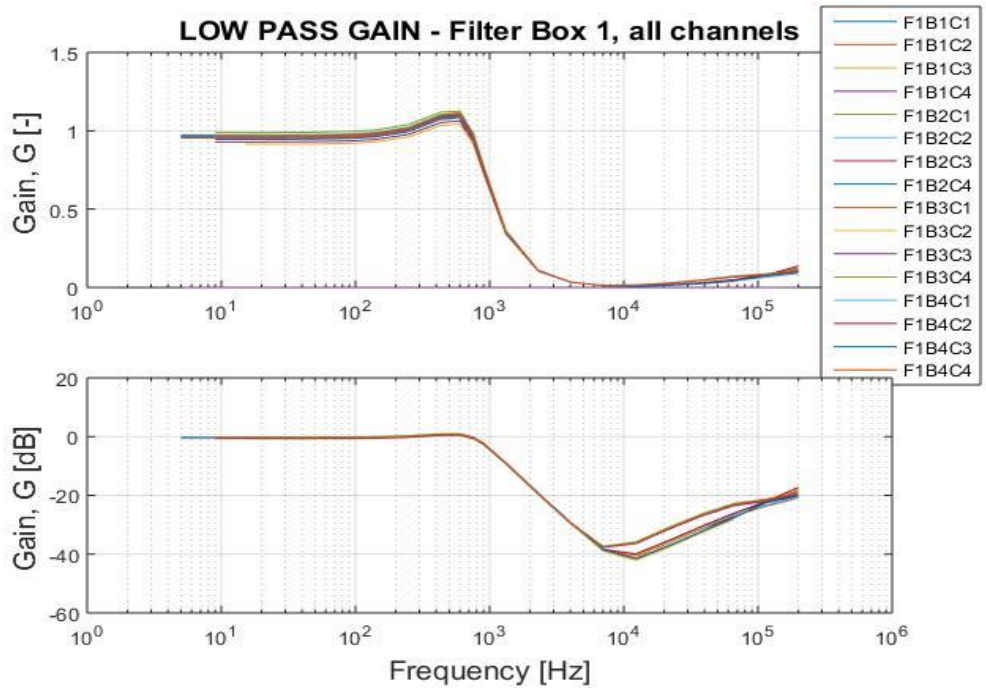

Figure 4.14

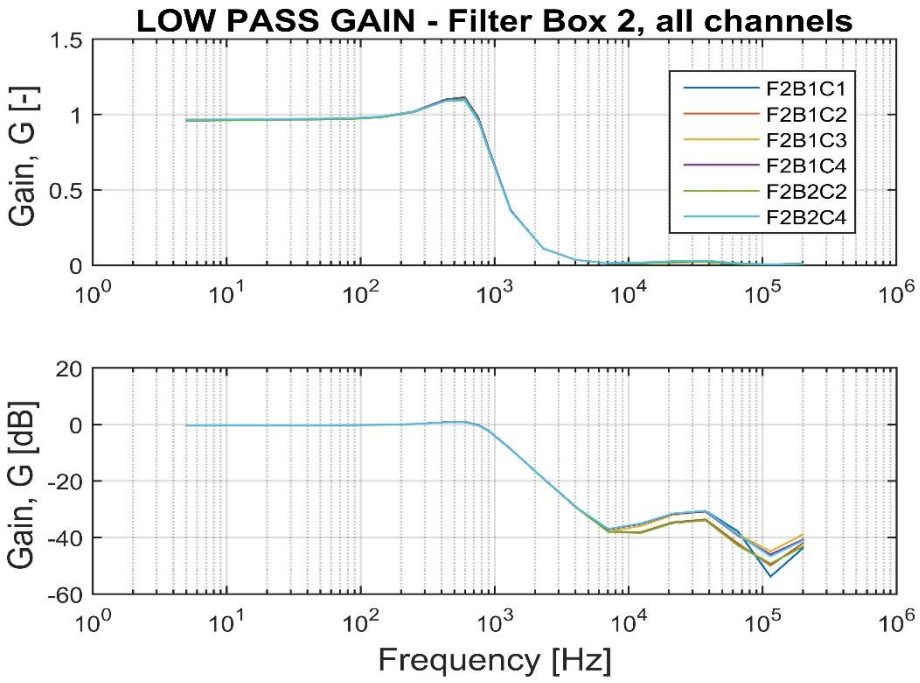

Figure 4.15

GAIN: Raw channel

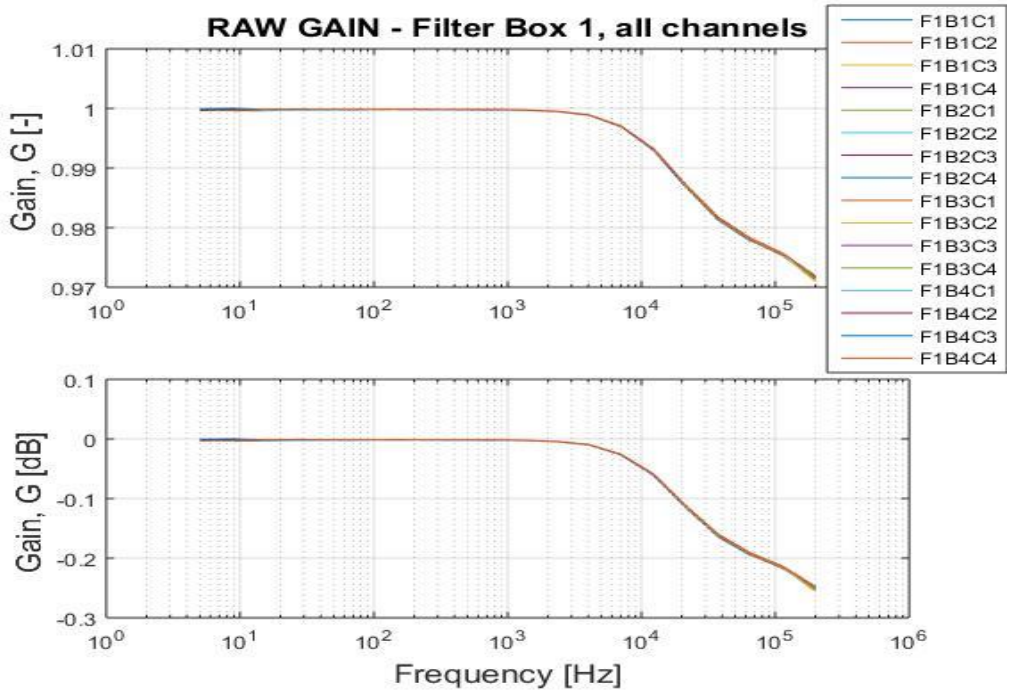

Figure 4.16

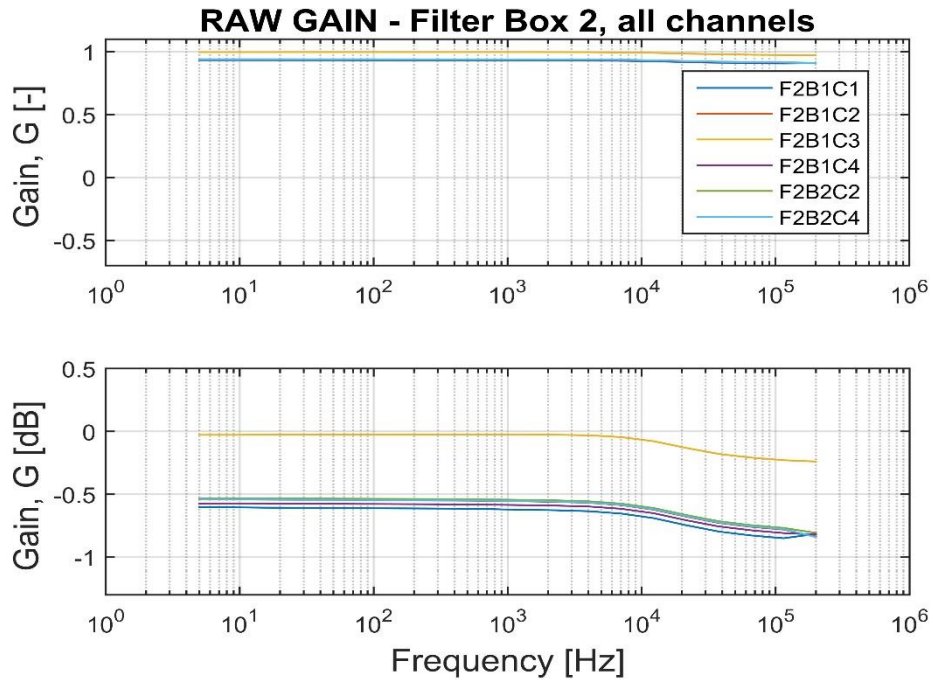

Figure 4.17

In these graphics is represented the gain (absolute and expressed in decibel) of all the channels belonging to the filter box 1 and filter box 2. It can be noticed that, as expected, the high-pass filter (shown in figures 4.12 and 4.13) has a cut-off frequency of 100 Hz as indicated in the box. The gain in the band-pass region is 20dB as was set in the electronic card: the signal is amplified by a factor 10 for frequencies between 100Hz and 12000Hz. Starting from 10000Hz the signal amplitude is attenuated since the filter box is equipped by an internal anti-aliasing filter. Looking the graphics in the bottom, those whose gain is expressed in decibel we can observe that the filter box behaves like a second-order filter: the gain increases by 40 decibel each decade.

The Low-Pass gain is shown in figures 4.14 and figure 4.15. The two filter boxes behaves correctly showing a 0 gain in the band-pass region and a cut-off frequency near 750 Hz as expected. The shape of the gain is different at higher frequencies (>10000 Hz): the gain of the second filter box shows an oscillating tendency while the gain of the first box increase monotonically after 10000Hz. The Low-Pass channels behave like a second-order filter too: the gain decreases by 40 dB each decade.

The Raw channel is the output channel that theoretically should reproduce the input signal with no phase shift and gain equal to one. As mentioned before we can observe clearly in these graphics that exists an internal low-pass anti-aliasing filter for frequencies higher than 10000Hz (the gain starts decreasing slightly before that value). The cutting frequency and the decreasing slope of the filter is visible in the graphics of the gain expressed in decibels (figures 4.16 and 4.17).

Channel three in board three in the first filter box is broken as can be seen in the related graphic: the gain curve is flat for all the frequencies.

Phase: High-Pass channel

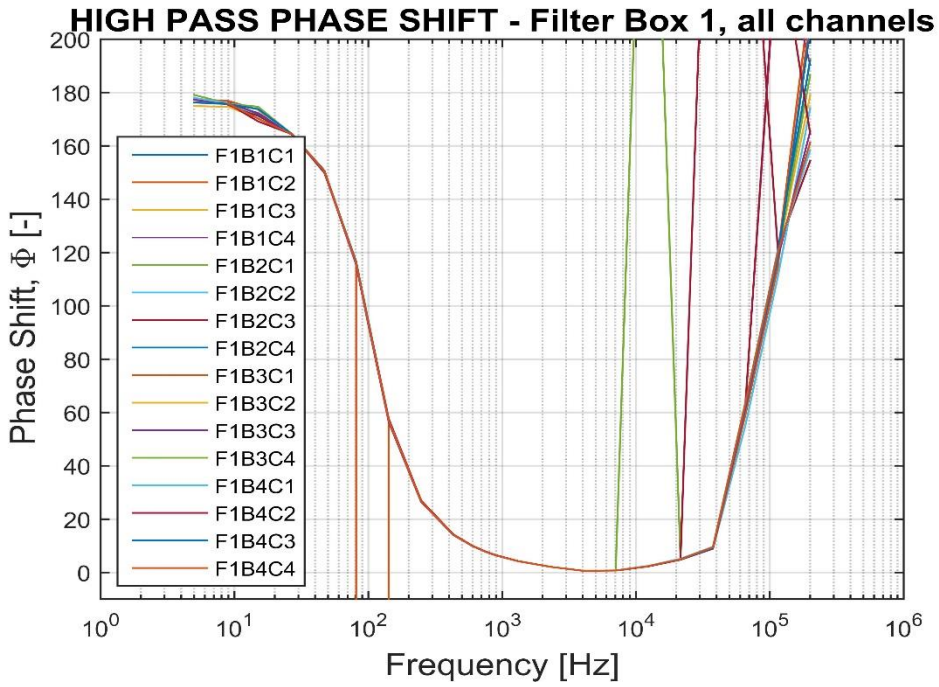

Figure 4.18

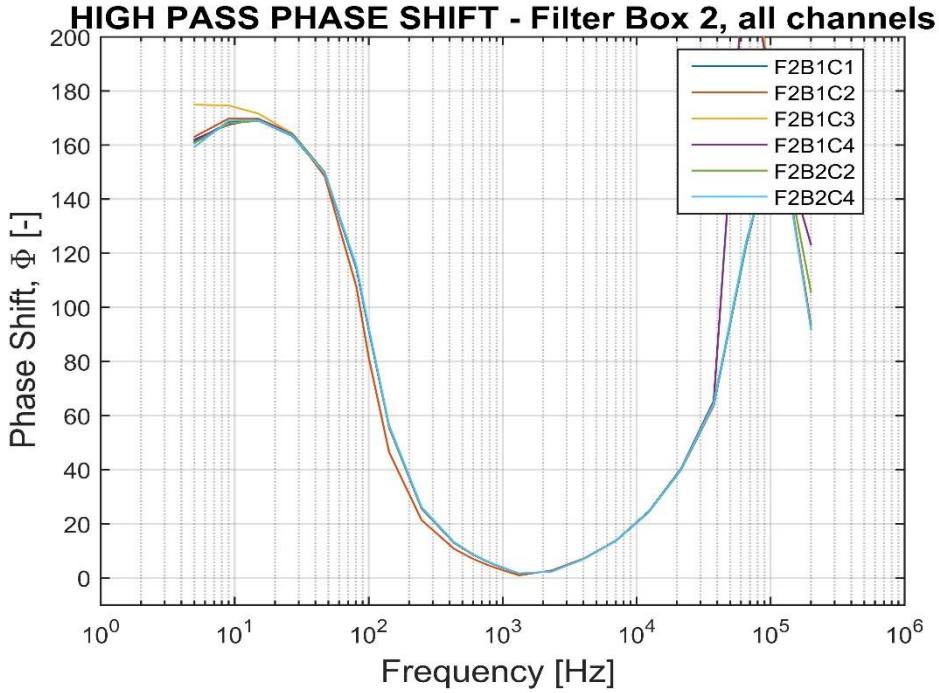

Figure 4.19

Phase: Low-Pass channel

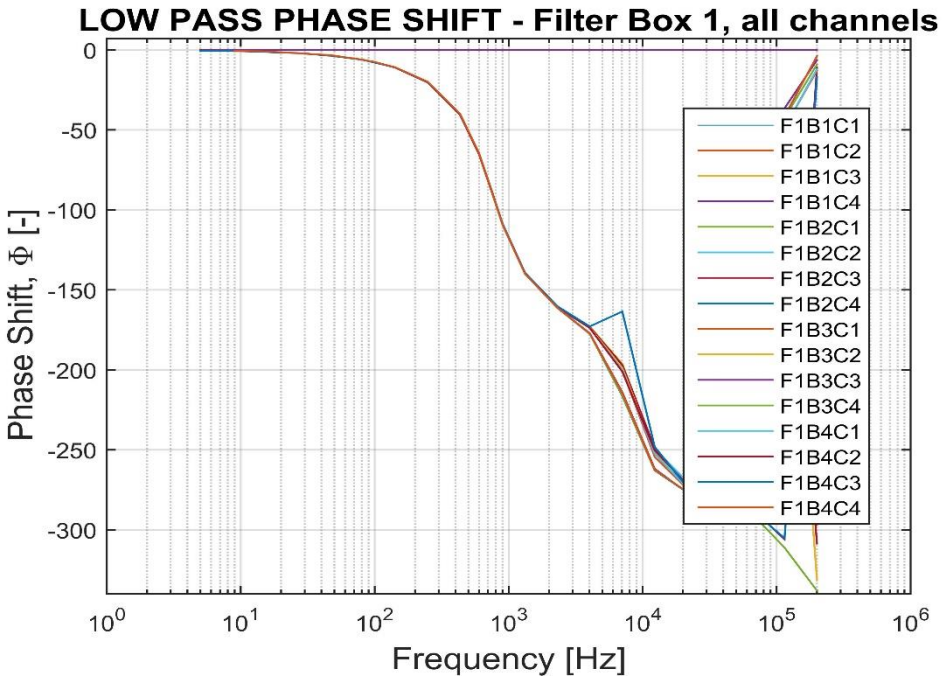

Figure 4.20

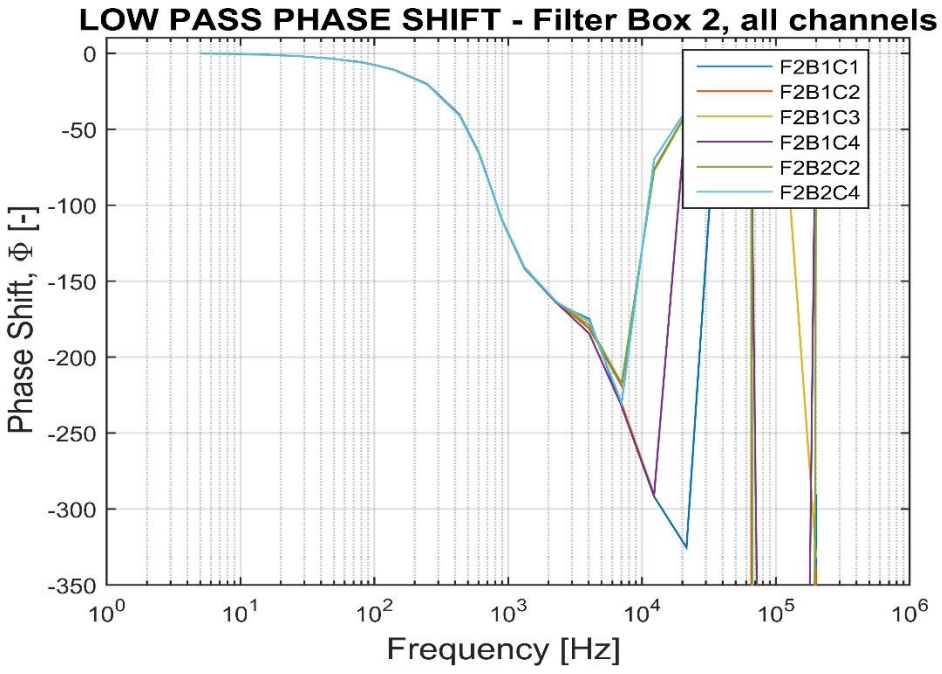

Figure 4.21

PHASE: Raw channel

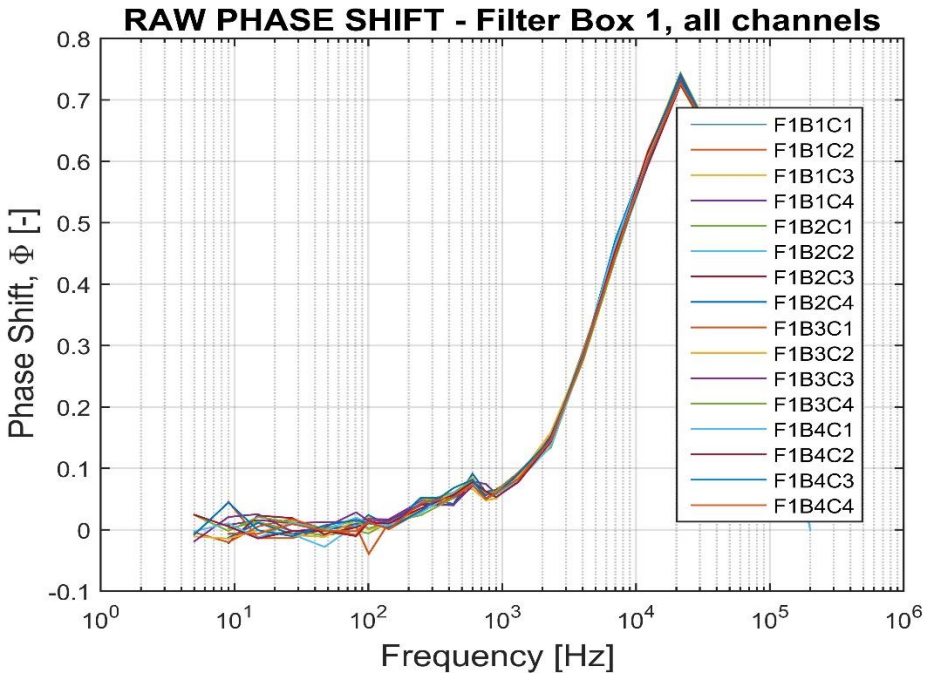

Figure 4.22

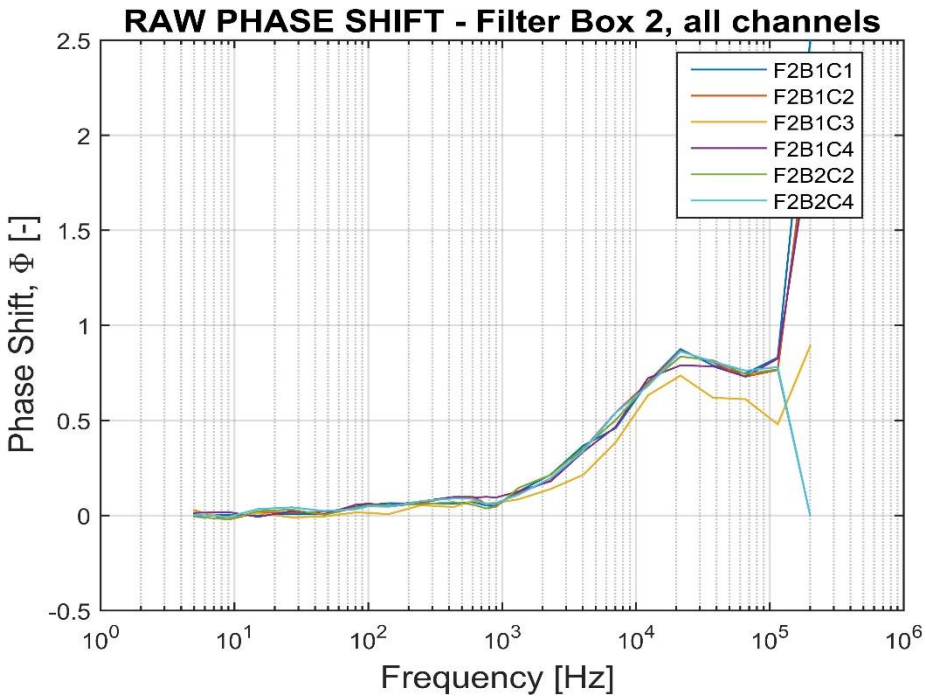

Figure 4.23

The phase shift of all the channels has been plotted grouping them as done in the previous graphics. It can be noticed that the shape of the curve agrees with the results obtained previously for the gain plot: the filter boxes behave like a second order filter. We can observe that the output signal of the high pass channel is shifted by 180 degrees at low frequencies respect to the input one; increasing the frequency the phase shift decreases approaching zero values. The high pass channel of the second filter box (Fig. 4.20) has a shape slightly different from that one the previous images: the phase shift starts at values lower than 180 degrees at low frequencies while we can observe that, after 1200 Hz, the phase shift tend to increase again.

For all the boxes we notice that the last three values (at frequencies 65555, 114503 and 200000 Hz) are completely wrong: this can be explained always considering that the filter box has an internal anti-aliasing filter after 10KHz.

There are some values of phase shift at medium frequencies which are manifestly wrong: the explanation has to be found inside the code written in Matlab. The code computes the phase shift as the difference between the position of two contiguous peaks (of the output and input signal, respectively). This difference is extended to all the peaks and a mean value is obtained (Fig. 4.18). The code has been written with a correction that considers only contiguous peaks: nevertheless this is not working perfectly and sometimes the code subtract the position of non-contiguous peaks causing a not-acceptable value of phase shift.

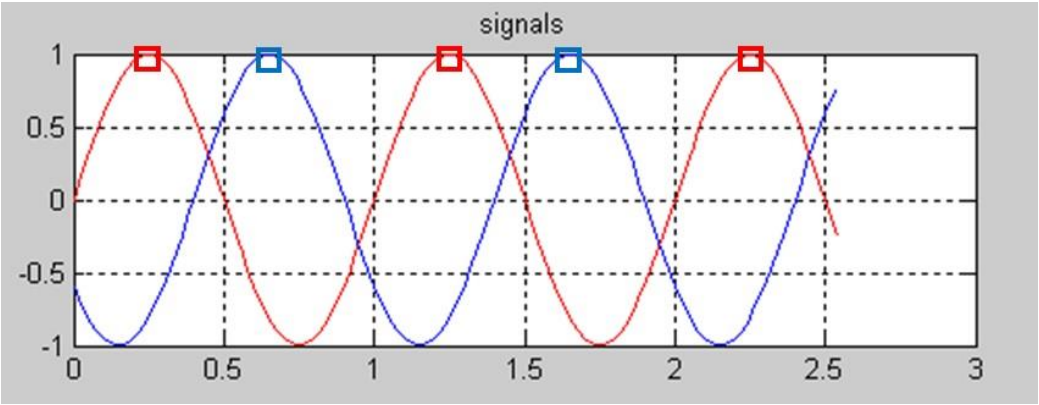

Figure 4.24: *The phase shift is obtained as the difference of the time position of two contiguous peaks.*

The graphics of the phase shift for the low pass channels show a trend which is different from the expected one: the filter box does not behave like a second order low pass filter as we expected from the gain plots. The phase shift starts with

values near 0° and decreases up to -300°/-310° rising the frequencies. The last three values of phase shift for all the boards show a manifestly wrong trend due to the internal anti-aliasing filter of the box. The results of certain channels relative to the second filter box are quite rather inaccurate for frequencies higher than 4032 Hz. In any case it is possible to extrapolate the shape of the filter obtaining reasonable values of phase shift.

The phase shift in the raw channel should be equal to zero for all the frequencies: nevertheless, as we can see, this value slightly increases (values lower than 1°) at higher frequencies. The results related to the second box show some mild differences among the six channels.

4.1.5 Conclusions

The tests with known input signals have shown some important results useful to understand the behaviour of filter boxes. It has been verified the type of filter used, its cut-off frequency and its band-pass. These data processing have led to some important conclusions on the nature of the filter:

- The filter boxes have an internal anti-aliasing filter, with a cut-off frequency positioned at 10kHZ.
- The High-Pass channels are second order high-pass filters: the signal is attenuated by 40 decibels each decade for frequencies below the cut-off frequency (100Hz); the phase starts at 180° and decreases to 0° at high frequencies.
- The Low-Pass channels are filters whose cut-off frequency is at 750Hz: for values higher than $f_{cut\text{-}off}$ the signal is attenuated by 40 decibel each decade. The phase starts at 0° and decreases up to -310°/-320° for frequencies higher than 10KHz.
- The Raw channels behaves correctly reproducing almost perfectly the input signal: a slight change of phase is evidenced for high frequencies.

4.2 Signal compensation

The experiments carried out in the CT3 facility have a short duration (~0.5s). The compressed air flows through the turbine which rotates at a fixed velocity: the phenomena analysed in the turbine are unsteady since the flow is extremely fast and complicated aerodynamic and thermodynamic mechanisms intervene in a reduced fraction of time. An acceptable experimental analysis can be obtained only with instrumentations able to sense high frequency fluctuations.

Restarting from the theory described in chapter 3, it has been done a study on the dynamic behaviour of the cold wire. The calibration conducted in the oven and inside the heated jet (see Chapter 3) has brought to a relation of the electrical output of the probe and the stationary physical input (temperature in this case). The results are valid only for a steady analysis since the output has been taken in steady conditions.

The dynamic analysis is much more complicated and has to be done using a physical model which describes the mechanisms occurring close to the wire. Later, this mathematical approach has to be confirmed by experimental tests to prove the validity of the model.

In this paragraph it will be explained in detail how it has been possible to compensate the signal of the cold wire through its transfer function. The compensation has been done following the works done by Dénos [4] and Arwatz [5].

4.2.1 Mathematical description of the problem

High speed flow is characterized by high frequency phenomena: the temperature fluctuation are extremely fast and even the more reliable instruments are not able to follow these variations. The necessity of the numerical compensation stems from the knowledge of the physical limits of a probe to sense high frequency fluctuations. Knowing the characteristics of the probe it is possible to obtain, with certain approximations, a transfer function that mathematically describes the dynamic behaviour of the probe. The raw signal sensed by the probe is “filtered” by the inverse of the transfer function and the compensation is obtained. An example of the compensated signal is shown in Fig. 4.31. The image comes from a step test done by Dénos: it can be noticed the recorded signal (raw signal), the theoretical jet temperature step and the compensated signal.

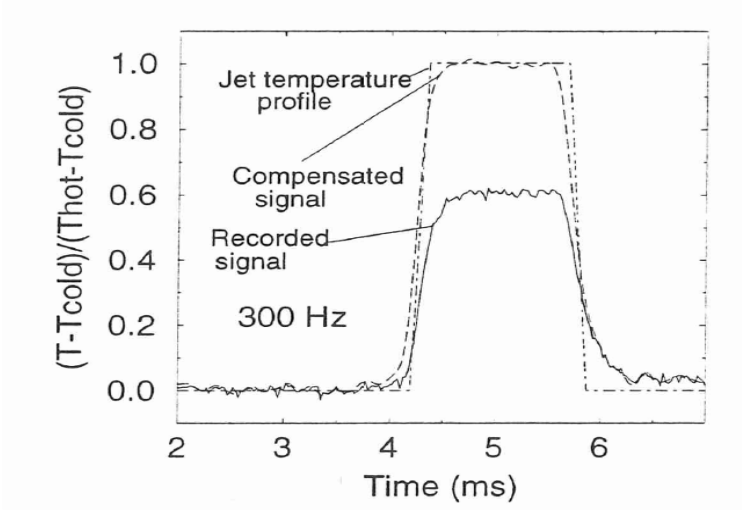

Figure 4.25: *Example of a cold wire step signal: through its transfer function it has been compensated and the result is not so different from the 'real' jet temperature profile.*

4.2.1.1 First order transfer function

The probe has been described mathematically with a first order transfer function. This result stems from an approximation of the heat exchange mechanisms occurring near the wire: temperature variations of the probe during the time depends only on the convective fluxes between air and wire. As a first approximation it has been neglected the heating caused by the Joule effect and the conduction phenomena originated by the prongs that hold the wire. These are some supports usually made of steel whose diameter is several order of magnitude bigger than that one of the wire. A typical configuration (Fig 4.32) of the cold wire considers also some smaller stubs between the wire and the prongs in such a way to reduce conduction phenomena.

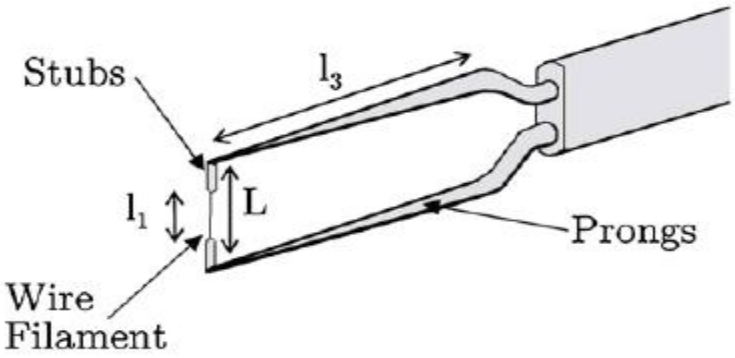

Figure 4.26: *Configuration of a cold wire: the wire filament is hold by stubs which are connected to some stain prongs.*

Getting back to the mathematical description of the cold wire done in chapter 3, the energy balance can be written as follow:

$$V_w \rho_w c_w \frac{\partial T_w}{\partial t} = -hS_w(T_w - T_g) \tag{4.8}$$

$$\tau \frac{\partial T_w}{\partial t} + T_w = f(t) = T_g \tag{4.9}$$

$\tau = \frac{V_w \rho_w c_w}{hS_w} = \frac{d_w \rho_w c_w}{4h}$ being the time constant of the prong, T_g the gas temperature, T_w the wire temperature. It's first order differential equation that can be described easily in the frequency domain by its transfer function

$$H(\omega) = \frac{1}{1 + \mathrm{j}\omega\tau} \tag{4.10}$$

Each transfer function can be described by its gain$|H(\omega)|$ and its phase $\hat{H}(\omega)$. An important parameter of a transfer function is the cut-off frequency defined as the frequency for which $|H(\omega)| = 0.707$. It can be easily computed as follow:

$$f_{cut} = \frac{1}{2\pi\tau} \tag{4.11}$$

The time constant has been computed in chapter 3. It depends on several parameter as can be seen in Eq. (4.12): the Nusselt number (expressed as a function of the Reynolds number) stems from experimental activities that allow to obtain its constants A, B, n.

$$\tau = \frac{{d_w}^2 {\rho_w}^2 c_w}{4k_g \left[A + B\left(\frac{\rho_g v_g d_w}{\mu_g}\right)^n\right]} \tag{4.12}$$

The first order transfer function has been implemented in Matlab considering the input parameter furnished by Dénos in [4]. In detail, it has been considered a

heated jet with velocity $v_g = 25m/s$ and total temperature $T_g = 340K$: the experiment has been done at atmospheric pressure. The density of air has been computed from perfect gas equation, the air being assumed as a perfect gas with R = 287 J/(kg K) and γ=1.4 ; the viscosity μ_g and conductivity k_g of air stem from experimental relations function of the temperature. The data of the wire relative to density and specific heat ratio come from experimental tables relative to tungsten. The constant A,B and n are defined with an experimental correlation that takes into account density and velocity variations. The diameter of the wire is 2.5 μm. All the data are reported in the following table.

Physical quantity	Description/unit	Value
v_g	[m/s]	25
T_{tot}	[K]	340
μ_g	[kg/(m s)]	0,0000217
k_g	[W/(m K)]	0.03
T_s	[K] $T_s = T_{tot} - {v_g}^2/2C_p$	339.8
ρ_g	[kg/m^3] $\rho_g = P/R\,T$	1.0253
d_w	[m]	0.0000025
ρ_w	[kg/m^3]	20000
c_w	[J/(kg K)]	134
A	Intercept of experimental relation Nu(Re)	0.458
B	Slope of experimental relation Nu(Re)	0.345
n	Exponent in experimental relation Nu(Re)	0.45
τ	[s]	0.0001369

***Table 4.2**: Data to compute the first order transfer function*

In order to compute the one first order transfer function the only data that have not been provided were the density of air and the static temperature. As mentioned before, density has been computed with perfect gas equation while the static temperature comes from the steady flow energy equation.

The following figures refer to the gain of the transfer function: the first one has been provided by Dénos in his work while the second one on the right is the transfer function computed with these data in Matlab.

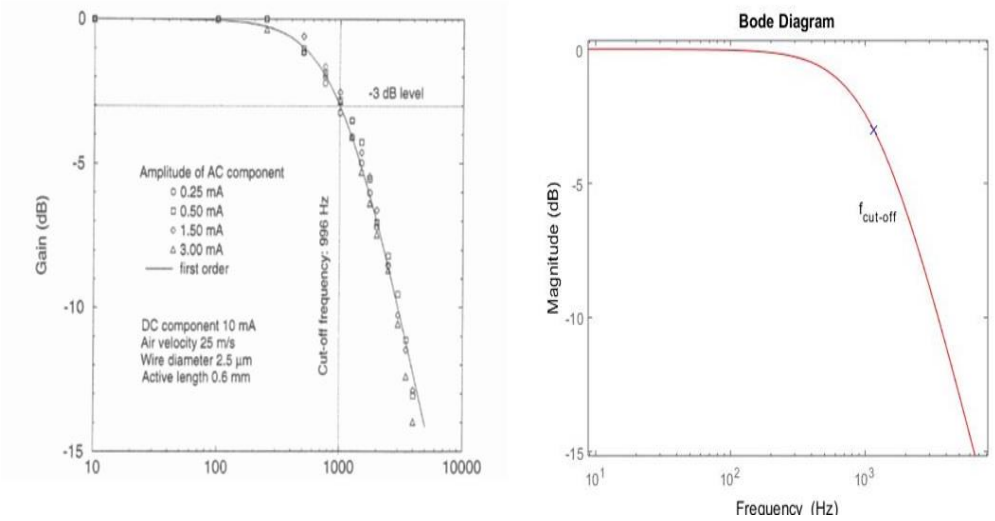

***Figure 4.27**: Comparison of the computed first order transfer function with the one found by Dénos*

The two transfer functions looks like each other: the cut-off frequency found in Matlab, $f_c = 1162Hz$ is not so different from that one found by Dénos ($f_c = 996Hz$). This small difference might be due to some differences in the computation of density or static temperature. The image on the left shows that the transfer function computed by Dénos perfectly fits with experimental data found for a 2.5 µm cold wire tested at 25 m/s. For this test Dénos used a frequency generator in order to test the dynamic response of the wire with a known input (in this case an input AC current was superimposed to a 10mA DC current). The experimental part to determine the dynamic behaviour of the wire has not been done due to a lack of time and to the risk to break the wire.

4.2.1.2 Two first order transfer function

The main source of inaccuracy of the model previously described is that it does not take into account the conduction phenomena between wire and prongs. Dénos provides a mathematical description of this mechanism dealing with the steady and unsteady case. In the steady condition he considers the prongs with an infinite thermal capacity (the prongs stay at an imposed temperature) while he neglects the Joule effect. The phenomenon is described by the following equation and its boundary conditions:

$$\frac{\partial^2 T_w}{\partial x^2} = \lambda^2 (T_w - T_g) \tag{4.13}$$

$$Q_{cond}\left(x = \frac{l}{2}\right) = 0 \tag{4.14}$$

$$T_w(x = 0) = T_p \tag{4.15}$$

where $\lambda^2 = \frac{4h}{k_w\, d_w}$, T_g is the gas temperature and T_p is the temperature of the prong; x = 0 states one extremity of the wire. This equation has an analytical solution that allows to compute an important parameter used to define the two first order transfer function: this parameter is g, defined as $\frac{T_w(mean)-T_p}{T_g-T_p}$. This value is an index of the heat transferred by convection respect to the whole heat transferred. Once defined g it is possible to implement the transfer function: this is realized as the weighted sum of two first order transfer functions. The first transfer function $H(s)$ is related to the wire and weighted with parameter g (associated with convective phenomena); the other transfer function $Hp(s)$ describes the behaviour of the prong and is weighted with (1-g):

$$G(s) = gH(s) + (1 - g)Hp(s) \tag{4.16}$$

As a consequence also the probe temperature results in a linear combination of the wire and prong temperatures.

The wire first order transfer function has been computed using as input parameters $v_g = 100m/s$, $T_{tot} = 340{,}15K$ and $d_w = 0{,}0000025m$. The time constant τ_w associated to its transfer function is equal to 0,00009227 s.

The prong first order transfer function has been computed using other experimental values. The prong time constant τ_p is defined as follow:

$$\tau_p = \frac{{d_p}^2 \rho_p c_p}{4k_g\left[A_p + B_p\left(\frac{\rho_g v_g L_p}{\mu_g}\right)^{n_p}\right]} \tag{4.17}$$

It's possible to notice that the Reynolds number has been defined respect to L_p, the length of the prong. Moreover, the time constant of the prong has been computed using a different Nusselt number: the correlation used is the one used by Paniagua [3] to describe the Nusselt number of air flowing parallel to a wire. In this case the prong has been assumed as a thicker wire with L_p as length. All the data have been reported in the following table:

Physical quantity	Description/unit	Value
v_g	[m/s]	100
T_{tot}	[K]	340
μ_g	[kg/(m s)]	0,0000217
k_g	[W/(m K)]	0.03
T_s	[K] $T_s = T_{tot} - {v_g}^2/2C_p$	335
ρ_g	[kg/m^3] $\rho_g = P/R\,T$	1.04
d_p	[m]	0.0004
ρ_p	[kg/m^3]	7750
c_p	[J/(kg K)]	452
A_p	Intercept of experimental relation Nu(Re)	0.085
B_p	Slope of experimental relation Nu(Re)	0.009
n_p	Exponent in experimental relation Nu(Re)	0.674
τ_p	[s]	1.0547

***Figure 4.3**: Data used to compute the second order transfer function*

The transfer function obtained with the weighted sum of two first order transfer function is a strictly proper transfer function with degree of denominator higher than that one of numerator (d=2 > n=1). The value of *g* used to compute this transfer function is obtained from an empirical correlation (that will be mentioned later) and it's equal to 0.7522. In Fig. 4.34 it's shown the computed transfer function and the one provided by Dénos computed using three different prong time constants. They differ a little especially for the length of the plateau region (the flat part between the two cut-off frequencies): this might be explained for the different value of *g* used in the formula. Dénos does not provide the value used to compute its transfer function.

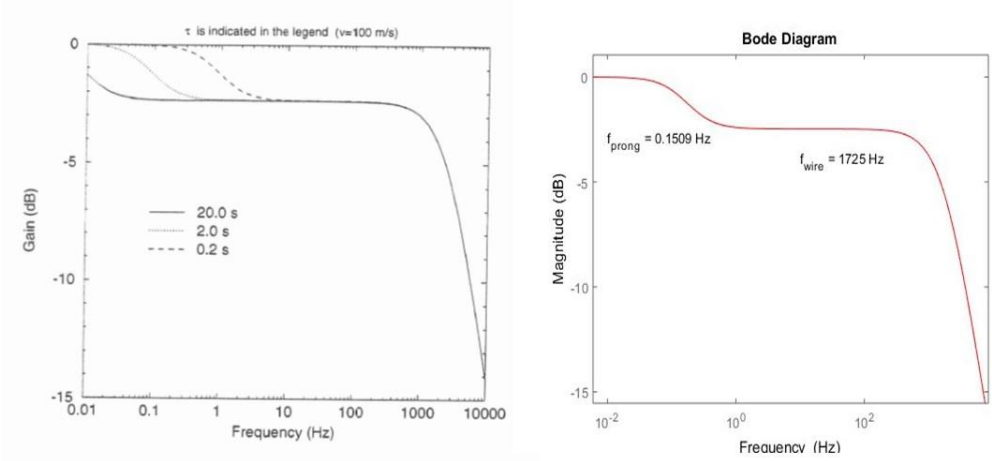

***Figure 4.28**: Comparison between the computed second order transfer function with the one found by Dénos*

4.2.1.3 Five first order transfer function

The accuracy of the physical model can be improved increasing the number of first order transfer functions used to obtain the final one. Following the example of Dénos it has been implemented the code to obtain a five first order transfer function: the first one is referred to the wire while the remaining ones describe the behaviour of the prongs.

The transfer function of the probe obtained by Dénos has been experimentally found with step tests. The time constants and the contributions of each (computed) first order system to the overall signal are adapted so that the system response to the reconstructed step fits the experimental response. Knowing the time constants of the five transfer functions and all the data relative to density, viscosity, conductivity and velocity of air it is possible to obtain the equivalent diameters. These data are reported in table 4.4 also with the values of (g_i) found experimentally.

In the Matlab code it has been chosen always the same wire made of tungsten keeping the characteristics used in the other cases; the heated jet has a total temperature of 340 K and a velocity of 200 m/s. The density of the gas was found with the perfect gas equation considering ambient pressure. The time constant of the wire has been obtained with the same experimental values (*A, B, n*) used in the previous cases for the wire transfer function: its value at 200 m/s is equal to 0.00007237 s.

The other four transfer functions have been written using the data furnished by Dénos (see table 4.5): the Reynolds number have been evaluated respect to the equivalent diameters while the Nusselt number have been defined with a new correlation:

$$Re_i = \frac{\rho_g v_g \, d_{pi}}{\mu_a} \tag{4.18}$$

$$Nu_i = -6{,}4511 + 0{,}438 {Re_i}^{0{,}45} \tag{4.19}$$

$$\tau_{pi} = \frac{{d_{pi}}^2 \rho_p c_p}{4 k_g Nu_i} \tag{4.20}$$

Equivalent diameter [mm]	**Percentage of contribution to $(\mathbf{1-g})_i$**
0.157	43
0.597	20
0.983	33
2.49	4

***Table 4.4**: The values of (1-g) have been found experimentally after having obtained the real transfer function. The equivalent diameters are obtained analitically.*

Knowing the values of the time constants τ_{pi} and τ_w it is possible to write the first order transfer functions in the generic formula and combine them knowing the values of g and $(\mathbf{1-g})_\mathbf{i}$:

$$Hp(s)_i = \frac{1}{1 + s\tau_{pi}} \tag{4.21}$$

$$H(s) = \frac{1}{1 + \tau_w s} \tag{4.22}$$

$$G(s) = gH(s) + \sum_{1}^{4} (1-g)_i Hp(s)_i \tag{4.23}$$

The computed transfer function $G(s)$is represented in figure with the one by Dénos. Nevertheless he does not provides the data of the time constants and the associated cut-off frequencies: it is possible to make only a qualitatively comparison between them.

The value of g stems from an analytical formula provided by Dénos:

$$g = 0.0596Re^{0.45} + 0.570 \qquad (4.23.1)$$

Physical quantity	Description/unit	Value
v_g	[m/s]	200
T_{tot}	[K]	340
μ_g	[kg/(m s)]	0,0000217
k_g	[W/(m K)]	0.03
T_s	[K] $T_s = T_{tot} - {v_g}^2/2C_p$	320
ρ_g	[kg/m^3] $\rho_g = P/R\,T$	1.088
d_{p1}	[m]	0.000157
d_{p2}	[m]	0.000597
d_{p3}	[m]	0.000983
d_{p4}	[m]	0.00249
ρ_p	[kg/m^3]	7750
c_p	[J/(kg K)]	452
A	Intercept of experimental relation Nu(Re)	-6,4511
B	Slope of experimental relation Nu(Re)	0,438
n	Exponent in experimental relation Nu(Re)	0.45
τ_w	[s]	0.00007237
τ_{p1}	[s]	0.0453
τ_{p2}	[s]	0.6555
τ_{p3}	[s]	1.7771
τ_{p4}	[s]	11.403

Table 4.5: *Data used to compute the five first order transfer function.*

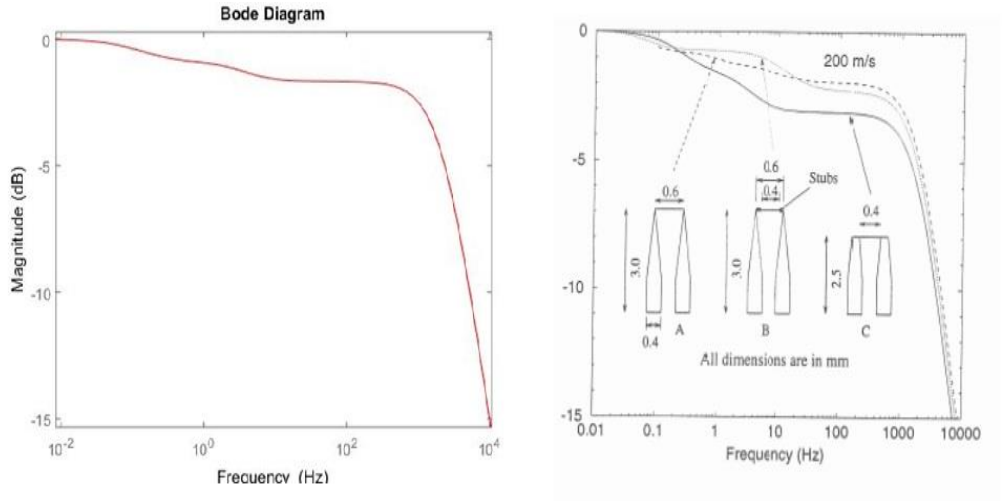

Figure 4.29: *Comparison between the computed five first order transfer function and the one obtained by Dénos*

As can be seen the computed transfer function looks like to the one referred to cold wire type A in Fig. 4.35. The value of cut-off frequency associated to the wire (τ_w) seems correct being for both the graphic around 1500Hz.

This computational part has been done in order to reproduce the work done by Dénos and having some ideas of the order of magnitude of the parameters involved in the dynamic calibration. Next chapter describes the experimental setup used to realize the dynamic calibration and shows the obtained results.

Chapter 5

Experimental activity

The experimental activity was firstly focused in finding the real dynamic model of the cold wire. After having found the transfer functions of the cold wire for different Mach number the cold wire has been tested inside the CT3 with the turbine stage working in transient vacuum-ambient pressure conditions.

5.1 Dynamic calibration of the cold wire

The cold wire has been first calibrated in static conditions as described in chapter 3: it has been tested in natural-convection conditions inside the oven and in forced-convection conditions in a heated jet. As a result we dispose of different calibration coefficients referred to the cold wire at different Mach numbers (table 3.4).

The problem of the instruments working in short duration experiments is that they have to senses physical variations in a small fraction of time. The analysed phenomena are extremely unstable and the static calibration shows its limits. It is necessary to develop a real dynamic model that describes the behaviour of the probe in unsteady conditions and that takes into account all the effects of conduction of prongs. The theoretical work has been described in the second part of chapter 4: according to the description provided by Dénos, we developed three different models for the cold wire using 1,2 and 5 first order transfer functions. It was possible to make qualitatively conclusions but there was no experimental data referred to the cold wire.

For this reasons different tests have been done in order to characterize the probe in unsteady conditions: the cold wire has been tested with step tests realized at different Mach number and different test durations; the data obtained have been processed and it was possible to extract the transfer function of the instrument. The following paragraphs illustrate the experimental procedure used to get these results and the code realized in order to analyse the data.

5.1.1 Experimental setup

For the dynamic calibration it has been chosen the cold wire DAO123A which has two transducers 1A and 2A placed at the extremity and at the centre of the probe, respectively. The tests have been done for both the heads but the transfer function has been computed referring to the results relative to head 1A because they were more accurate. The probe is shown in Fig. 5.1 and the physical characteristics and the coefficients of calibration at different Mach number are reported in Table 5.1.

Probe	**Head**	**Electronics**	**Mach** (0 = oven)	T = a*V + b **a**	**b**	**R^2**
DAO123A	**1A**	Black Box - CH1	0	29,9297205	21,2746	0,99923
			0,05	43,1686293	25,0399	0,99981
			0,2	41,6652308	26,8696	0,99922
			0,3	43,5803606	19,1749	0,99973
	2A	White Box - CH1	0	17,8797016	16,862	0,9993
			0,3	25,4295907	24,203	0,9996

Table 5.1: *Calibration coefficients of the cold wire at different Mach numbers.*

As mentioned before, the tests realized to evaluate the transfer function of the probe consisted in step tests in which the transducer experienced an abruptly change of temperature due to the passage of a hot jet. In order to realize these tests, in addition to the cold wire, two thermocouples and a differential pressure probe were used. The two thermocouples, 2R and 4R, are the same used in the static experiment described in chapter 3; the pressure transducer is the 12V8 that has been calibrated before the test. The coefficients of the calibration are reported in table 5.2.

Figure 5.1: *Cold wire DAO123A.*

Calibration $(P = a*V+b)$	12V8 (relative pressure sensor)
a	0.298707271
b	0.125502363
R^2	0.999999619

Table 5.2: *Calibration coefficients of the pressure transducer 12V8.*

As done for the static jet in the heated jet, also in this case it has been used almost the same experimental setup. The air jet is blown by a nozzle mounted on a support and linked by pipes to a heat exchanger and to the air reservoir. It was possible to increase or decrease the temperature of the air using a handle that changes the current flowing into the resistances of the heat exchanger. The pressure and total temperature were monitored by the 12V8 Sensym transducer

and 4R thermocouple placed inside the nozzle. The thermocouple 2R and the cold wires were mounted close each other using mechanical supports and placed just behind the nozzle exit. In order to realize the temperature steps the two probes (2R and DAO123A) were shielded by a rectangular piece of wood that separated the nozzle from the transducers. In this case the piece of wood was mounted on a support that could run along a guide up and down thus exposing the probes to the hot flow. It was possible to control the moving support through a pneumatic system that made the wooden shield move only pressing a bottom. The nominal velocity of the moving support is 0.5 m/s.

Also for this experiment the two thermocouples have been linked to the amplifiers (2R TC to TU07; 4R TC to TU04); the pressure transducer is the 12V8, powered by a 15V power supply; the cold wire is linked to a Wheatstone bridge which, in turn is linked to a power supply. The head 1A, the one on the bottom, is linked to the black box TUCW3; the head 2A, the one on the middle, is linked to the white box TUCW2.

These four transducers have been connected to a data acquisition system and to a computer in order to use a software and set the acquisition parameters. Before setting the parameters for the acquisition, it has been done a preliminary computation for the expected maximum and minimum values in the experiment. In particular, in order to give an adequate sampling rate it has been easily quantified the test step. Since the nominal velocity of the support is 0.5 m/s and the diameter of the hole of the nozzle is 12 mm, the expected time necessary to characterize the step is 24 ms, which is associated to 41.67Hz. In order to respect the Nyquist criterion, the minimum sampling frequency has to be the double, 83.3 Hz. The modern calculators allow to sample at a far higher frequency rate: the limit to sample with a high rate is that there is less memory to record data and the observation time is reduced.

5.1.2 Step tests

The step tests have been realised at different Mach number setting a temperature difference of 40°C at least. The nominal Mach number decided for the tests are 0.05, 0.1, 0.2 and 0.3. In order to achieve the correct Mach number it must be set the total pressure value in the air reservoir which is computed with the following formula:

$$P_{tot} = P_s \left[1 + \left(\frac{\gamma - 1}{2}\right) M^2\right]^{\frac{\gamma}{\gamma-1}} \qquad (5.1)$$

Being P_s the ambient static pressure and $\gamma = 1.4$. The value was displayed in volt in a multimeter linked to the pressure transducer 12V8 and the related value in bar was obtained using the calibration coefficients. Once the temperature of the air inside the nozzle reached the desired value, it was possible to start the experiments. The experiments should have been realized at constant ΔT in the four different tests at different Mach numbers: nevertheless the heating system is rather simple and it was not possible to set the temperature with accuracy.

In Fig. 5.2 it is possible to see the results from a step test at Mach number 0.05and jet-total temperature of about 60°C when the head 1A is tested. In the figure the signals are displayed in Celsius degrees since the calibration coefficients have been applied. In this case we used the coefficients obtained in static conditions in the oven test for the 2R (grees), 4R (red) and cold wire (blue) outputs. The 2R thermocouple and the cold wire show the same temperature in the initial phase before the step.

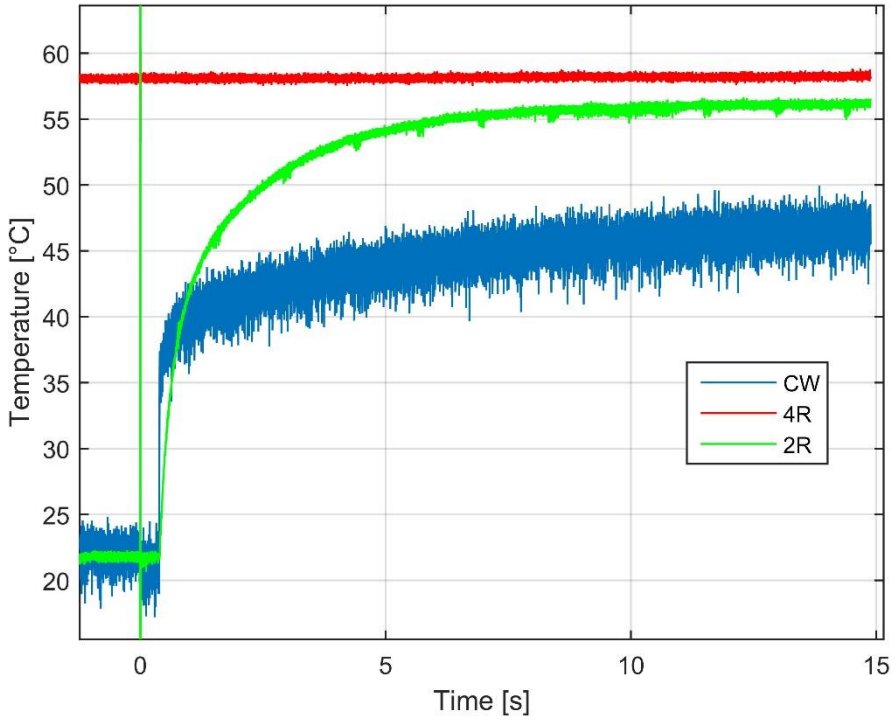

***Figure 5.2**: Step test: the electrical outputs of the 4R (red), 2R (green) and 1A (blues) have been converted into degrees using the calibration coefficients obtained in the still air test (Mach = 0).*

The test has been done at Mach 0.05 and the calibration coefficients of the cold wire at that velocity are rather different from those obtained in the oven at Mach 0 (see table. 5.1). The electrical signal of the cold wire has been converted in degrees with the coefficients obtained in the calibration at Mach 0.05 keeping the same coefficients for the signals of 2R and 4R thermocouples (coming from a static calibration in natural convective conditions, i.e. Mach 0). The resulting temperature curves are displayed in Fig 5.3. In this case, in the initial phase at constant temperature, the 2R and cold wire transducers show a different temperature: this difference is due to the use of calibration coefficients coming from two different type of conditions (natural and forced convections)

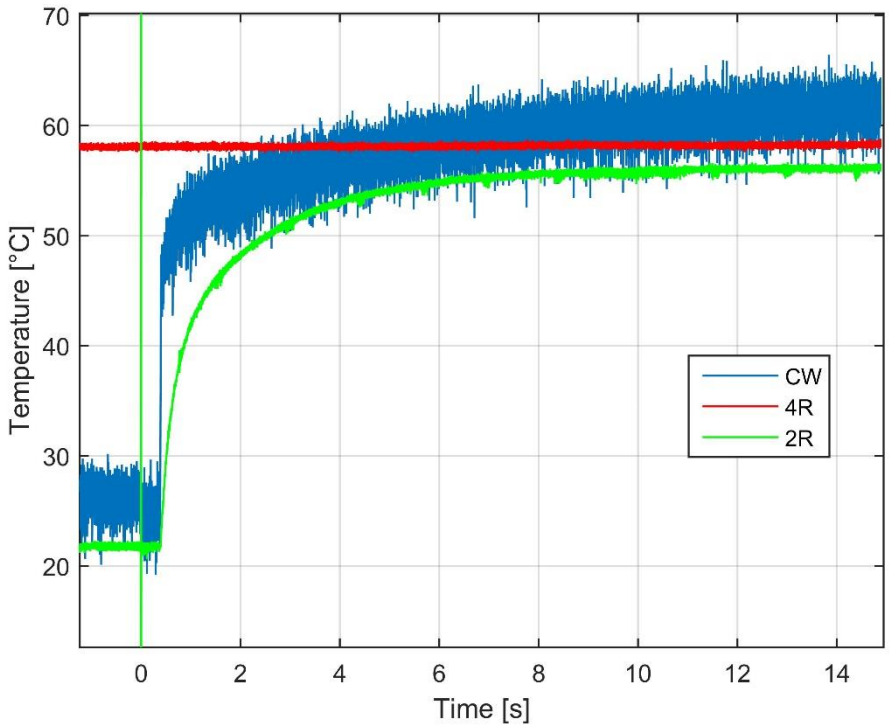

***Figure 5.3**: Step test: the electrical outputs of the 4R (red), 2R (green) have been converted into degrees using the calibration coefficients obtained in the still air test (Mach = 0); the cold wire output (blue) has been converted with calibration coefficients obtained in a test at Mach = 0.05.*

Nevertheless it has been decided to use these last coefficients (referring to the forced convection) subtracting the temperature shift existing between the two curves and obtaining the results depicted in the following figure.

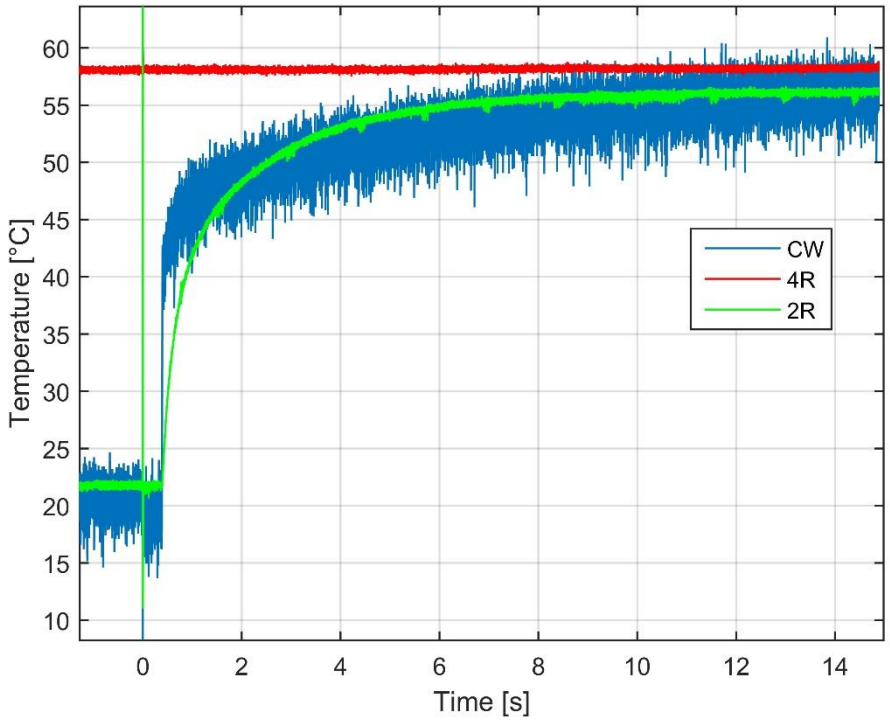

***Figure 5.4**: For all the step tests it has been decided to use the static calibration coefficients at Mach=0 for the 2R and 4R thermocouples. The cold wire output has been modified with coefficients of calibration relative to the correct Mach number subtracting a shift of temperature.*

The signal, especially the one of the cold wire, is extremely noisy: before doing any qualitative analysis it has been cleaned using a digital low pass filter. The high peaks observed at around 0 seconds are due to the drop of electric current occurring when the bottom controlling the shield movement is pressed.

5.1.2.1 First step test

A first step test has been done using a sampling frequency of 8000Hz and an observation time of 8 seconds. In the following pictures it has been plotted the cold wire signal relative to head 1A (filtered and cleaned from the spurious peaks), the 2R and 4R signals in function of time for different Mach numbers. As mentioned before, due to the inaccuracy of the heating system it was not possible to set easily the step temperature to a fixed value in the four tests. The cold wire signal has been filtered with a Butterworth filter of the fourth order and a cut-off frequency of 10Hz.

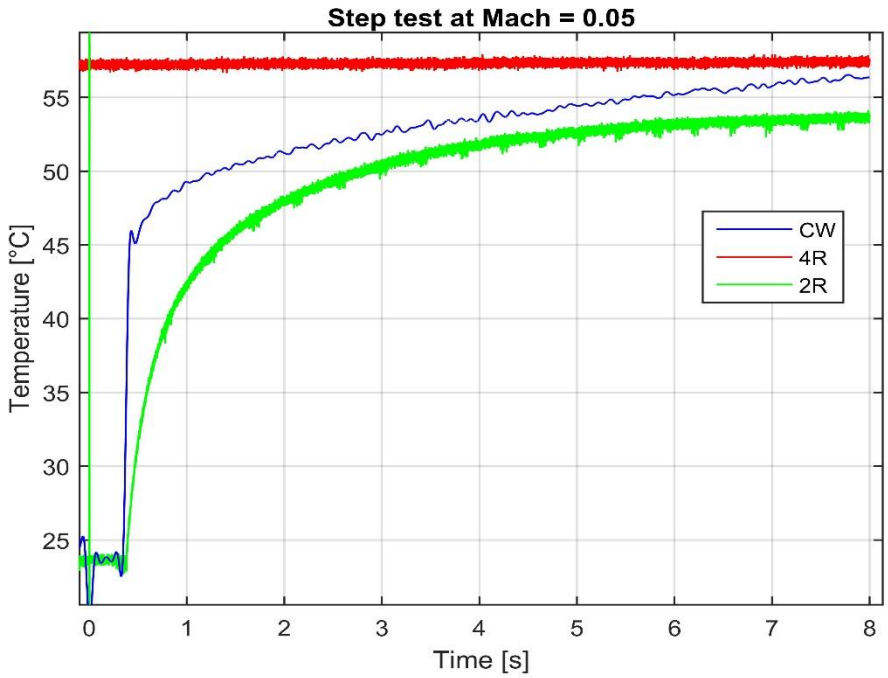

***Figure 5.5**: Step test 1 at Mach 0.05*

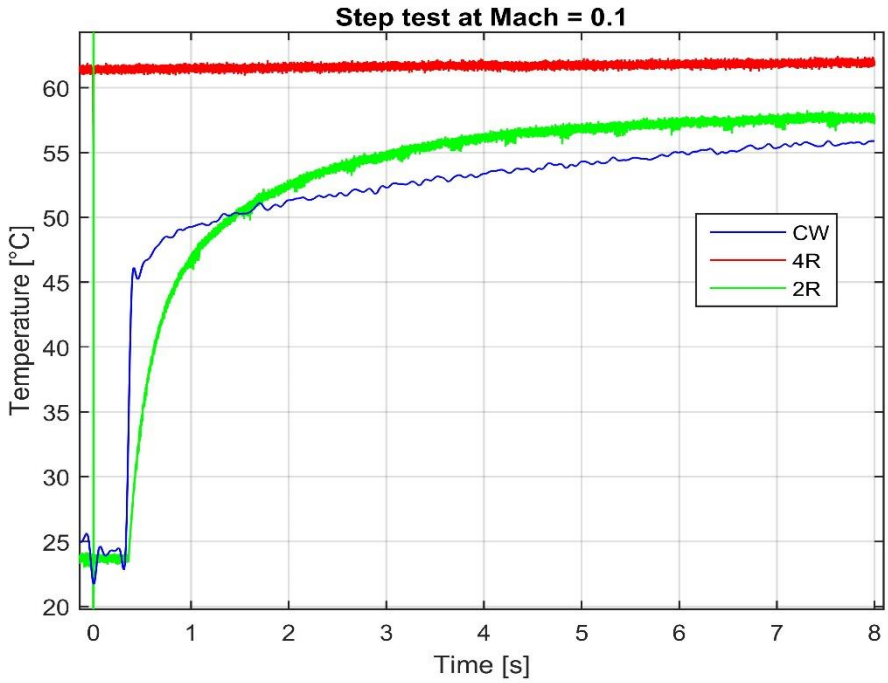

***Figure 5.6:** Step test 1 at Mach 0.1*

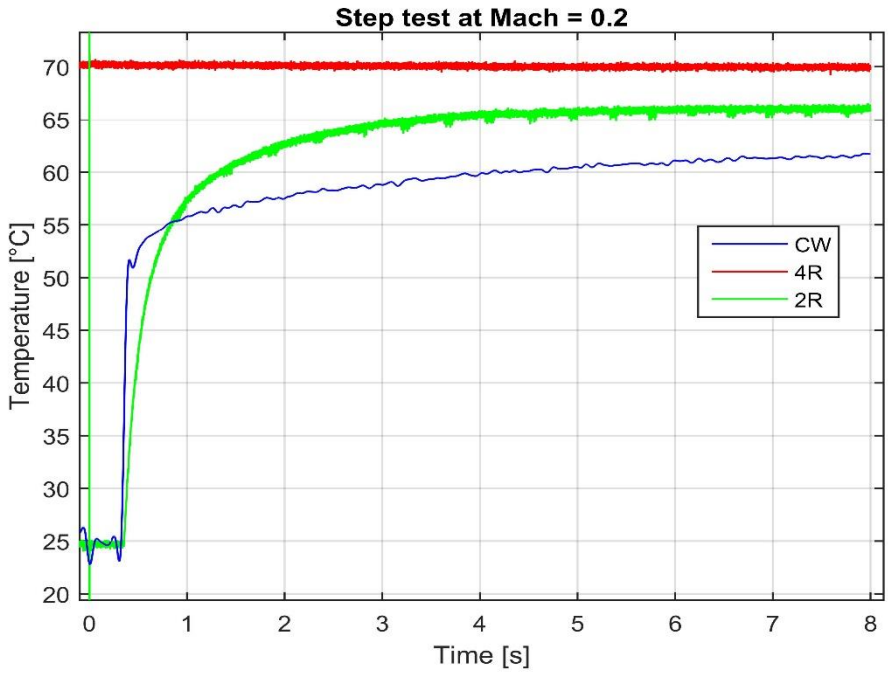

Figure 5.7: Step test 1 at Mach 0.2

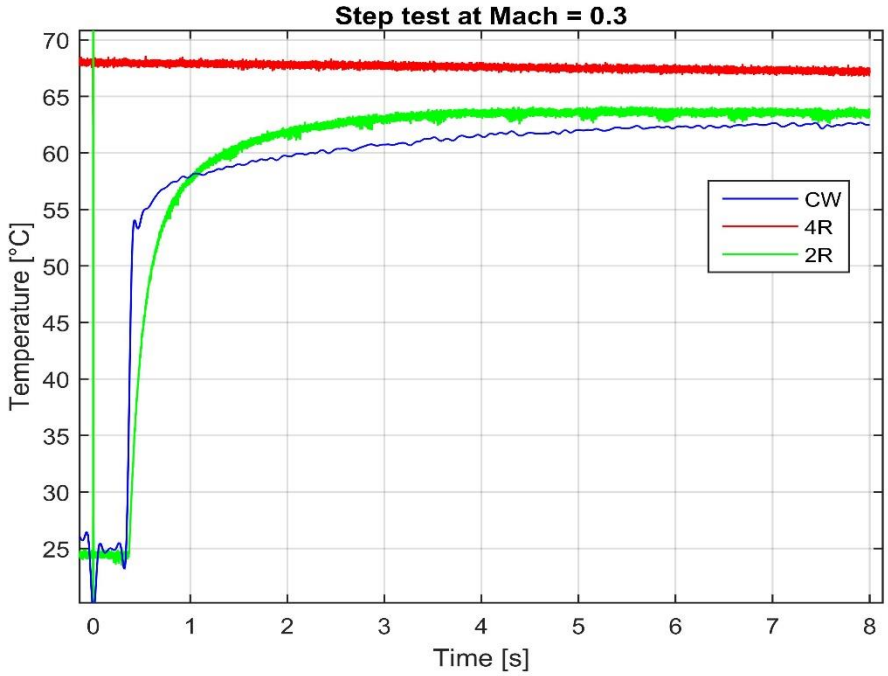

Figure 5.8: Step test 1 at Mach 0.3

The reactivity of head 1A of the cold wire is much higher than the one of the thermocouple 2R in the initial phase of the step. However the thermocouple seems reaching a stable final value while the cold wire curve has a final positive slope. It needs some more time to reach a stable final value. A second step test has been done increasing the observation time and modifying slightly the position of the probes.

5.1.2.2 Second step test

In this test it has been decided to place the 2R thermocouple and the cold wire head 1A as close as possible each-others in such a way that they could sense the same temperature variations. Moreover, the two transducers have been placed closer to the exit of the nozzle in such a way to reduce the heat losses. A picture of the "modified" setup is shown in Fig. 5.9. For this experiment we changed the sampling frequency reducing it from 8000 to 4000Hz in order to increase the observation time: finally the step test was analysed for about 16 seconds without affecting significantly the accuracy of the sampling.

Figure 5.9: *The setup used to realize the step tests. The two probes are shielded by a rectangular piece of wood that closes the flow blown by the nozzle.*

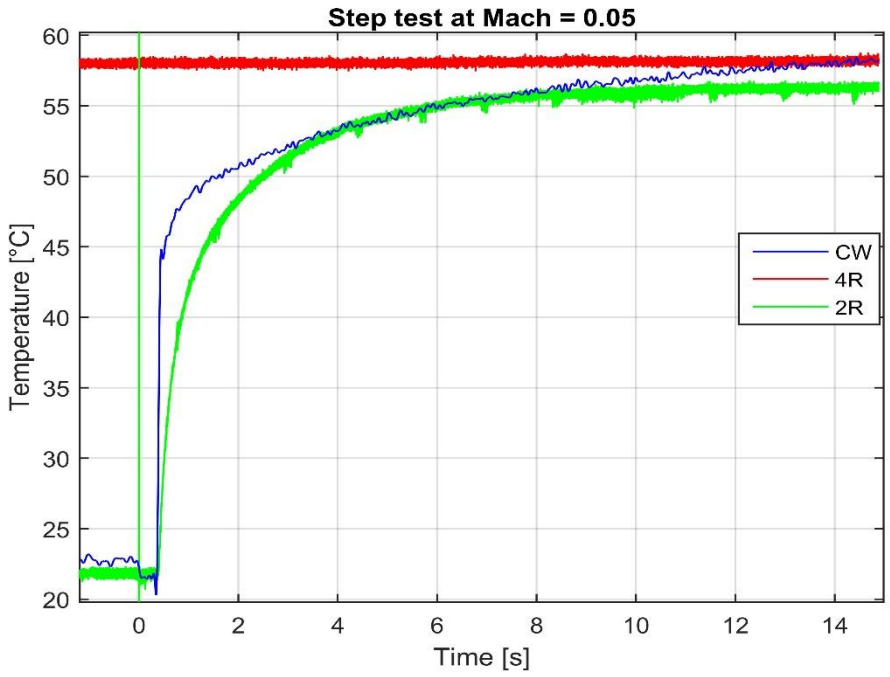

Figure 5.10: Step test 2 at Mach 0.05

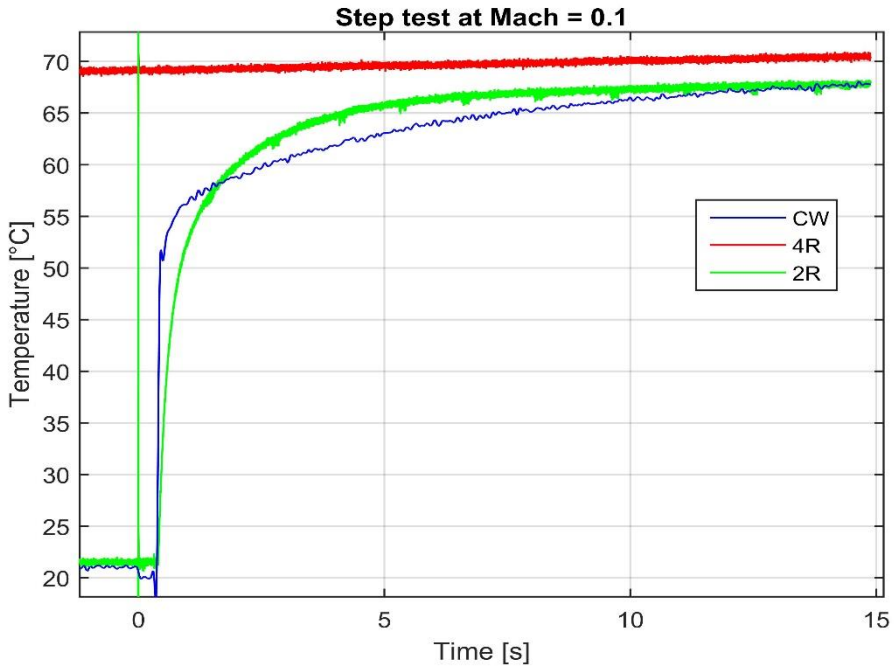

Figure 5.11: Step test 1 at Mach 0.1

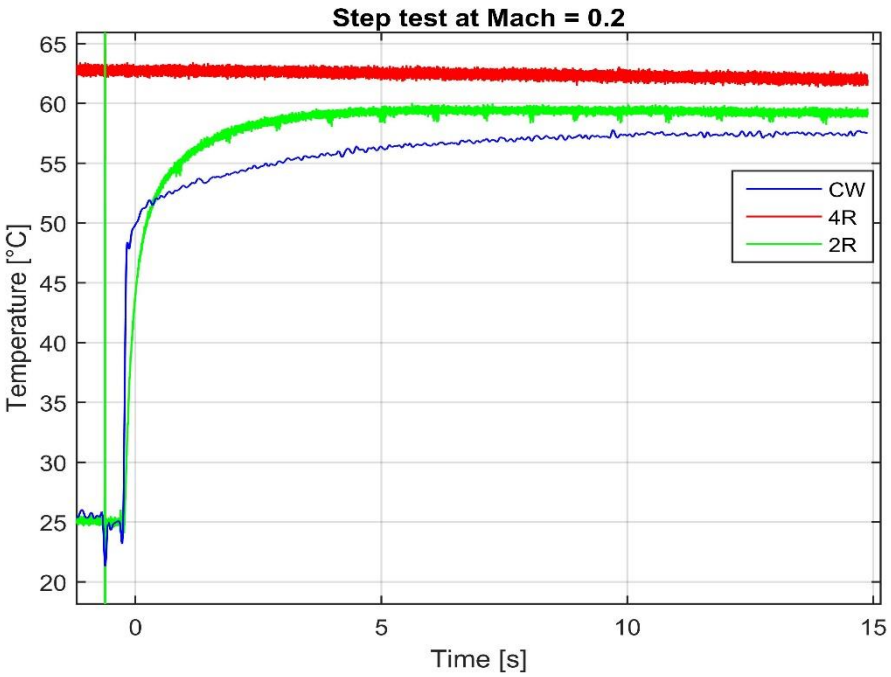

Figure 5.12: Step test 2 at Mach 0.2

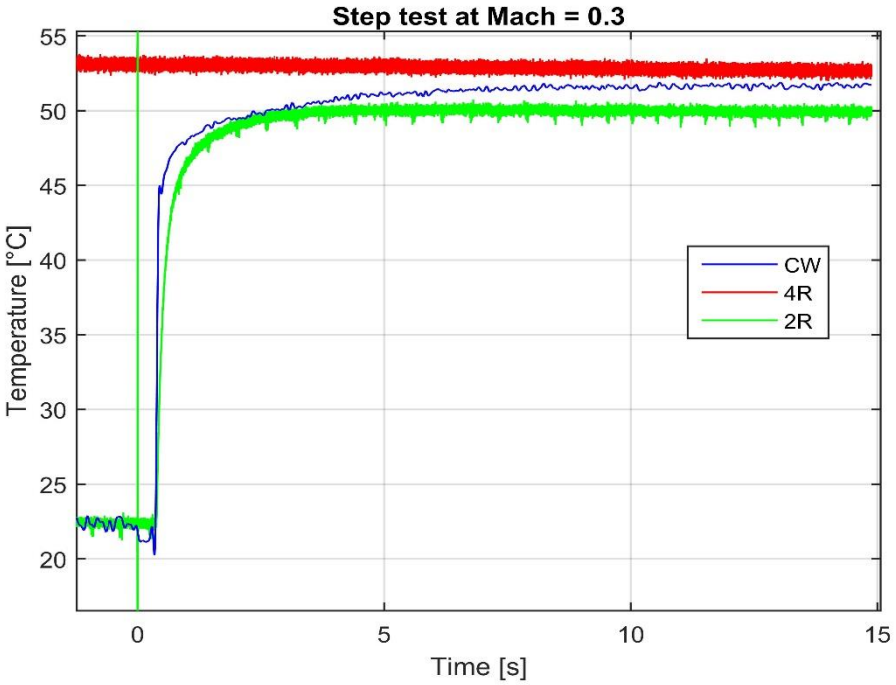

Figure 5.13: Step test 2 at Mach 0.3

The first thing that can be observed is that doubling the observation time allows to get curves with a final stable value. Nevertheless the curves of head 1A of the cold wire at low Mach numbers (0.05, 0.1) show always a slight positive final slope, which means that the velocity of the flow interferes on the reactivity of the probe. In any way, the new setup and a longer observation time brought to better results: the final temperature registered by the cold wire and 2R thermocouple are closer respect to the first case. The difference of temperature existing between the two probes and the "nominal" total temperature sensed inside the nozzle can be explained with the velocity error described in chapter 3. While the 4R thermocouple placed inside the nozzle senses the total temperature of the flux at extremely low velocity, the two probes placed outside are submerged into a flow of a certain velocity. The flow around the probes is not brought to rest isentropically but, due to the viscous stresses and heat losses, the conversion of kinetic energy into thermal enthalpy is incomplete and the total temperature registered by the probes immersed in the flow is lower than the nominal stagnation temperature.

Since the second step test give better results, the research of the experimental transfer function will be lead using these last data referred to the head 1A of the cold wire.

5.2 Compensation of the signal

The necessity to compensate the signal has been explained in the previous chapter where it has been illustrated the concept of transfer function of a probe. In particular, it has been described how to compute transfer functions of different orders.

The compensation of the signal is a technique used to overcome the physical limits of a transducer to react to external unsteady excitations. In effect, each transducer is characterized by a static behaviour, related to the ability to reproduce the response of a stationary input and a dynamic behaviour which allows to get the response of the probe to unsteady inputs. Once the dynamic behaviour of the probe is known, knowing its transfer function, the compensation is obtained simply applying the inverse of its transfer function to the signal.

The aim of this experimental work is to obtain the experimental transfer function of head 1A of the cold wire DAO123A starting from the outputs sampled in the second step tests previously described. Three approaches will be described in

order to compute the transfer function and it will be chosen the one that gives the more reliable results.

5.2.1 FFT ratio approach

The most known technique used to compute an experimental transfer function consists in doing the ratio between the Fast Fourier Transform (FFT) of the output signal and the FFT of the input signal:

$$H(\omega) = \frac{Y(\omega)}{X(\omega)} \tag{5.2}$$

In our experiment, the output $Y(\omega)$ is the Fourier transform of the recorded cold wire signal while the input $X(\omega)$ is the Fourier transform of the theoretical step. The cold wire signal, tested in this case at Mach 0.05 for 14 seconds, has been filtered with a Butterworth low-pass filter of the fourth order with a cut-off frequency of 10 Hz and has been adimensionalized in this manner:

$$T_{ad} = \frac{T_{cw} - \min(T_{cw})}{\max(T_{cw}) - min(T_{cw})} \tag{5.3}$$

The two signals (output and input) are depicted in Fig. 5.14. The problem of this technique is that it can be used when the input signal has a Fast Fourier Transform whose values are above a certain minimum value. In this case the input signal is a step and the Fourier transform of a step has values close to zero as the frequency increases (see Fig 5.15). For this reasons when dividing the two vectors $Y(\omega)$ and $X(\omega)$ the resulting transfer function shows meaningless peaks that makes the results unusable (see Fig. 5.16).

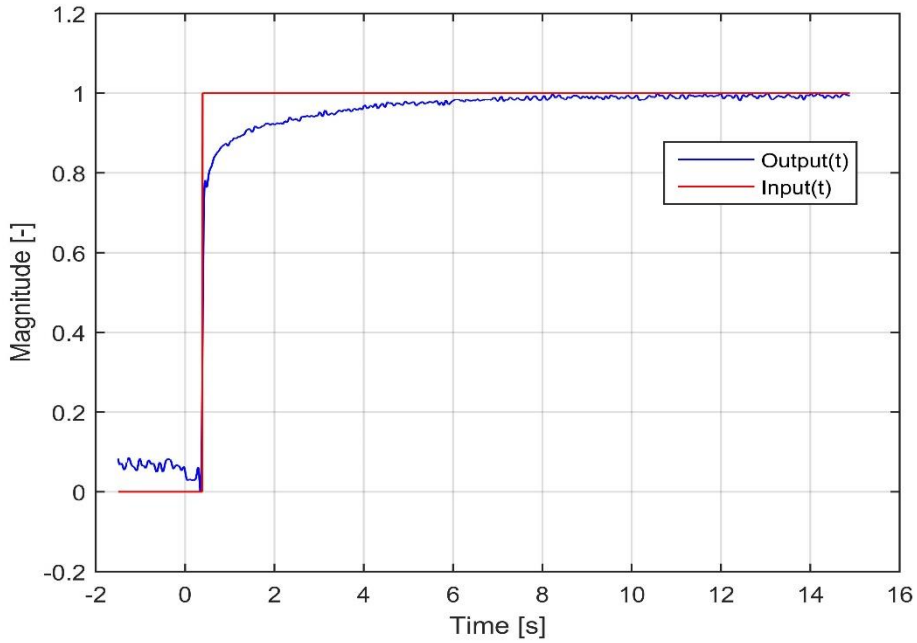

***Figure 5.14**: Comparison between the cold wire step signal and the theoretical Heaviside step.*

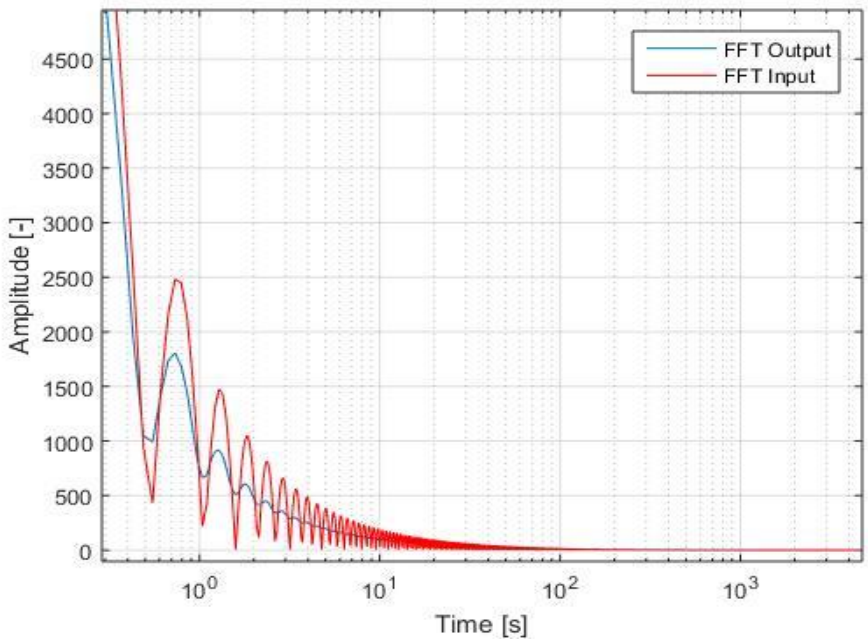

***Figure 5.15**: Fast Fourier Transform of the cold wire signal (blue) and of the Heaviside signal (red).*

The resulting transfer function is shown in the following picture.

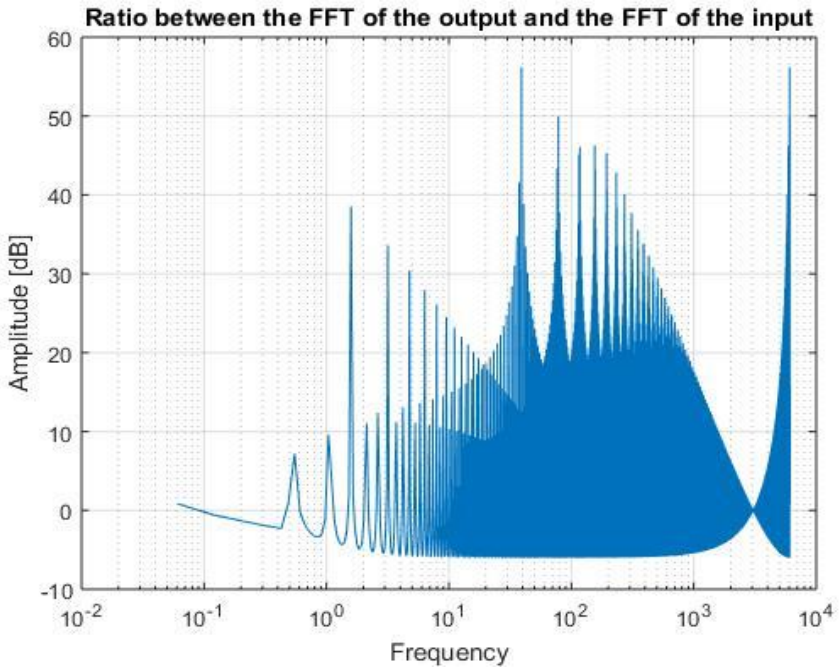

***Figure 5.16**: The ratio of the FFT of the cold wire signal and the FFT of the Heaviside input signal gives the experimental transfer function*

5.2.2 Differentiation approach

The step tests are generally easy to realize in the practice: the problem is that their results cannot be used directly to obtain the transfer function of the transducer. Another alternative to obtain an experimental transfer function is to "redefine" the step-time signal: this is differentiated, subtracting two consecutively values of the step signal and dividing each by the delta time between them. What we obtain is, as expected, an impulse signal because the impulse is the derivative of the step. The resulting signal is shown in the following picture.

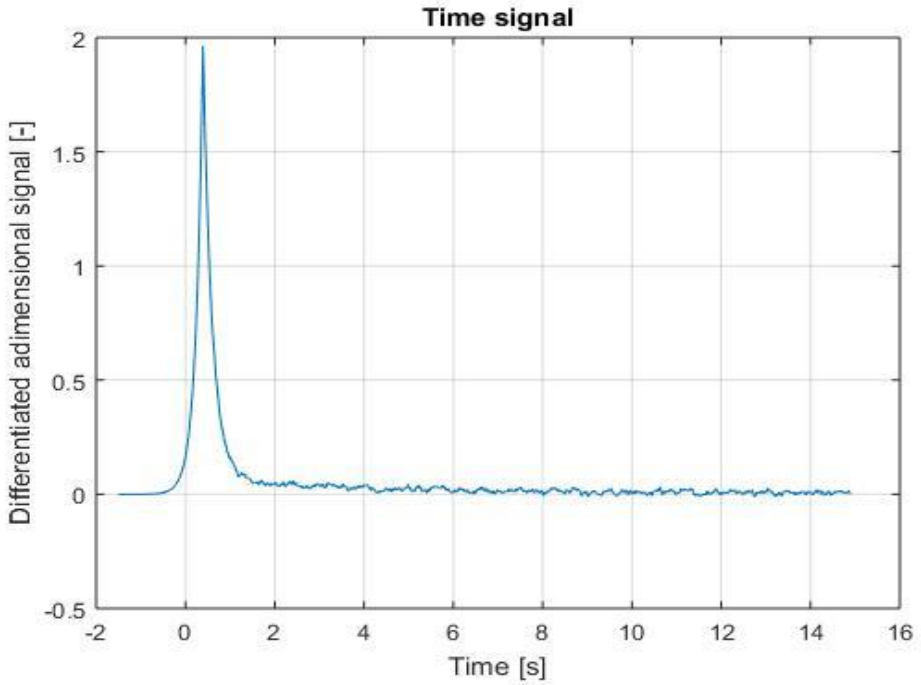

Figure 5.17: *The impulse signal has been obtained subtracting two consecutively values of the original step signal and dividing this value by the delta time between them.*

The advantage of using this technique is that when we want to apply the Fourier Fast transform to the theoretical impulse signal we obtain one, from the theory. In this case, being the FFT of the input $X(\omega) = 1$, the experimental transfer function coincides with the FFT of the output $Y(\omega)$.

$$H(\omega) = Y(\omega) \tag{5.4}$$

The FFT of the differentiated signal produce this transfer function:

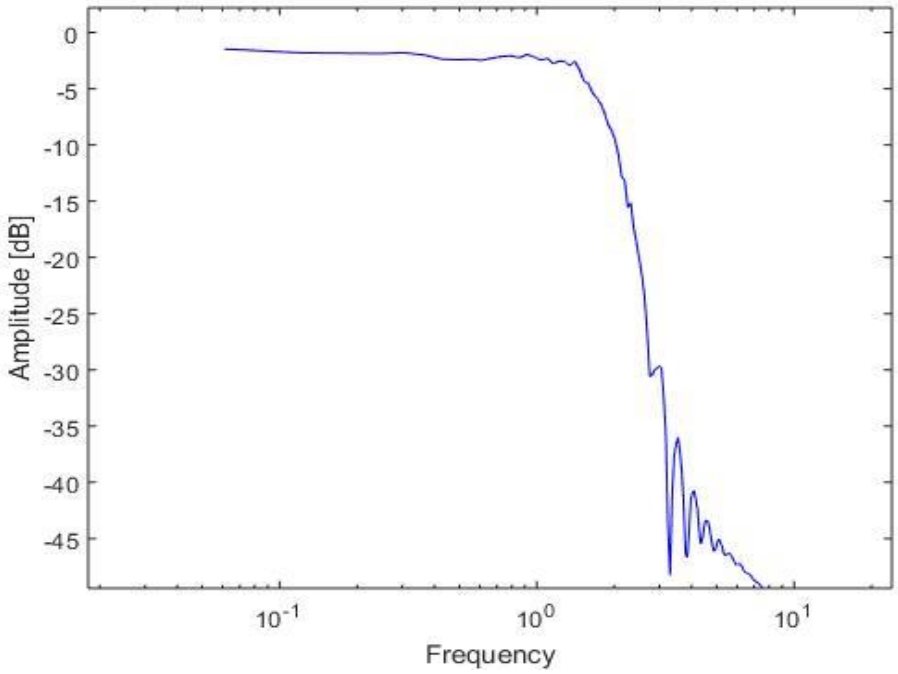

***Figure 5.18**: The resulting transfer function obtained after having redefined the step as impulse.*

The transfer function obtained is less noisy respect to the one obtained with the approach of the ratio of the FFT and has an abrupt drop at 1 Hz. Nevertheless it does not look like to the transfer function that Dénos obtained in its work. The problem of these approaches is that they are extremely depending on how the cold wire signal is defined. Different tests have been made cutting the initial constant part, or increasing this initial constant part adding zeros: the resulting transfer functions extracted from these modified vectors are rather different. It was not possible to find the "best" shape of the step signal that produce a reliable transfer function.

5.2.3 TFEST approach

The last method used to compute the experimental transfer function is a function defined in Matlab, TFEST. The basic inputs of this function are the recorded data of the signal and the number of poles and zeros of the expected transfer function. This code takes the data of the cold wire step signal, those of the theoretical true step, the sampling time and evaluates a transfer function with the number of zeros and poles imposed as inputs. The theoretical true step is the step generated from

the movement of finite velocity of the wooden shield (0.5 m/s in this case). In Fig. 5.19 it is shown the theoretical true step and theoretical step (Heaviside).

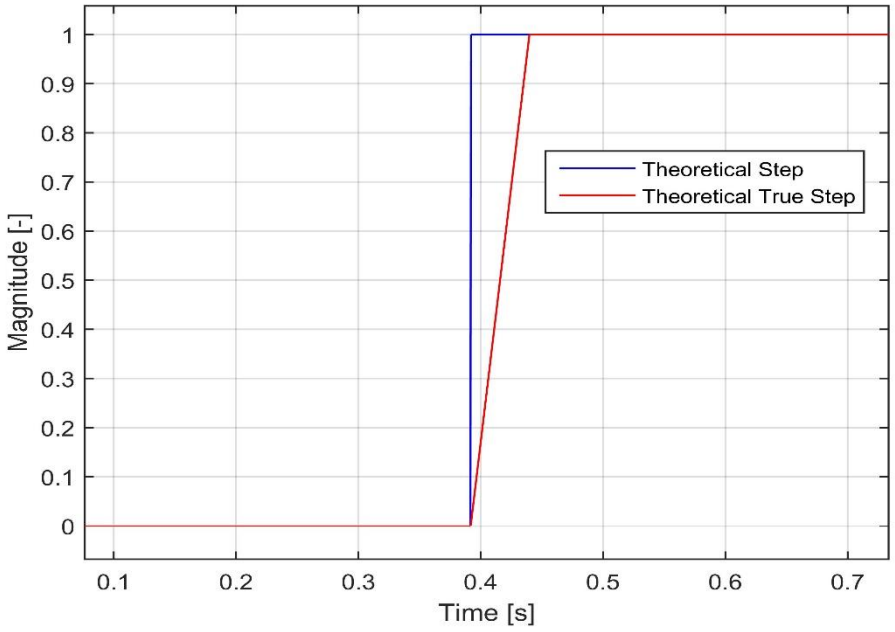

***Figure 5.19**: The theoretical true step is the step generated by the movement of the shield. Since the nozzle has a diameter of 12 mm and the support moves the shield at a finite velocity, 0.5 m/s, the step lasts 0.024 seconds.*

The details of the code are not available: it tries to compute an analytical transfer function that best matches the transfer function that it finds experimentally with the data. The output it's a transfer function characterized by a "Fit to estimation data" value: it is a percentage that shows how much the computed transfer function reproduces the behaviour of the experimental one.

It has been written a code that loads the experimental results of the step test of the cold wire. The signal has been cleaned from the spurious peaks, low-pass filtered and adimensionalized as described before: it is shown in the following picture.

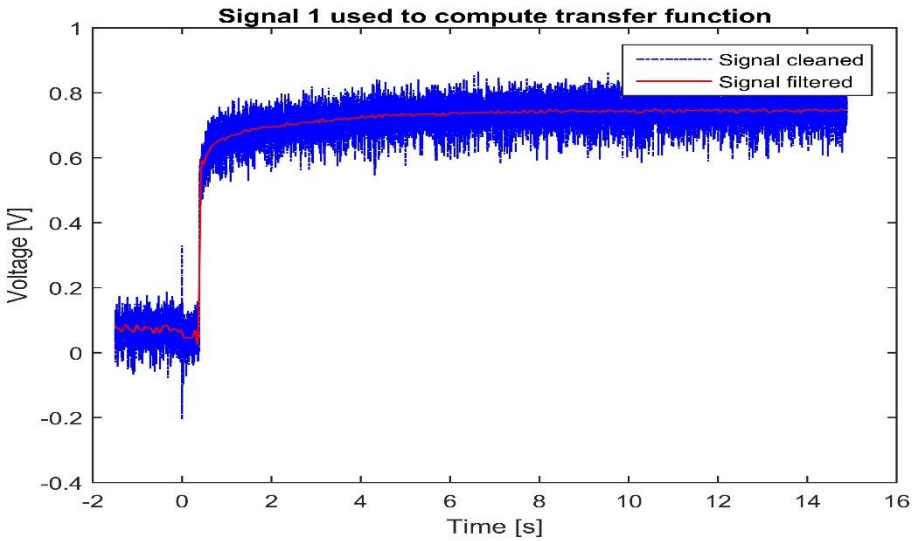

Figure 5.20: *The signal of the cold wire has been cleaned from spurious peaks, low-pass filtered and adimnesionalized.*

The modified data have been used to compute the transfer function with 'tfest'. According with the work done by Dénos, the transfer functions used to describe the probe are of the first, second and fifth order. For this work it has been chosen to test the data imposing a second, third, fourth and fifth order transfer functions (selecting two, three, four, five poles respectively in the options of 'tfest'). The transfer functions obtained at Mach 0.05 are depicted in figure.

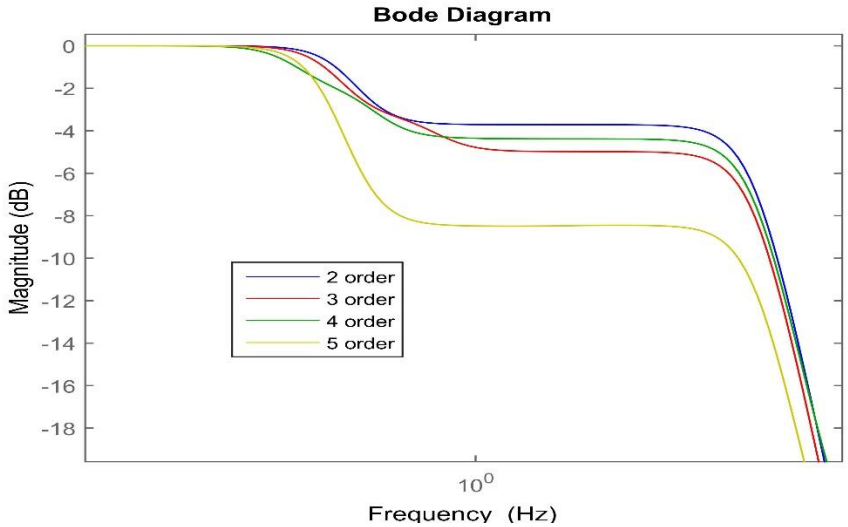

Figure 5.21*: The experimental transfer functions found with 'tfest' with a different number of poles with tests at Mach number 0.05*

Among the four transfer functions, the one that gives the higher 'Fit to estimation data' value is the 3rd order transfer function with 96.45%. The experimental transfer functions seem describing correctly the behaviour at low frequency: the effect of the conduction of the prongs is visible in the magnitude bode diagram with the small steps and with a reduction of the amplitude of the output. The abruptly drop of magnitude at around 10 Hz is due to the finite probe injection speed (0.5 m/s) and to the existence of a shear layer on both sides of the jet: these combined effects allow to analyse only phenomena in a restricted field of frequencies. This result is not sufficient to obtain a realistic dynamic description of the cold wire. The main element of the probe, the tungsten wire, is not taken into account in this analysis.

The wire, as widely descripted in chapter three, behaves as a first order system and it is possible to evaluate its transfer function with a formula that includes experimental data of Reynolds number, Nusselt number, physical and geometrical data of the wire (density, diameter). It is the main element of the probe that permits to sense high frequency fluctuations: its contribute in the experimental transfer function is not visible since the step experiments allow to analyse only the low frequencies phenomena.

In order to obtain a realistic description of the dynamic phenomena we decided to combine the results of the experimental transfer function (related to low frequencies phenomena, i.e. conductions of prongs) and those obtained analytically (with the first order transfer function). In the following picture it's depicted the experimental transfer function obtained with 'tfest' imposing two poles and one zeros (TF), the first order transfer function obtained analytically (TF_1ORDER) and the transfer function that combines both (TF_mod).

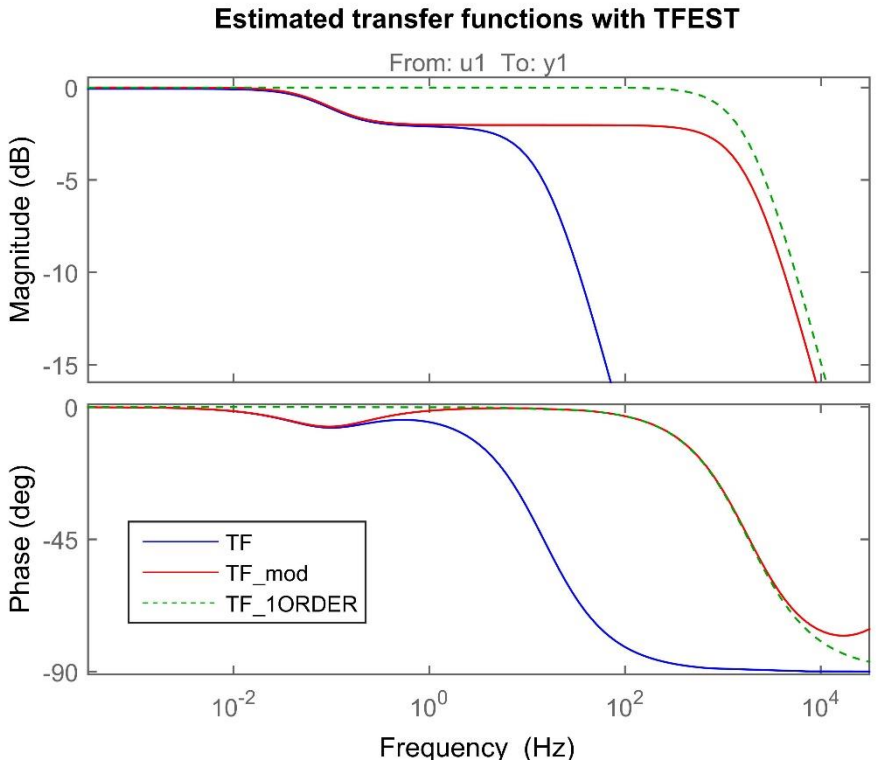

Figure 5.22: *The modified transfer function (TF_mod) combines the low frequency behaviour of the experimental transfer function found with 'tfest' and the high frequency behaviour which stems from the dynamic behaviour of the tungsten wire (described with a first order transfer function).*

The blue transfer function (TF in the picture) has been modified artificially substituting the pole at 1Hz with the one found in the first order transfer function with cut-off frequency of about 1000Hz. The resulting transfer function is the red one (TF_mod).

One source of inaccuracy of the obtained transfer function has to be found in the value of the cut-off frequency of the tungsten wire: this has not experimentally computed. Not disposing of the experimental setup we found this value analytically with formula provided by Dénos and described previously in chapter 4.

The transfer functions used in this test at Mach 0.3 are here reported:

$$G_1(s) = \frac{11472.79}{s + 11472.79} \tag{5.5}$$

$$G_2(s) = \frac{s + 0.6675}{(s + 92.914)(s + 0.52833)} \tag{5.6}$$

$$G_{2mod}(s) = \frac{(s + 0.6675)(s + 1000000)}{(s + 11472.79)(s + 0.52833)} \tag{5.7}$$

In the modified transfer function $G_{2mod}(s)$ we added a high frequency zero at 1MHz in order to obtain a proper transfer function that can be reversed without modify its shape before that value of frequency.

The main limit of this method is that it does not take into account what happens in the plateau region. Realizing step tests with a higher injection velocity of the shield (in this case it was 0.5 m/s) it is possible to analyse the dynamic behaviour in a wider range of frequencies.

The transfer functions found at Mach 0.3 have been modified adding the cut-off frequency of the tungsten wire (equal to $\frac{1}{2\pi\tau}$). The results are depicted in Fig. 5.23.

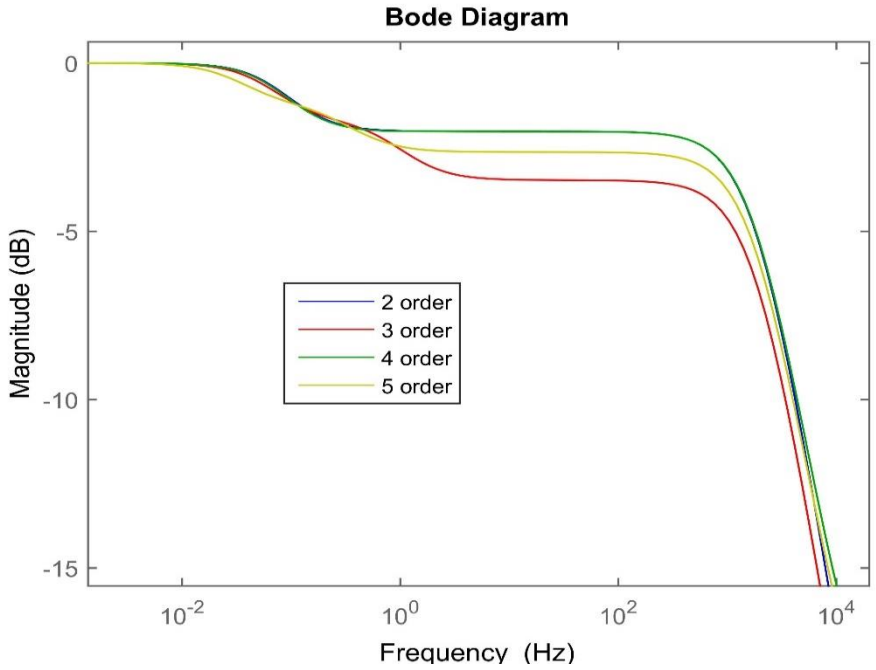

Figure 5.23: *The transfer functions found with 'tfest' imposing different numbers of poles in step tests at Mach number 0.3.*

The 3rd order transfer function is the one that gives the higher 'Fit to estimation data value'. The analytical expression (which stems from a step test at Mach = 0.3) is here reported:

$$G(s) = \frac{0.007686s^3 + 7686s^2 + 59280s + 28000}{s^3 + 11480s^2 + 72280s + 28000} \qquad (5.9)$$

This transfer function has been inverted and used to compensate the cold wire signal in order to reproduce the theoretical step; in Fig. 5.24 is shown the original signal of the cold wire, the reconstructed step and the theoretical step. The figure on the bottom (Fig. 5.25) shows the computed transfer function in blue and the inverse transfer function in red. The reconstructed signal was obtained doing the FFT of the cold wire signal and multiplying this outcome with the vector resulting from the 'freqresp' function. This function has as inputs the inverse of the transfer function and the frequency range expressed in radians.

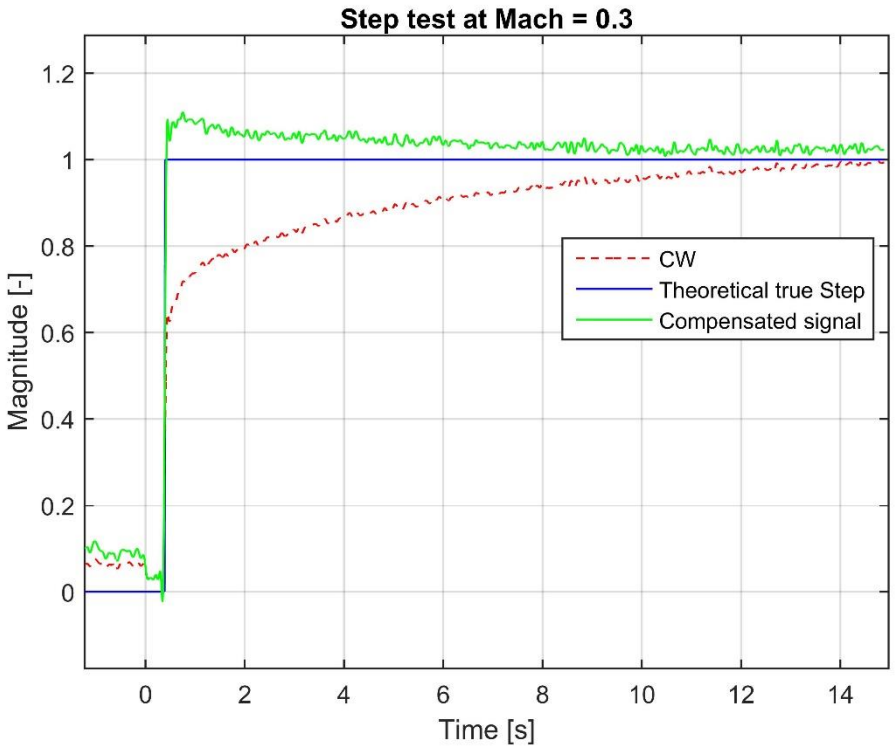

Figure 5.24: *The cold wire signal has been compensated using the inverse of the transfer function. The reconstructed step fits well the theoretical true step.*

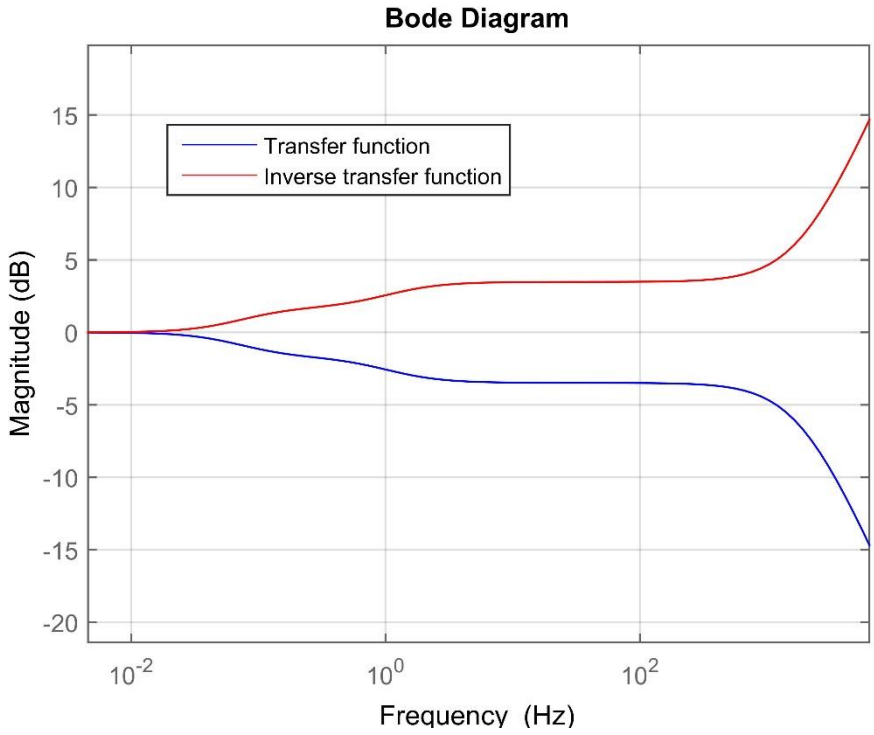

Figure 5.25: *The transfer function (blue) and it inverse (red) used for the compensation.*

5.2.4 Conclusions

The step tests realized with the moving support allowed to get the experimental transfer function of head 1A of the cold wire DAO123A.

The transfer function is defined in three parts: the low frequency part described with the transfer function obtained with 'tfest'; the medium frequency part which is approximate with a flat region; the high frequency part defined starting from the cut-off frequency found with a first order transfer function.

As mentioned before, the main limit of this approach is the undefined medium region which has been approximate as flat. A higher injection velocity of the support would allow to find the real behaviour in this medium frequency region. The cut-off frequency of the tungsten wire stems from an analytical formula but no experimental tests have been realised to confirm this trend.

The other two methods used to compute the transfer function gave erroneous results. They are extremely dependant on how the step vector has been defined.

The obtained 3rd order TF has been used to compensate the cold wire step signal. The results are good: the compensated signal well fits the theoretical one. For the test in turbine will be generated four transfer functions of the 3rd order at different Mach number (0.05, 0.1, 0.2, 0.3) in such a way to see the differences of the compensated signal in the four cases.

5.3 Cold wire test in CT3

The CT3 is a facility in Von Karman Institute used to test turbine stages in similarity conditions with aero-engines. It has been done an experiment to understand the effect of energy dissipation due to the injection of air at ambient pressure in the settling chamber. The rotor is brought to a stable rotating velocity in a vacuum ambient and it is analysed how the injection of air affects the working conditions when it rotates only for inertia.

5.3.1 Description of the test

It has been analysed the transient phenomena occurring when the turbine, initially rotating in vacuum ambient at constant speed, encounters flow at ambient pressure.

The turbine test section has been equipped by several instruments to sense pressure and temperature variations. First of all the turbine test section has been brought to vacuum (under 30mbar absolute pressure). The rotor of the turbine is spun up to the desired speed by an auxiliary power turbine, for this test at about 2200 rpm. As a stable value of rotating speed is reached, the power turbine is turned off: the rotor keeps rotating for inertia always in vacuum conditions. Several valves are opened: air at ambient temperature and pressure enters in the turbine test section and the aero-brakes are activated. Due to the increase of pressure and density inside the chamber the rotors experiences drag and the aero-brakes produce an opposite momentum respect to the direction of rotation. After few minutes the rotor is brought to rest; rpm, temperature and pressure conditions are monitored during all the test.

The aim of the test is to use the cold wire which has been calibrated for static and dynamic conditions and understand which mechanisms intervene during the transient replenishment phase.

5.3.2 Experimental setup

The main facility for this test is the CT3 test rig. The complete description is provided in chapter two: it's a facility used to test turbine stages in aero-engines working conditions. A light piston of 1.6 m of diameter can course inside a 8 meters long cylinder: from the back of the piston some pressurized air is provided thus generating a pressure difference in the two chambers separated by the piston itself. An isentropic compression is realised: as the air inside the second chamber of the piston reaches the desired temperature and pressure a valve is opened and the compressed air is blown in the test chamber. The turbine to be tested is rotating at a certain speed and for a short time the flow passes through it. During the test several instruments are used to register some parameters. In our experiment the CT3 has been used to bring the turbine to a desired velocity (2200 rpm) in vacuum conditions. A vacuum pump has been used to reach a total pressure under 30 mbar.

In order to understand the mechanisms occurring during the open-valves-phase it has been used the cold wire DAO123A, described in the previous chapters and 3 differential pressure probes. All the four transducers have been placed inside the CT3, behind the rotor.

The electronic used for the cold wire DAO123A is always the same used during the calibration: head 1A has been linked to the black box TUCW3, head 2A has been linked to the white box TUCW2. The cold wire outputs have been connected to the Wheatstone bridge through a longer cable: it has been registered a higher value of resistance respect the one obtained registered during the calibration of cold wire. This will results in a shift of the electrical output. This effect has to be taken into account in order to get a correct conversion voltage-temperature.

The DAO123A is a cold wire which has been calibrated in static and dynamic conditions. It has two heads, one placed in the middle and the other at the extremity of the probe (respectively head 2A and head 1A). The CT3 facility is designed in order to easily insert transducers: in effect there are some holes realised for this purpose. The DAO123A can be mounted into the facility through a metallic support which is depicted in Fig. 5.26. The metallic piece, named 3904-46, is pierced with 5 holes with 8 millimeters of diameter and the probe can be easily inserted having a slightly smaller diameter. The assembly of the probe can be quite complicated due to the extreme fragility of the wire: for this purpose it has been used the tool descripted in chapter 2.

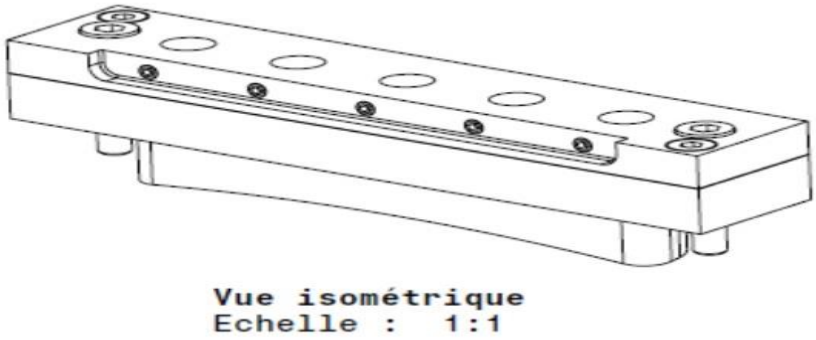

***Figure 5.26**: The probes are inserted in these metallic supports which, in turn, are inserted in the CT3 facility.*

The objective is to fix the probe at the correct height and angle in the turbine channel trying to move as less as possible the transducer. The metallic support is mounted on the tool and the variable-height instrument is placed under the tool as depicted in Fig. 5.27. With the Excel program descripted in chapter two it is possible to set the correct eight of the variable-height instrument in such a way to obtain the correct value of deep of the probe inside the turbine channel. The probe courses inside the metallic support till it touches the surface of the variable-height-tool. For this experiment head 1A, the one placed at the extremity of the probe DAO123A, has been inserted at 75% of the total length of the turbine channel with a 0° angle (computed respect to the axis of the turbine).

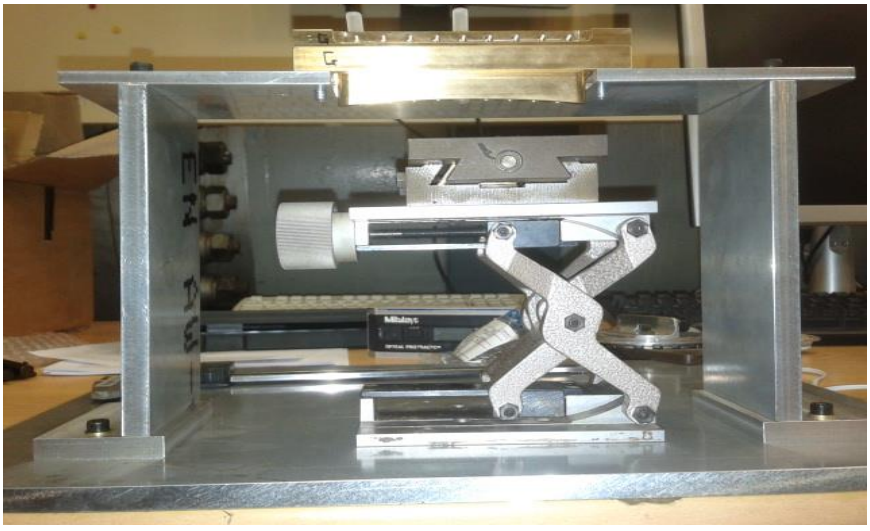

***Figure 5.27:** The setup used to set the depth and the angle of the probe in the turbine channel.*

The pressure transducers used in this experiment are always differential pressure transducers, as the other used in other tests. In this case the SENSYMs are the SENSA1, SENSA2 and SENSA3. These probes have been calibrated with the process descripted in chapter 3 and the following tables are referred to the values of slope and intercept obtained after the calibration.

Calibration *(P = a*V+b)*	SENSA1 (relative pressure sensor)
A	-540.22
b	1621.844
R^2	0.999976

Calibration *(P = a*V+b)*	SENSA2 (relative pressure sensor)
A	-551.788
b	1661.067
R^2	0.999992412

Calibration *(P = a*V+b)*	SENSA3 (relative pressure sensor)
A	-543.423
b	1634.398
R^2	0.99998555

Table 5.3: *Calibration coefficients of the differential pressure probes SENSA1, SENSA2 and SENSA3.*

Another transducer has been used to compute the round per minutes of the turbine in order to have a graphic of the velocity of rotor during the test.

The 5 probes have been linked to GENESIS the data acquisition system used also for the analogue filter tests, described in the first part of chapter four. In this test we acquired the signals for 192 seconds with a sampling frequency of 5000 Hz. A low pass filter with a cut-off frequency of 500 Hz has been used. The head 1A of cold wire DAO123A has been sampled at 5000 Hz (for the whole duration, 192 seconds) and also at 200000 Hz (for a shorter duration). For the higher sampling frequency case we used a low-pass filter with a cut-off frequency of 50000Hz. The aim of this double sampling was to get the differences of the cold wire signal during the unsteady phase (at the opening of the valves). Due to a setting error the

higher sampling signal has been recorded in the wrong period and we recorded a stable (high sampled) signal.

5.3.3 Test and results

The test has a length of almost 5 minutes since the rotor needs to be spun up to 2200 rpm. When the desired rotating speed is reached the data acquisition system starts acquiring data for a total length of 3 minutes. The test ends when the turbine is brought to zero velocity due to the intervention of the aero-brakes after the injection of air. The results of the experiment are reported in the following graphs.

The first images analysed are those referred to the velocity of rotor and to the trend of pressure inside the test chamber.

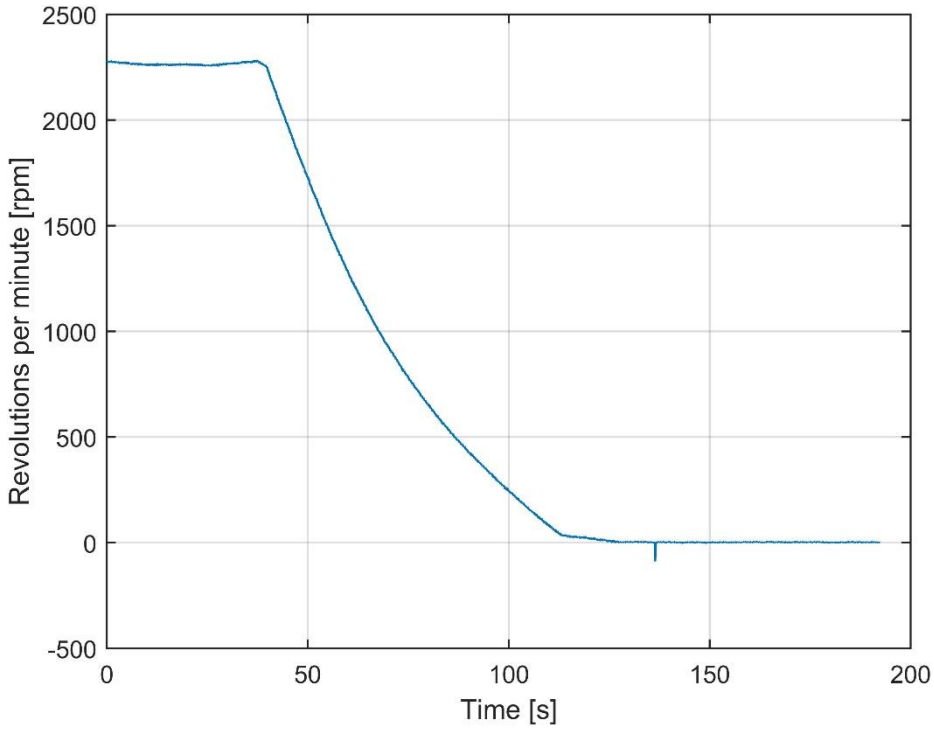

Figure 5.28: *The RPM during the test in the turbine rig.*

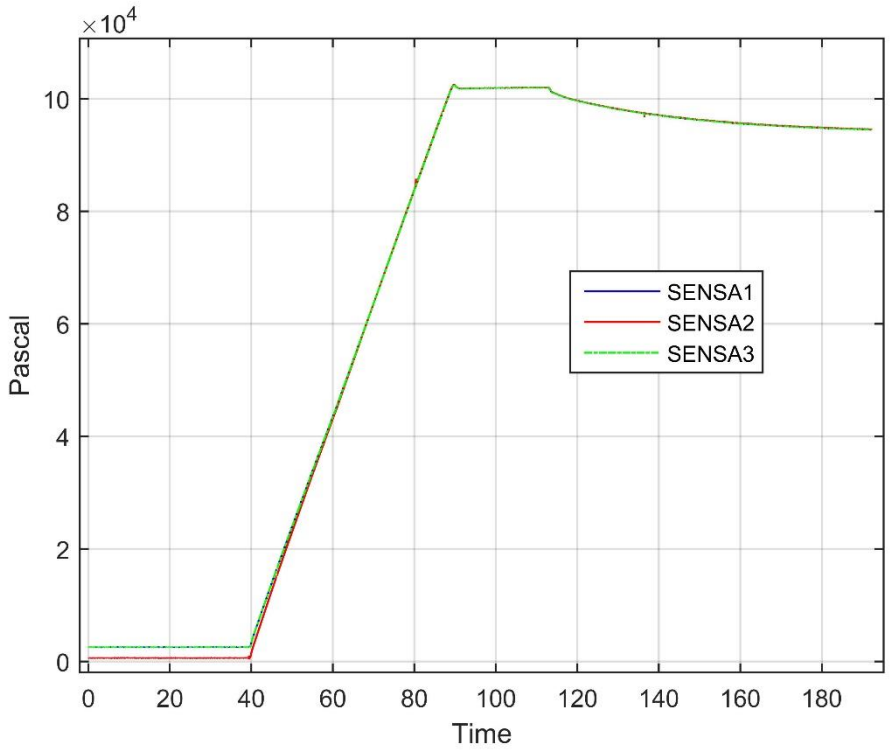

Figure 5.29: *The pressure sensed by the differential pressure transducers during the test in the turbine rig.*

It can be noticed that in the first 40 seconds the measured quantities are constant: the RPM sensor displays 2200 revolutions per minute and the three differential pressure probes have a low constant value. The sensor SENSA2 shows a slight shift of almost 2000 Pascal respect to the other probes: this can be due to electronics. At 40 seconds the valves are opened and the pressure inside the test chamber increases linearly during 50 seconds while the rotor, which is rotating only for inertia, starts decelerating. The turbine stops rotating and the pressure is monitored one minute more: after having reached a stable value for few seconds, pressure slowly decreases to the final ambient pressure (94495 Pa).

The results of the cold wire are shown in the following pictures. One is referred to head 1A, placed more deeply in the turbine channel (75% of the total length of the channel); the second one, head 2A, is placed at 25% of the total length of the channel. As mentioned before, the probe has been linked to the Wheatstone bridge through a cable which has a higher electrical resistance respect to the one used during the calibrations: this results in a shift of the temperature. Knowing the ambient temperature by a thermometer and the initial temperature registered by

the cold wire (in the first 40 seconds) it is possible to find the shift. The corrected results are plotted here below.

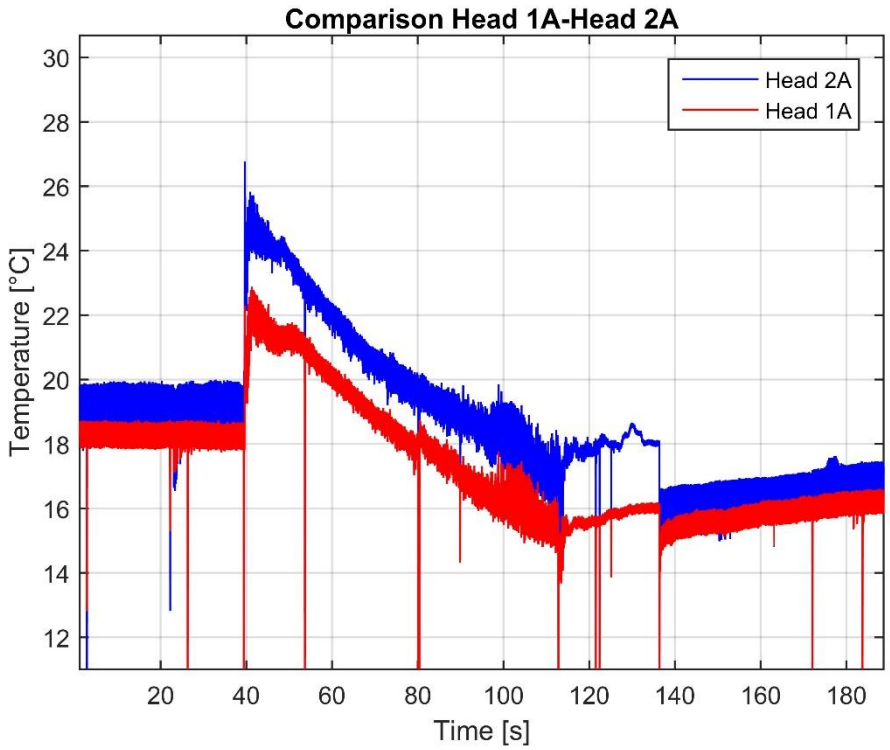

Figure 5.30: *Comparison of the signals of the two heads of cold wire DAO123A*

The initial temperature is almost the same for both the transducers (there is a difference of less than 1 degree). The physical phenomenon of kinetic energy dissipation (observed previously with the RPM graphic) can be interpreted in another way with the graphics of the cold wire. We observe that, as the valves are opened at 40 seconds, the temperature registered by the cold wire rises abruptly: the air enters in the chamber and is accelerated by the movement of the rotor. In this phase there is a conversion of kinetic energy of the turbine into thermal energy of air. During this phase the kinetic energy of the turbine decreases due to the effect of aero-brakes which generates an opposite momentum respect to the rotation. As the RPM decreases also the conversion of kinetic energy decreases: after the abrupt peak, the temperature decreases. We can observe that the temperature sensed by the two sensors is different during the open-valve-phase: head 1A, which is the transducer placed at the extremity (i.e. at a lower radial distance from the axe of the turbine), senses a lower temperature respect to the

other head. This result can be related to a difference of kinetic energy: the tangential velocity of air increases with the radius from the axis of the turbine. Since head 2A has a radial distance greater respect to the one of head 1A, the air impacting on this first probe will have a higher kinetic energy, which will result in a higher total temperature. In both graphics, that have been plotted together in figure, we observe a similar phenomenon between 115 and 135 seconds. In this phase the turbine decelerate from 35 RPM to 0 and temperature registered from both the transducers increases slightly. In the last minute of recording, when the RPM is 0, temperature slowly increases from 16°C to 17°C while the pressure stabilises to the final ambient pressure value.

5.3.4 Compensation of the cold wire

Once obtained the results of cold wire DAO123A we tried to compensate the signal registered from head 1A using the transfer functions obtained with the step tests. The abrupt open of the valves is associated with the peak of temperature which occurs in a small fraction of time (~0.05s). In order to compensate the signal we used the transfer functions of 3rd order (those one that gave the highest 'Fit to estimation data' value) obtained at different Mach number (0.05, 0.1, 0.2, 0.3): the transfer functions are shown in the following figure.

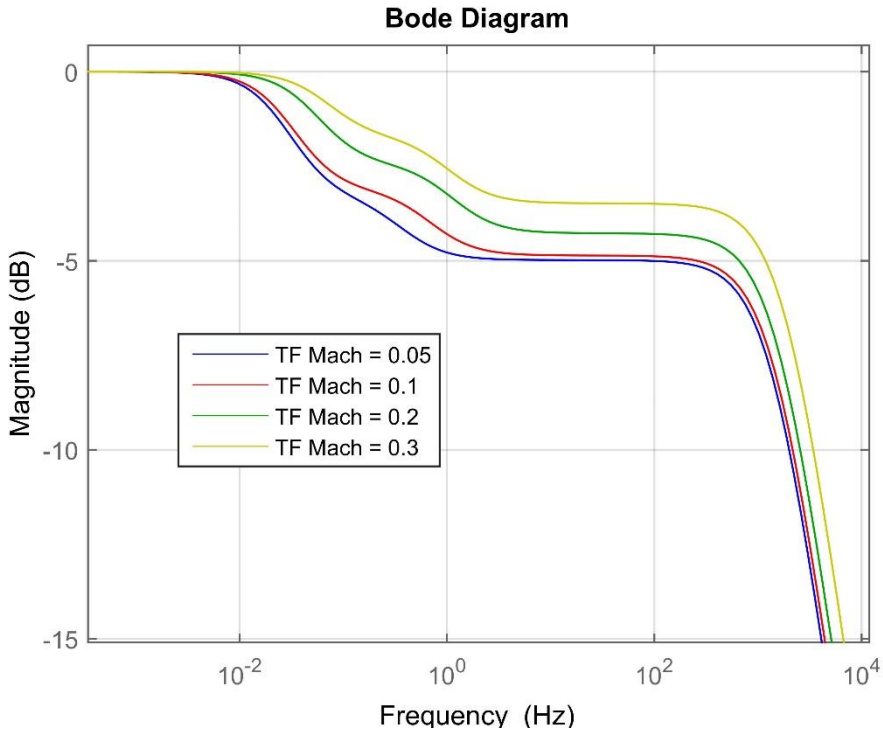

Figure 5.31: *The transfer function of 3rd obtained with the step tests for different Mach numbers. It is possible to see the effect of velocity on the shape of the transfer function.*

It can be noticed that the four transfer functions have a similar shape with a cut-off frequency of the wire at around 1000Hz. The increase of Mach number causes a higher convection which results in a faster response of the probe. The transfer function has been inverted and, through the use of the 'lsim' function in Matlab, it was possible to obtain the compensation of the signal of head 1A of the probe.

The results of the raw signal and the compensated one are shown in Fig. 5.32. Later, the signal has been filtered with a fourth order low-pass Butterworth filter with a cut-off frequency of 5 Hz. The compensation has been applied to this filtered signal with the four inverse transfer functions and the results are depicted in figures 5.33, 5.34, 5.35, 5.36.

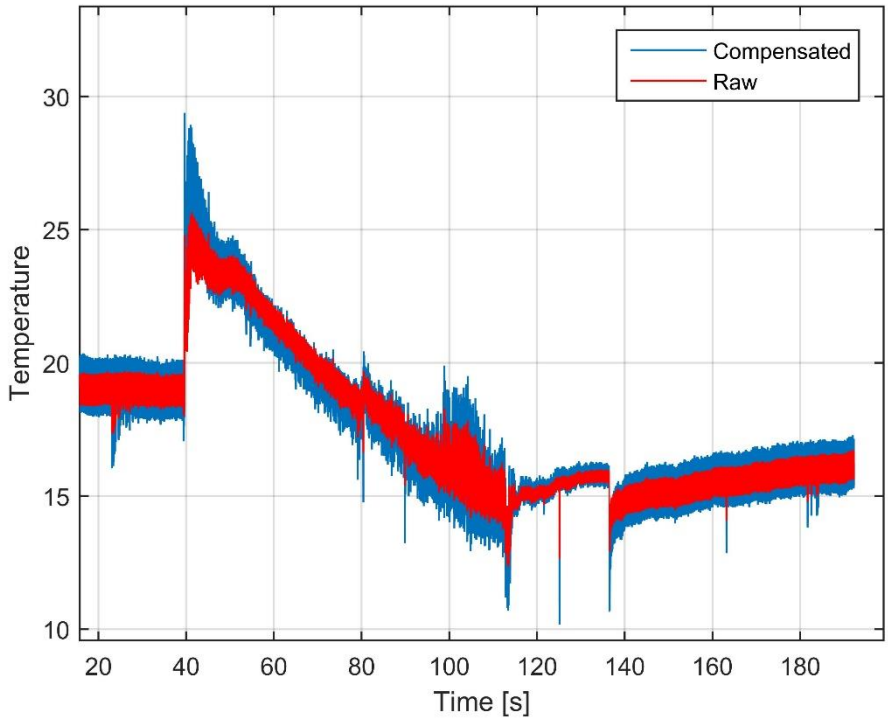

Figure 5.32: *Comparison of the raw signal of the cold wire and the compensated raw signal of the cold wire (head 1A with a transfer function obtained in a step test at Mach = 0.05).*

The transfer functions that have been applied to compensate the signal stem from step tests realized at different Mach numbers. All the step tests have been realised with a known time constant equal to 0.024 seconds. This time constant is obtained as the ratio of the diameter of the nozzle injecting air and the velocity of the variable height support. The time constant of the experiment in the CT3 is about 0.05 seconds (this value has been checked manually in the four tests and it is referred to the time required to reach the peak of temperature). The two experiments (step test and test in CT3) have a time constants of the same order: it is interesting to see how the Mach number influences the compensation. As observed in Fig. 5.31, the transfer functions differ among them and the effect of velocity (i.e. convection) interferes on the shape of the transfer function. This means that it does not exist a unique transfer function that can describe a dynamic phenomenon in all the frequencies: there is a certain dependence on the velocity of the flow. The question is which transfer function is more adapted to compensate the cold wire tested in the CT3.

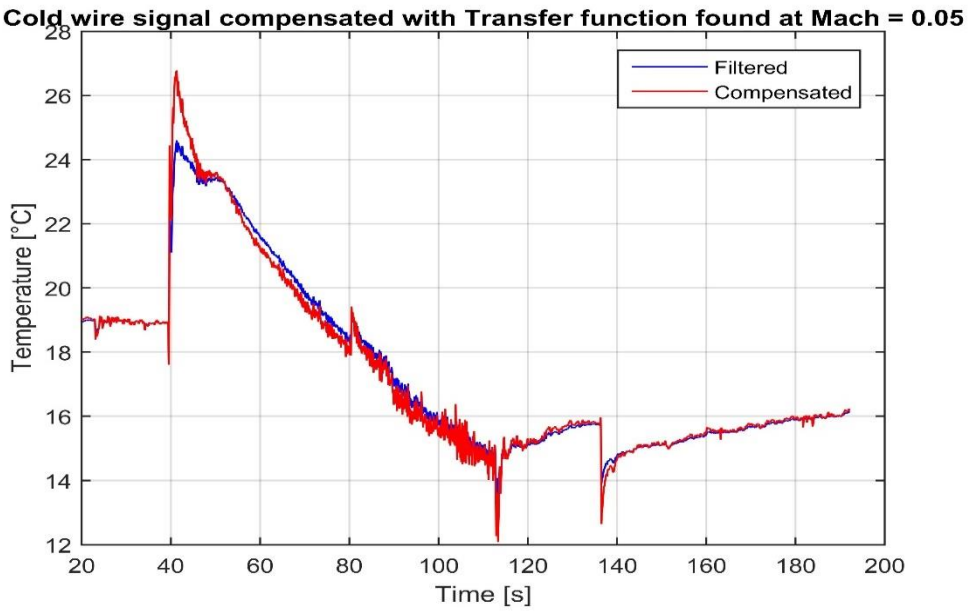

Figure 5.33: *Compensation with the transfer function obtained at Mach= 0.05.*

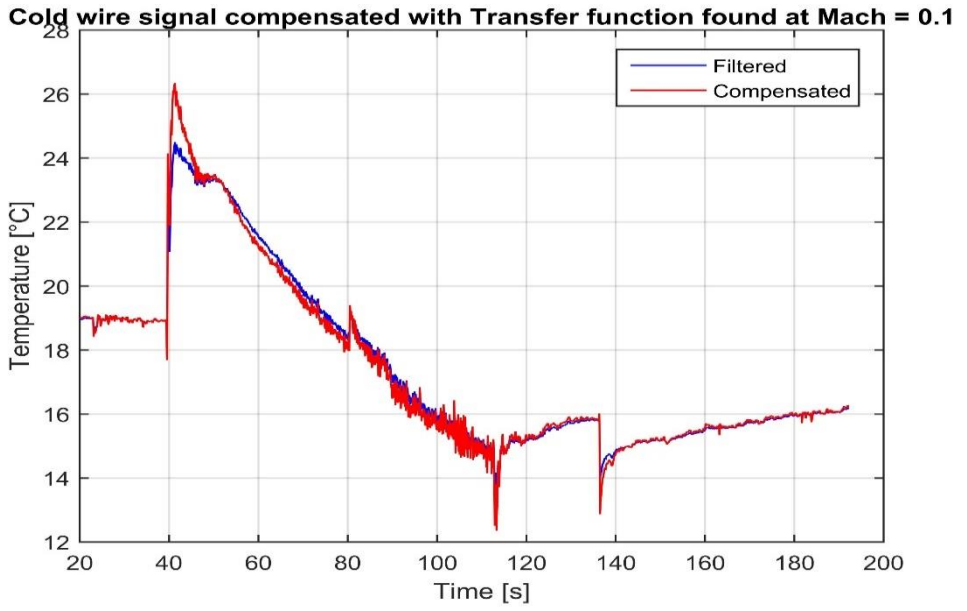

Figure 5.34: *Compensation with the transfer function obtained at Mach= 0.1.*

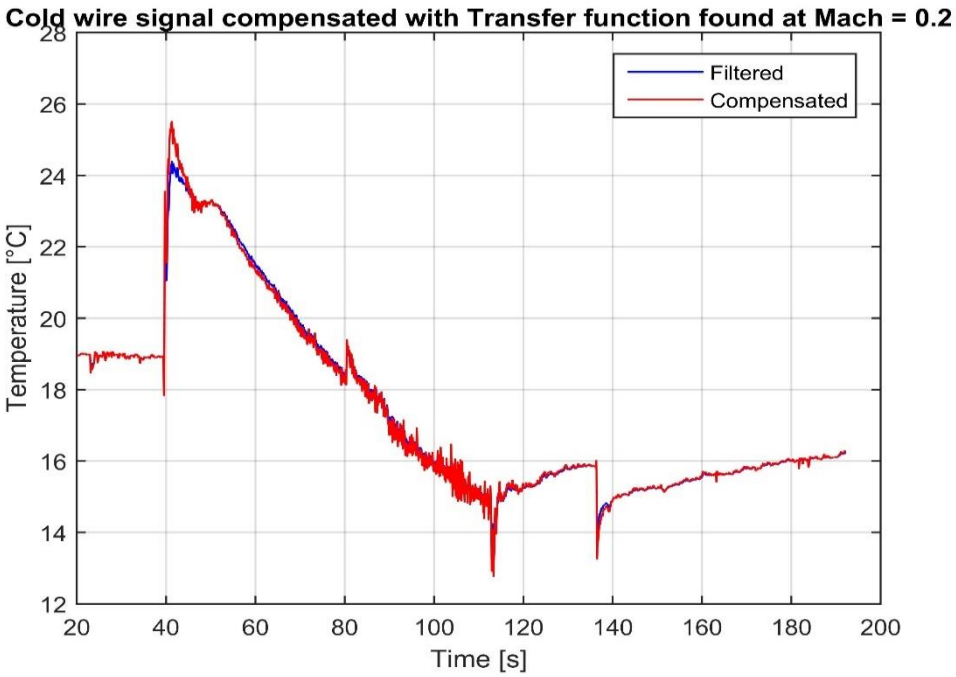

Figure 5.35: *Compensation with the transfer function obtained at Mach= 0.2.*

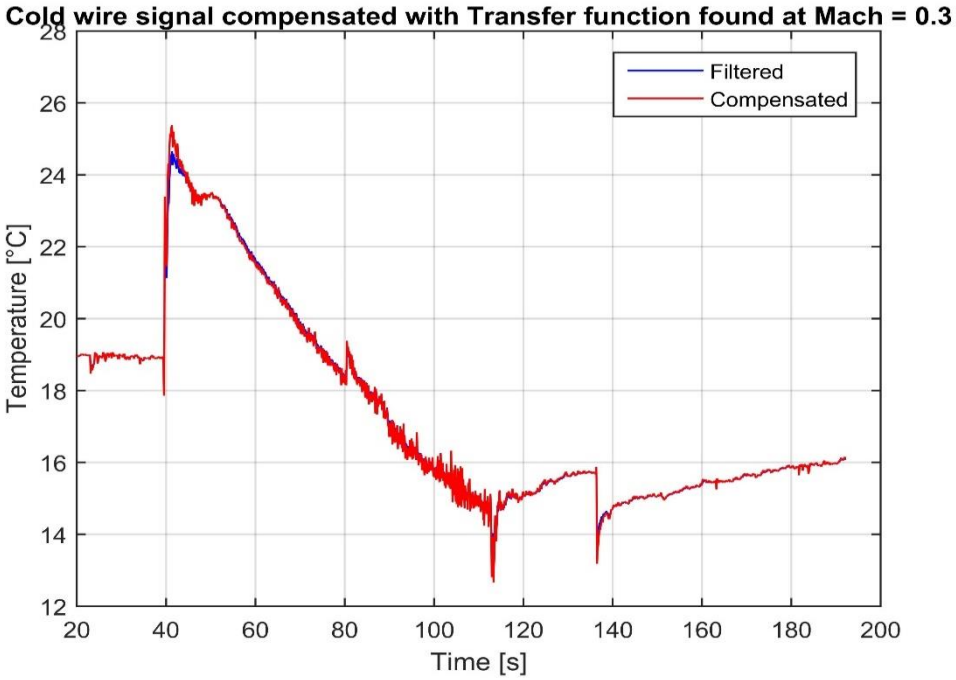

Figure 5.36: *Compensation with the transfer function obtained at Mach= 0.3.*

The test in CT3 has been done to test the cold wire in transient conditions when air at ambient pressure is injected in the test chamber and the turbine is rotating in vacuum conditions. The cold wire has to sense temperature variations in a different condition respect to the test done for the calibration. In effect the step test it's easy to be described: the air has a certain temperature, Mach number and impacts the cold wire perpendicularly as a narrow heated jet. The fluid dynamic inside the CT3 during this test is much more complicated and would deserve another study since we deal with a transient phenomenon from vacuum to ambient pressure conditions. The air enters in the chamber and two main events occur simultaneously: the 'chaotic' expansion inside the test chamber and the interaction of the flow with the rotating turbine. The flow impacting on the cold wire is not a jet with a known direction and velocity. A correct analysis should take into account the velocity and direction of the flow hitting the probe but no other transducers have been used in this test. For this reason the description of the results will be qualitative.

They are visible four different phases of this test: the first part at vacuum conditions; the second one when air is injected and impact the aero-brakes causing the rotor to decelerate; the third one when the rotor is brought to rest; the fourth one when air expands uniformly in the chamber without the interference of the rotor. The final temperature is lower respect the ambient temperature but we can see that it's not the final stable value (it's required a longer acquisition). There are some differences in the four compensated signals: the one with the highest peak at 40 seconds is the signal compensated with the transfer function obtained in the step test at Mach 0.05; as the Mach number increases the same peak is less compensated (has a smaller amplitude) and the compensated signal approaches the raw one. Aside from this peak, there are no significant differences in the compensation among the cases at different Mach number: the cold wire responds rather accurately also without compensation. We can conclude that for these tests the use of a transfer function respect to another is rather indifferent since the Mach number does not play an important influence. The cold wire is enough fast to reproduce the temperature in this kind of test. It would be interesting to see how behaves the cold wire in experiments with a smaller time constant using the same transfer functions used in this test (which has a time constant of 0.024 seconds).

5.3.5 Conclusions

The test in the CT3 has highlighted the effects of heating caused by the interaction of air with the rotor. After the abrupt peak caused by the contact of the turbine with air, the total temperature sensed by the cold wire decreases with the velocity of the rotor: the test chamber is slowly filled by air at ambient pressure which causes the rotor to decelerate.

The effect of compensation in this test are not particularly visible: the fast peak of temperature experienced at the opening of valves is compensated using four different transfer functions (obtained in step tests at 4 different Mach number and same time constant). The difference of temperature of the compensated signal respect to the raw signal is of about 1-2 degrees which means that the cold wire is enough fast for this test. The differences in the four compensations are not so clear: the more suitable transfer function should be the one that has been obtained in conditions similar to those experienced during the test in CT3. This comparison is not possible not disposing of enough accurate information of the flow around the cold wire.

A better characterization of the dynamic behaviour of the cold wire would be obtained realizing step tests with a lower step time constant (i.e higher injection velocity). It would be interesting to test these transfer functions for faster phenomena, for example increasing the velocity of the rotor and generating a higher and a faster temperature peak.

Bibliography

[1] IATA Economic Briefing. Airline Fuel and Labour cost share. February 2010

[2] J. Anthoine, T. Arts, H.L. Boerrigter, J.-M. Buchlin, M. Carbonaro, G. Degrez, R. Denos, D. Fletcher, D. Olivari, M.L. Riethmuller, R.A. Van den Braembussche, Measurement techniques in fluid dynamics, An introduction

[3] G. Paniagua, R. Dénos, M. Oropesa, Thermocouple probes for accurate temperature measurements in short duration facilities, April 2002

[4] R. Dénos, Sieverding CH (1997) Assessment of the cold wire resistance thermometer for high speed turbomachinery applications. Transactions of ASME: J. Turbomach 119: 1140-148

[5] Gilad Arwatz, Carla Bahri, Alexander J Smits and Marcus Hultmark, 28 August 2013. Dynamic calibration and modelling of a cold wire for temperature measurements. Mechanical and Aerospace Engineering. Princeton University, USA.

[6] D. Sergio Lavagnoli, DR. D. José Marìa Desantes, DR. D. Guillermo Paniagua, On the Aerothermal Flow Field in a Transonic HP Turbine Stage with a Multi-Profile LP Stator Vane.

Appendix A – Results of the analogue filter

Filterbox 1-Board 1-Channel 1

FILTERBOX	1		BOARD		1		CHANNEL		1			
FREQUENCY	RAW GAIN	RAW GAIN	LP GAIN	LP GAIN	HP GAIN	HP GAIN	RAW PHASE	RAW PHASE	LP PHASE	LP PHASE	HP PHASE	HP PHASE
[Hz]	[-]	[dB]	[-]	[dB]	[-]	[dB]	[deg]	[µs]	[deg]	[µs]	[deg]	[µs]
0,100	0,999	-0,009	1,008	0,071	0,051	-25,909	0,000	0,000	0,000	0,000	0,000	0,000
5,000	1,000	-0,002	0,959	-0,366	0,023	-32,619	-0,023	-12,667	-0,419	-233,000	177,036	98353,500
9,000	1,000	-0,002	0,959	-0,364	0,075	-22,494	-0,025	-7,714	-0,604	-186,571	176,401	54444,667
15,000	1,000	-0,002	0,964	-0,322	0,208	-13,629	-0,012	-2,308	-1,016	-188,231	171,622	31781,917
27,000	1,000	-0,002	0,959	-0,361	0,690	-3,225	-0,002	-0,200	-2,058	-211,760	164,412	16914,800
47,000	1,000	-0,002	0,960	-0,353	2,211	6,892	-0,009	-0,533	-3,705	-218,978	149,906	8859,682
81,000	1,000	-0,002	0,964	-0,315	6,888	16,762	0,006	0,203	-6,168	-211,532	116,295	3988,177
100,000	1,000	-0,002	0,967	-0,291	9,466	19,524	0,024	0,673	-7,666	-212,939	93,843	2606,745
142,000	1,000	-0,002	0,975	-0,217	11,323	21,079	0,007	0,136	-10,977	-214,721	57,108	1117,136
248,000	1,000	-0,002	1,008	0,071	10,595	20,502	0,051	0,573	-20,155	-225,752	26,676	298,789
433,000	1,000	-0,002	1,086	0,715	10,077	20,067	0,042	0,271	-40,357	-258,898	14,086	90,364
600,000	1,000	-0,002	1,095	0,789	9,946	19,953	0,091	0,423	-64,892	-300,428	9,912	45,890
757,000	1,000	-0,002	0,958	-0,371	9,893	19,906	0,061	0,224	-90,003	-330,262	7,714	28,306
900,000	1,000	-0,002	0,761	-2,376	9,866	19,883	0,061	0,189	-109,248	-337,184	6,420	19,815
1322,000	1,000	-0,003	0,355	-8,999	9,831	19,852	0,089	0,186	-139,799	-293,745	4,203	8,830
2308,000	0,999	-0,005	0,107	-19,397	9,812	19,835	0,153	0,185	-161,050	-193,831	2,074	2,496
4032,000	0,999	-0,010	0,034	-29,368	9,811	19,834	0,283	0,195	-173,788	-119,728	0,589	0,406
7043,000	0,997	-0,027	0,012	-38,541	9,821	19,843	0,473	0,187	-198,576	-78,319	0,763	0,301
12302,000	0,993	-0,061	0,010	-40,365	9,845	19,864	0,613	0,138	-251,139	-56,707	2,399	0,542
21487,000	0,987	-0,116	0,016	-35,918	9,873	19,889	0,734	0,095	-273,193	-35,318	5,027	0,650
37531,000	0,981	-0,165	0,027	-31,399	9,832	19,853	0,642	0,048	-283,298	-20,968	9,299	0,688
65555,000	0,978	-0,196	0,042	-27,536	6,820	16,676	0,437	0,019	-290,548	-12,311	62,759	2,659
		900 <fc< 1000 Hz			100< fc<142 Hz	37531 <fc< 65555 Hz						
	0,997	-0,028	0,989	-0,264	9,843	19,992						

Filterbox 1-Board 1-Channel 2

FILTERBOX	1		BOARD		1		CHANNEL		2			
FREQUENCY	RAW GAIN	RAW GAIN	LP GAIN	LP GAIN	HP GAIN	HP GAIN	RAW PHASE	RAW PHASE	LP PHASE	LP PHASE	HP PHASE	HP PHASE
[Hz]	[-]	[dB]	[-]	[dB]	[-]	[dB]	[deg]	[µs]	[deg]	[µs]	[deg]	[µs]
0,100	1,122	0,999	1,122	0,998	1,005	0,041	0,000	0,000	0,000	0,000	0,000	0,000
5,000	1,000	-0,002	0,962	-0,335	0,024	-32,452	-0,051	-28,333	-0,394	-219,000	177,012	98340,000
9,000	1,000	-0,004	0,962	-0,334	0,077	-22,313	0,046	14,143	-0,721	-222,571	175,305	54106,429
15,000	1,000	-0,002	0,962	-0,333	0,212	-13,481	-0,014	-2,539	-1,161	-214,923	172,351	31916,923
27,000	1,000	-0,002	0,963	-0,328	0,703	-3,066	-0,014	-1,400	-2,068	-212,720	164,439	16917,560
47,000	1,000	-0,002	0,964	-0,316	2,256	7,067	0,001	0,044	-3,469	-205,044	150,147	8873,932
81,000	1,000	-0,002	0,968	-0,285	7,015	16,921	0,006	0,190	-6,172	-211,671	116,024	3978,859
100,704	1,000	-0,002	0,970	-0,262	9,720	19,754	-0,039	-1,087	-7,607	-209,826	-467233,043	-12887948,642
142,000	1,000	-0,001	0,979	-0,185	11,464	21,187	0,011	0,221	-10,965	-214,496	56,818	1111,471
248,000	1,000	-0,002	1,012	0,106	10,716	20,601	0,046	0,518	-20,113	-225,276	26,559	297,478
433,000	1,000	-0,002	1,091	0,757	10,194	20,167	0,056	0,360	-40,279	-258,397	14,026	89,981
600,000	1,000	-0,002	1,101	0,839	10,062	20,054	0,077	0,356	-64,836	-300,166	9,879	45,734
757,000	1,000	-0,002	0,964	-0,320	10,008	20,007	0,059	0,217	-90,051	-330,438	7,702	28,262
900,000	1,000	-0,002	0,765	-2,330	9,981	19,983	0,058	0,180	-109,339	-337,467	6,398	19,748
1322,000	1,000	-0,002	0,356	-8,959	9,946	19,953	0,080	0,169	-139,698	-293,533	4,187	8,798
2308,000	1,000	-0,004	0,108	-19,302	9,927	19,937	0,142	0,171	-160,464	-193,125	2,096	2,523
4032,000	0,999	-0,009	0,034	-29,328	9,926	19,936	0,278	0,192	-173,578	-119,583	0,635	0,437
7043,000	0,997	-0,026	0,012	-38,445	9,936	19,944	0,458	0,181	-198,109	-78,135	0,698	0,275
12302,000	0,993	-0,060	0,009	-40,689	9,961	19,966	0,617	0,139	-251,374	-56,760	2,285	0,516
21487,000	0,987	-0,114	0,015	-36,229	9,989	19,991	0,735	0,095	-271,427	-35,089	4,808	0,622
37531,000	0,981	-0,163	0,027	-31,481	9,936	19,945	0,645	0,048	-278,430	-20,607	9,521	0,705
65555,000	0,978	-0,195	0,045	-26,918	6,694	16,514	0,431	0,018	-285,533	-12,099	63,735	2,701
114503,000	0,975	-0,217	0,076	-22,334	3,571	11,055	0,285	0,007	-64,219	-1,558	119,153	2,891
200000,000	0,972	-0,250	0,122	-18,266	1,911	5,626	0,000	0,000	-297,013	-4,125	216,000	3,000
		900 < fc < 1000 Hz			1322 <fc< 37531 Hz	100<fc<37531 Hz						
	0,995	-0,046	0,966	-0,166	9,946	20,102						

Filterbox 1-Board 1-Channel 3

FILTERBOX	1		BOARD		1		CHANNEL		3			
FREQUENCY	RAW GAIN	RAW GAIN	LP GAIN	LP GAIN	HP GAIN	HP GAIN	RAW PHASE	RAW PHASE	LP PHASE	LP PHASE	HP PHASE	HP PHASE
[Hz]	[-]	[dB]	[-]	[dB]	[-]	[dB]	[deg]	[µs]	[deg]	[µs]	[deg]	[µs]
0,100	1,000	0,000	0,951	-0,435	0,041	-27,727	0,000	0,000	0,000	0,000	0,000	0,000
5,000	1,000	-0,001	0,913	-0,787	0,022	-32,988	0,021	11,667	-0,403	-223,667	178,291	99050,667
9,000	1,000	-0,002	0,914	-0,784	0,072	-22,858	-0,022	-6,714	-0,690	-213,000	174,316	53801,167
15,000	1,000	-0,002	0,914	-0,785	0,200	-13,980	-0,006	-1,154	-1,149	-212,692	173,379	32107,167
27,000	1,000	-0,001	0,914	-0,780	0,663	-3,564	0,015	1,560	-2,079	-213,840	164,191	16892,083
47,000	1,000	-0,002	0,915	-0,769	2,124	6,542	0,000	-0,022	-3,257	-192,511	150,096	8870,909
81,000	1,000	-0,002	0,919	-0,736	6,589	16,377	0,010	0,354	-6,154	-211,051	115,854	3973,051
100,000	1,000	-0,002	0,921	-0,711	9,024	19,108	0,021	0,571	-7,656	-212,653	93,434	2595,398
142,000	1,000	-0,002	0,929	-0,637	10,781	20,653	0,008	0,150	-11,016	-215,493	57,033	1115,679
248,000	1,000	-0,002	0,960	-0,350	10,118	20,102	0,048	0,541	-20,140	-225,577	26,737	299,472
433,000	1,000	-0,002	1,034	0,289	9,634	19,676	0,055	0,353	-40,389	-259,102	14,130	90,647
600,000	1,000	-0,002	1,043	0,362	9,512	19,565	0,086	0,396	-64,859	-300,273	9,952	46,074
757,000	1,000	-0,002	0,913	-0,793	9,461	19,519	0,049	0,180	-89,985	-330,195	7,762	28,483
900,000	1,000	-0,002	0,725	-2,790	9,436	19,496	0,051	0,157	-109,078	-336,661	6,439	19,872
1322,000	1,000	-0,002	0,339	-9,396	9,404	19,466	0,087	0,183	-139,513	-293,143	4,222	8,871
2308,000	1,000	-0,004	0,103	-19,724	9,386	19,450	0,158	0,190	-160,459	-193,119	2,089	2,515
4032,000	0,999	-0,010	0,033	-29,731	9,385	19,449	0,286	0,197	-172,951	-119,152	0,607	0,418
7043,000	0,997	-0,026	0,011	-38,991	9,395	19,458	0,445	0,175	-196,256	-77,404	0,725	0,286
12302,000	0,993	-0,061	0,008	-42,103	9,419	19,480	0,614	0,139	-249,711	-56,384	2,368	0,535
21487,000	0,987	-0,115	0,013	-37,728	9,447	19,506	0,744	0,096	-273,811	-35,397	4,967	0,642
37531,000	0,981	-0,164	0,023	-32,881	9,425	19,485	0,640	0,047	-284,201	-21,035	8,997	0,666
65555,000	0,978	-0,195	0,039	-28,231	6,767	16,607	0,441	0,019	-290,115	-12,293	60,552	2,566
			900 < fc <1000 Hz		900<fc<37531 Hz	100<fc< 37531 Hz						
	0,997	-0,027	0,925	-0,693	9,412	19,601						

Filterbox 1-Board 1-Channel 4

FILTERBOX	1		BOARD		1		CHANNEL		4			
FREQUENCY	RAW GAIN	RAW GAIN	LP GAIN	LP GAIN	HP GAIN	HP GAIN	RAW PHASE	RAW PHASE	LP PHASE	LP PHASE	HP PHASE	HP PHASE
[Hz]	[-]	[dB]	[-]	[dB]	[-]	[dB]	[deg]	[µs]	[deg]	[µs]	[deg]	[µs]
0,100	1,122	0,998	1,118	0,967	1,005	0,040	0,000	0,000	0,000	0,000	0,000	0,000
5,000	1,000	-0,002	0,929	-0,643	0,022	-32,963	-0,042	-23,500	-0,455	-252,750	180,050	100027,500
9,000	1,000	-0,002	0,929	-0,642	0,073	-22,689	0,008	2,429	-0,680	-209,857	174,814	53955,000
15,000	1,000	-0,002	0,929	-0,640	0,202	-13,900	0,016	2,923	-1,154	-213,769	171,756	31806,692
27,000	1,000	-0,002	0,929	-0,637	0,671	-3,462	0,011	1,120	-2,059	-211,880	164,263	16899,500
47,000	1,000	-0,001	0,931	-0,621	2,155	6,669	0,012	0,733	-3,422	-202,267	150,277	8881,622
81,000	1,000	-0,002	0,934	-0,592	6,688	16,506	0,013	0,456	-6,149	-210,861	115,571	3963,329
100,000	1,000	-0,002	0,937	-0,568	9,143	19,222	0,018	0,490	-7,635	-212,092	92,958	2582,153
142,000	1,000	-0,002	0,945	-0,494	10,854	20,712	0,017	0,332	-10,940	-214,007	56,514	1105,514
248,000	1,000	-0,002	0,977	-0,204	10,149	20,129	0,047	0,524	-20,032	-224,378	26,457	296,341
433,000	1,000	-0,002	1,053	0,446	9,660	19,700	0,053	0,343	-40,173	-257,717	13,991	89,758
600,000	1,000	-0,002	1,063	0,534	9,536	19,588	0,079	0,366	-64,671	-299,401	9,853	45,614
757,000	1,000	-0,002	0,932	-0,613	9,486	19,541	0,074	0,273	-89,884	-329,825	7,668	28,139
900,000	1,000	-0,002	0,740	-2,613	9,460	19,518	0,059	0,183	-109,107	-336,749	6,369	19,658
1322,000	1,000	-0,002	0,345	-9,242	9,428	19,488	0,087	0,183	-139,677	-293,489	4,168	8,757
2308,000	1,000	-0,004	0,105	-19,607	9,410	19,472	0,151	0,182	-161,092	-193,882	2,063	2,483
4032,000	0,999	-0,010	0,033	-29,650	9,409	19,471	0,287	0,198	-177,156	-122,049	0,595	0,410
7043,000	0,997	-0,026	0,013	-37,716	9,418	19,479	0,464	0,183	-213,998	-84,402	0,747	0,295
12302,000	0,993	-0,060	0,015	-36,427	9,443	19,502	0,610	0,138	-261,856	-59,127	2,354	0,532
21487,000	0,987	-0,114	0,026	-31,602	9,471	19,528	0,739	0,096	-276,739	-35,776	4,946	0,639
37531,000	0,981	-0,163	0,044	-27,130	9,444	19,503	0,640	0,047	-285,844	-21,156	9,243	0,684
65555,000	0,978	-0,195	0,067	-23,526	6,522	16,288	0,441	0,019	-293,089	-12,419	62,951	2,667
114502,000	0,975	-0,217	0,079	-22,007	3,472	10,811	0,286	0,007	-36,522	-0,886	239,707	5,815
200000,000	0,971	-0,253	0,108	-19,361	1,990	5,978	0,287	0,004	-6,357	-0,088	190,411	2,645
			900 < fc <1000		900 < fc < 37531 Hz	100 <fc < 37531						
	1,000	-0,004	0,938	-0,452	9,435	19,632						

Filterbox 1-Board 2-Channel 1

FILTERBOX	1,000		BOARD		2,000		CHANNEL		1,000			
FREQUENCY	RAW GAIN	RAW GAIN	LP GAIN	LP GAIN	HP GAIN	HP GAIN	RAW PHASE	RAW PHASE	LP PHASE	LP PHASE	HP PHASE	HP PHASE
[Hz]	[-]	[dB]	[-]	[dB]	[-]	[dB]	[deg]	[µs]	[deg]	[µs]	[deg]	[µs]
0,100	1,122	1,000	1,125	1,022	1,003	0,030	0,000		0,000		0,000	
5,000	1,000	-0,001	0,989	-0,099	0,023	-32,907	-0,002	-1,333	-0,336	-186,667	174,248	96804,500
9,000	1,000	-0,002	0,988	-0,101	0,074	-22,627	0,002	0,714	-0,725	-223,857	175,866	54279,714
15,000	1,000	-0,001	0,989	-0,098	0,205	-13,785	0,013	2,385	-1,198	-221,923	171,782	31811,461
27,000	1,000	-0,002	0,989	-0,095	0,679	-3,357	-0,002	-0,160	-2,036	-209,440	164,126	16885,440
47,000	1,000	-0,002	0,990	-0,086	2,178	6,761	-0,009	-0,556	-3,704	-218,933	149,787	8852,644
81,000	1,000	-0,002	0,994	-0,051	6,770	16,612	-0,001	-0,037	-6,185	-212,089	116,193	3984,679
100,000	1,000	-0,002	0,997	-0,025	9,294	19,364	-0,006	-0,163	-7,692	-213,673	93,762	2604,490
142,000	1,000	-0,001	1,006	0,049	11,120	20,922	0,012	0,229	-11,046	-216,086	57,136	1117,686
248,000	1,000	-0,002	1,039	0,336	10,421	20,358	0,045	0,502	-20,298	-227,358	26,729	299,380
433,000	1,000	-0,002	1,119	0,974	9,916	19,927	0,061	0,390	-40,605	-260,490	14,112	90,529
600,000	1,000	-0,002	1,126	1,030	9,788	19,814	0,081	0,375	-65,235	-302,015	9,943	46,033
757,000	1,000	-0,002	0,982	-0,155	9,736	19,768	0,062	0,226	-90,324	-331,442	7,751	28,442
900,000	1,000	-0,002	0,779	-2,175	9,710	19,744	0,065	0,200	-109,481	-337,904	6,425	19,831
1322,000	1,000	-0,002	0,363	-8,795	9,676	19,714	0,090	0,189	-139,699	-293,535	4,212	8,850
2308,000	1,000	-0,004	0,111	-19,130	9,657	19,697	0,134	0,161	-160,547	-193,226	2,090	2,515
4032,000	0,999	-0,010	0,035	-29,168	9,656	19,696	0,281	0,194	-173,646	-119,630	0,609	0,420
7043,000	0,997	-0,026	0,012	-38,410	9,665	19,704	0,458	0,181	-200,421	-79,047	0,725	0,286
12302,000	0,993	-0,060	0,010	-40,159	9,691	19,727	0,606	0,137	-252,180	-56,942	357,660	80,759
21487,000	0,987	-0,114	0,017	-35,619	9,718	19,752	0,741	0,096	-274,458	-35,481	4,909	0,635
37531,000	0,981	-0,163	0,028	-30,921	9,684	19,721	0,624	0,046	-283,258	-20,965	8,910	0,659
65555,000	0,978	-0,194	0,045	-26,908	6,833	16,692	0,441	0,019	-289,965	-12,287	61,361	2,600
114503,000	0,975	-0,217	0,067	-23,493	3,632	11,202	0,289	0,007	-311,106	-7,547	117,264	2,845
200000,000	0,971	-0,253	0,095	-20,414	2,055	6,255	0,264	0,004	-338,010	-4,695	192,621	2,675
			900<fc<1000 Hz		81< fc < 100 Hz	37531<fc<65555 Hz						
	0,995	-0,046	0,998	0,038	9,682	19,851						

Filterbox 1-Board 2-Channel 2

FILTERBOX	1,000		BOARD		2,000		CHANNEL		2,000			
FREQUENCY	RAW GAIN	RAW GAIN	LP GAIN	LP GAIN	HP GAIN	HP GAIN	RAW PHASE	RAW PHASE	LP PHASE	LP PHASE	HP PHASE	HP PHASE
[Hz]	[-]	[dB]	[-]	[dB]	[-]	[dB]	[deg]	[µs]	[deg]	[µs]	[deg]	[µs]
0,100	1,122	1,001	1,121	0,994	1,004	0,032	0,000		0,000		0,000	
5,000	1,000	-0,002	0,969	-0,269	0,021	-33,541	0,018	9,750	-0,369	-204,750	180,587	100326,333
9,000	1,000	-0,003	0,969	-0,269	0,068	-23,301	-0,007	-2,286	-0,604	-186,571	174,908	53983,833
15,000	1,000	-0,003	0,969	-0,269	0,190	-14,429	-0,001	-0,154	-1,131	-209,385	172,099	31870,231
27,000	1,000	-0,002	0,970	-0,264	0,630	-4,012	-0,007	-0,760	-2,061	-212,080	164,392	16912,760
47,000	1,000	-0,002	0,972	-0,251	2,025	6,127	-0,028	-1,644	-3,653	-215,889	150,332	8884,864
81,000	1,000	-0,002	0,975	-0,221	6,334	16,033	0,007	0,253	-6,200	-212,620	116,410	3992,115
100,000	1,000	-0,002	0,978	-0,196	8,711	18,801	0,010	0,265	-7,704	-214,010	93,723	2603,408
142,000	1,000	-0,001	0,986	-0,124	10,377	20,321	0,012	0,243	-11,080	-216,750	56,757	1110,279
248,000	1,000	-0,002	1,018	0,157	9,663	19,702	0,045	0,504	-20,289	-227,256	26,421	295,931
433,000	1,000	-0,002	1,093	0,776	9,179	19,256	0,039	0,253	-40,567	-260,244	13,960	89,555
600,000	1,000	-0,002	1,099	0,819	9,058	19,140	0,082	0,380	-65,021	-301,022	9,825	45,485
757,000	1,000	-0,002	0,960	-0,353	9,008	19,093	0,058	0,212	-89,934	-330,008	7,660	28,107
900,000	1,000	-0,002	0,763	-2,345	8,983	19,069	0,060	0,186	-108,989	-336,386	6,347	19,589
1322,000	1,000	-0,002	0,358	-8,922	8,951	19,038	0,089	0,187	-139,290	-292,675	4,165	8,752
2308,000	1,000	-0,004	0,109	-19,233	8,934	19,021	0,146	0,175	-160,200	-192,808	2,088	2,513
4032,000	0,999	-0,009	0,034	-29,257	8,933	19,020	0,285	0,196	-173,343	-119,422	0,632	0,435
7043,000	0,997	-0,026	0,012	-38,373	8,942	19,029	0,466	0,184	-197,620	-77,942	0,672	0,265
12302,000	0,993	-0,060	0,010	-40,325	8,967	19,053	0,614	0,139	-249,430	-56,321	2,215	0,500
21487,000	0,987	-0,114	0,016	-35,945	8,995	19,080	0,734	0,095	-269,817	-34,881	4,713	0,609
37531,000	0,982	-0,162	0,027	-31,226	8,988	19,073	0,630	0,047	-276,342	-20,453	8,870	0,657
65555,000	0,978	-0,194	0,047	-26,566	6,885	16,759	0,438	0,019	-282,809	-11,984	55,087	2,334
114503,000	0,975	-0,216	0,077	-22,275	3,639	11,221	0,292	0,007	-65,161	-1,581	110,772	2,687
200000,000	0,971	-0,256	0,136	-17,347	1,987	5,966	0,267	0,004	-330,755	-4,594	174,168	2,419
			900 < fc < 1000		81<fc<100 Hz	37531<fc<65555 Hz						
	0,995	-0,046	0,979	-0,130	8,962	19,193						

Filterbox 1-Board 2-Channel 3

FILTERBOX	1		BOARD		2		CHANNEL		3			
FREQUENCY	RAW GAIN	RAW GAIN	LP GAIN	LP GAIN	HP GAIN	HP GAIN	RAW PHASE	RAW PHASE	LP PHASE	LP PHASE	HP PHASE	HP PHASE
[Hz]	[-]	[dB]	[-]	[dB]	[-]	[dB]	[deg]	[µs]	[deg]	[µs]	[deg]	[µs]
0,100	1,122	1,001	1,122	1,003	1,004	0,032	0,000		0,000		0,000	0,000
5,000	1,000	-0,002	0,969	-0,277	0,023	-32,655	-0,010	-5,667	-0,436	-242,333	177,179	98432,500
9,000	1,000	-0,003	0,969	-0,277	0,076	-22,435	-0,022	-6,714	-0,711	-219,571	174,874	53973,429
15,000	1,000	-0,002	0,969	-0,275	0,210	-13,574	0,023	4,308	-1,174	-217,461	171,235	31710,167
27,000	1,000	-0,001	0,969	-0,272	0,696	-3,153	0,019	1,960	-2,082	-214,160	164,318	16905,167
47,000	1,000	-0,001	0,971	-0,254	2,230	6,965	-0,007	-0,422	-3,445	-203,600	150,675	8905,136
81,000	1,000	-0,001	0,974	-0,228	6,934	16,820	0,004	0,139	-6,222	-213,380	116,478	3994,430
100,000	1,000	-0,001	0,977	-0,202	9,538	19,589	0,012	0,347	-7,734	-214,845	94,102	2613,939
142,000	1,000	-0,001	0,985	-0,130	11,452	21,177	0,009	0,186	-11,091	-216,964	57,406	1122,957
248,000	1,000	-0,001	1,018	0,155	10,739	20,620	0,041	0,455	-20,332	-227,728	26,850	300,736
433,000	1,000	-0,002	1,094	0,782	10,217	20,187	0,040	0,258	-40,648	-260,765	14,164	90,868
600,000	1,000	-0,002	1,100	0,828	10,085	20,073	0,079	0,366	-65,198	-301,844	9,981	46,209
757,000	1,000	-0,002	0,960	-0,356	10,030	20,026	0,058	0,213	-90,237	-331,119	7,778	28,540
900,000	1,000	-0,002	0,762	-2,365	10,003	20,003	0,065	0,202	-109,350	-337,499	6,454	19,921
1322,000	1,000	-0,002	0,356	-8,962	9,968	19,972	0,088	0,184	-139,572	-293,268	4,228	8,885
2308,000	1,000	-0,004	0,109	-19,277	9,950	19,956	0,147	0,176	-160,316	-192,947	2,098	2,525
4032,000	0,999	-0,009	0,034	-29,292	9,948	19,955	0,282	0,195	-173,207	-119,328	0,622	0,428
7043,000	0,997	-0,026	0,012	-38,593	9,958	19,964	0,452	0,178	-196,939	-77,673	0,731	0,288
12302,000	0,993	-0,059	0,008	-41,456	9,985	19,987	0,615	0,139	-248,837	-56,187	2,367	0,535
21487,000	0,987	-0,113	0,014	-37,157	10,012	20,011	0,737	0,095	-273,419	-35,347	4,968	0,642
37531,000	0,982	-0,162	0,024	-32,276	9,973	19,977	0,631	0,047	-283,600	-20,990	349,812	25,891
65555,000	0,978	-0,193	0,042	-27,536	6,663	16,473	0,432	0,018	-286,870	-12,156	295,051	12,502
114503,000	0,975	-0,216	0,078	-22,181	3,548	11,001	0,285	0,007	-305,921	-7,421	121,519	2,948
200000,000	0,972	-0,251	0,101	-19,956	1,850	5,342	0,000	0,000	-10,866	-0,151	154,374	2,144
			900<fc<1000		81<fc<100 Hz	37531<fc<65555 Hz						
	0,995	-0,046	0,978	-0,133	9,969	20,107						

Filterbox 1-Board 2-Channel 4

FILTERBOX	1		BOARD		2		CHANNEL		4			
FREQUENCY	RAW GAIN	RAW GAIN	LP GAIN	LP GAIN	HP GAIN	HP GAIN	RAW PHASE	RAW PHASE	LP PHASE	LP PHASE	HP PHASE	HP PHASE
[Hz]	[-]	[dB]	[-]	[dB]	[-]	[dB]	[deg]	[µs]	[deg]	[µs]	[deg]	[µs]
0,100	1,122	1,001	1,119	0,977	1,003	0,028	0,000		0,000		0,000	0,000
5,000	1,000	-0,002	0,945	-0,493	0,023	-32,782	0,023	13,000	-0,561	-311,667	175,978	97765,667
9,000	1,000	-0,002	0,945	-0,493	0,073	-22,699	-0,013	-4,000	-0,691	-213,286	176,559	54493,667
15,000	1,000	-0,001	0,945	-0,493	0,204	-13,824	0,011	2,077	-1,124	-208,231	171,888	31831,167
27,000	1,000	-0,002	0,945	-0,489	0,675	-3,412	-0,007	-0,720	-2,035	-209,400	164,237	16896,800
47,000	1,000	-0,002	0,946	-0,478	2,167	6,718	-0,001	-0,044	-3,679	-217,444	149,830	8855,222
81,000	1,000	-0,001	0,950	-0,444	6,731	16,561	0,010	0,329	-6,153	-211,025	116,154	3983,342
100,000	1,000	-0,002	0,953	-0,420	9,239	19,312	0,014	0,378	-7,622	-211,714	93,722	2603,402
142,000	1,000	-0,001	0,961	-0,344	11,049	20,866	0,004	0,071	-10,947	-214,143	57,105	1117,079
248,000	1,000	-0,002	0,994	-0,051	10,351	20,300	0,053	0,589	-20,076	-224,870	26,709	299,159
433,000	1,000	-0,002	1,072	0,606	9,849	19,868	0,051	0,329	-40,297	-258,513	14,102	90,469
600,000	1,000	-0,002	1,083	0,693	9,723	19,756	0,077	0,355	-64,901	-300,470	9,937	46,005
757,000	1,000	-0,002	0,947	-0,473	9,670	19,709	0,062	0,229	-90,225	-331,075	7,750	28,440
900,000	1,000	-0,002	0,750	-2,493	9,644	19,686	0,064	0,197	-109,505	-337,978	6,432	19,853
1322,000	1,000	-0,002	0,349	-9,147	9,611	19,655	0,092	0,192	-139,940	-294,042	4,210	8,847
2308,000	1,000	-0,004	0,106	-19,522	9,593	19,639	0,144	0,173	-161,313	-194,147	2,079	2,503
4032,000	0,999	-0,009	0,033	-29,571	9,592	19,638	0,282	0,194	-177,542	-122,315	0,608	0,419
7043,000	0,997	-0,026	0,013	-37,565	9,601	19,647	0,448	0,177	-216,356	-85,331	0,713	0,281
12302,000	0,993	-0,059	0,016	-35,988	9,627	19,670	0,608	0,137	-262,911	-59,365	2,360	0,533
21487,000	0,987	-0,113	0,028	-31,102	9,655	19,695	0,742	0,096	-276,562	-35,753	4,960	0,641
37531,000	0,982	-0,162	0,047	-26,610	9,623	19,666	0,636	0,047	-284,840	-21,082	9,506	0,704
65555,000	0,978	-0,193	0,071	-22,937	6,573	16,356	0,435	0,018	-292,890	-12,411	63,555	2,693
114503,000	0,975	-0,216	0,085	-21,372	3,500	10,882	0,294	0,007	-41,577	-1,009	120,556	2,925
200000,000	0,971	-0,252	0,113	-18,939	1,992	5,986	0,261	0,004	-3,846	-0,053	192,018	2,667
			900< fc <1322		81<fc<100 Hz	37531<fc<65555 Hz						
	0,995	-0,046	0,954	-0,314	9,618	19,793						

Filterbox 1-Board 3-Channel 1

FILTERBOX	1		BOARD		3		CHANNEL		1			
FREQUENCY	RAW GAIN	RAW GAIN	LP GAIN	LP GAIN	HP GAIN	HP GAIN	RAW PHASE	RAW PHASE	LP PHASE	LP PHASE	HP PHASE	HP PHASE
[Hz]	[-]	[dB]	[-]	[dB]	[-]	[dB]	[deg]	[µs]	[deg]	[µs]	[deg]	[µs]
0,100	1,122	1,001	1,121	0,991	1,003	0,029	0,000	0,000	0,000	0,000	0,000	0,000
5,000	1,000	-0,003	0,954	-0,412	0,023	-32,818	-0,004	-2,333	-0,505	-280,667	177,518	98621,000
9,000	1,000	-0,001	0,954	-0,409	0,073	-22,699	-0,020	-6,286	-0,624	-192,571	176,850	54583,429
15,000	1,000	-0,001	0,954	-0,409	0,203	-13,837	0,005	1,000	-1,294	-239,539	173,554	32139,692
27,000	1,000	-0,002	0,955	-0,404	0,674	-3,426	0,017	1,800	-2,077	-213,640	164,443	16918,040
47,000	1,000	-0,002	0,955	-0,396	2,163	6,702	0,001	0,044	-3,452	-204,000	150,440	8891,273
81,000	1,000	-0,002	0,959	-0,363	6,772	16,614	-0,008	-0,291	-6,185	-212,089	116,700	4002,063
100,000	1,000	-0,001	0,962	-0,337	9,333	19,401	0,017	0,469	-7,617	-211,582	94,110	2614,163
142,000	1,000	-0,001	0,970	-0,264	11,168	20,960	0,001	0,014	-10,979	-214,763	57,109	1117,164
248,000	1,000	-0,001	1,002	0,019	10,417	20,355	0,030	0,341	-20,116	-225,313	26,586	297,785
433,000	1,000	-0,001	1,078	0,650	9,896	19,909	0,053	0,339	-40,215	-257,984	14,026	89,981
600,000	1,000	-0,002	1,087	0,725	9,765	19,793	0,074	0,341	-64,563	-298,903	9,876	45,722
757,000	1,000	-0,002	0,954	-0,414	9,711	19,745	0,051	0,187	-89,518	-328,483	7,700	28,254
900,000	1,000	-0,002	0,759	-2,393	9,684	19,721	0,064	0,196	-108,749	-335,645	6,381	19,695
1322,000	1,000	-0,002	0,356	-8,978	9,649	19,690	0,093	0,196	-139,266	-292,624	4,182	8,786
2308,000	1,000	-0,004	0,108	-19,312	9,631	19,673	0,147	0,176	-160,421	-193,074	2,071	2,493
4032,000	0,999	-0,009	0,034	-29,354	9,629	19,672	0,292	0,201	-173,629	-119,619	0,605	0,417
7043,000	0,997	-0,026	0,012	-38,489	9,639	19,680	0,447	0,176	-200,204	-78,961	0,701	0,276
12302,000	0,993	-0,059	0,010	-40,366	9,664	19,703	0,603	0,136	-254,410	-57,445	2,319	0,524
21487,000	0,987	-0,113	0,016	-35,731	9,692	19,728	0,733	0,095	-274,466	-35,482	4,866	0,629
37531,000	0,982	-0,161	0,028	-30,977	9,671	19,709	0,635	0,047	-284,002	-21,020	8,895	0,658
65555,000	0,978	-0,193	0,045	-27,026	7,074	16,994	0,437	0,019	-288,923	-12,243	59,017	2,501
114503,000	0,975	-0,215	0,065	-23,692	3,759	11,501	0,295	0,007	-48,489	-1,176	114,463	2,777
200000,000	0,971	-0,251	0,090	-20,877	1,952	5,810	0,000	0,000	-12,884	-0,179	208,328	2,893
			900 < fc < 1000		81< fc < 100 Hz	37531 < fc < 65555 Hz						
	0,995	-0,046	0,963	-0,244	9,649	19,839						

Filterbox 1-Board 3-Channel 2

FILTERBOX	1		BOARD		3		CHANNEL		2			
FREQUENCY	RAW GAIN	RAW GAIN	LP GAIN	LP GAIN	HP GAIN	HP GAIN	RAW PHASE	RAW PHASE	LP PHASE	LP PHASE	HP PHASE	HP PHASE
[Hz]	[-]	[dB]	[-]	[dB]	[-]	[dB]	[deg]	[µs]	[deg]	[µs]	[deg]	[µs]
0,100	1,122	1,000	1,124	1,013	1,004	0,034	0,000	0,000	0,000	0,000	0,000	0,000
5,000	1,000	0,000	0,974	-0,226	0,023	-32,655	-0,011	-6,000	-0,484	-269,000	174,899	97166,333
9,000	1,000	-0,001	0,975	-0,224	0,075	-22,466	-0,014	-4,429	-0,600	-185,143	174,635	53899,714
15,000	1,000	-0,002	0,975	-0,223	0,209	-13,615	-0,001	-0,154	-1,096	-203,000	170,303	31537,667
27,000	1,000	-0,001	0,975	-0,219	0,691	-3,210	-0,009	-0,880	-2,027	-208,520	164,110	16883,792
47,000	1,000	-0,001	0,976	-0,208	2,213	6,900	-0,012	-0,689	-3,492	-206,400	150,019	8866,400
81,000	1,000	-0,001	0,980	-0,175	6,854	16,719	0,016	0,544	-6,107	-209,418	115,771	3970,190
100,000	1,000	-0,001	0,983	-0,150	9,381	19,445	0,000	0,010	-7,579	-210,520	93,380	2593,898
142,000	1,000	-0,001	0,991	-0,076	11,205	20,988	0,008	0,150	-10,928	-213,771	57,036	1115,721
248,000	1,000	-0,002	1,025	0,212	10,523	20,443	0,033	0,374	-20,007	-224,089	26,769	299,829
433,000	1,000	-0,001	1,104	0,862	10,023	20,020	0,060	0,385	-40,076	-257,098	14,139	90,703
600,000	1,000	-0,002	1,116	0,957	9,896	19,909	0,066	0,308	-64,487	-298,551	9,966	46,139
757,000	1,000	-0,002	0,980	-0,175	9,844	19,863	0,048	0,176	-89,594	-328,760	7,779	28,543
900,000	1,000	-0,002	0,779	-2,165	9,818	19,840	0,051	0,157	-108,954	-336,279	6,469	19,967
1322,000	1,000	-0,002	0,364	-8,779	9,784	19,810	0,087	0,183	-139,498	-293,111	4,235	8,899
2308,000	1,000	-0,004	0,111	-19,127	9,766	19,794	0,153	0,184	-160,467	-193,129	2,101	2,528
4032,000	0,999	-0,009	0,035	-29,165	9,765	19,794	0,288	0,198	-173,633	-119,621	0,630	0,434
7043,000	0,997	-0,026	0,012	-38,285	9,776	19,803	0,446	0,176	-198,848	-78,426	0,689	0,272
12302,000	0,993	-0,059	0,010	-40,336	9,802	19,826	0,608	0,137	-251,714	-56,837	2,301	0,520
21487,000	0,987	-0,113	0,016	-35,837	9,831	19,852	0,726	0,094	-271,539	-35,104	4,856	0,628
37531,000	0,982	-0,161	0,028	-31,057	9,805	19,829	0,635	0,047	-278,553	-20,616	9,173	0,679
65555,000	0,978	-0,192	0,047	-26,485	6,742	16,575	0,425	0,018	-285,319	-12,090	63,096	2,674
114503,000	0,976	-0,215	0,079	-22,013	3,589	11,099	0,294	0,007	-64,023	-1,553	119,328	2,895
200000,000	0,971	-0,256	0,132	-17,584	1,916	5,647	0,249	0,003	-331,117	-4,599	178,893	2,485
			900 < fc < 1000 Hz		81< fc < 100 Hz	37531 < fc < 65555 Hz						
	0,995	-0,046	0,984	-0,057	9,793	19,944						

Filterbox 1-Board 3-Channel 3

FILTERBOX	1		BOARD		3		CHANNEL		3			
FREQUENCY	RAW GAIN	RAW GAIN	LP GAIN	LP GAIN	HP GAIN	HP GAIN	RAW PHASE	RAW PHASE	LP PHASE	LP PHASE	HP PHASE	HP PHASE
[Hz]	[-]	[dB]	[-]	[dB]	[-]	[dB]	[deg]	[µs]	[deg]	[µs]	[deg]	[µs]
0,100	1,122	1,000	1,000	0,000	1,003	0,026	0,000	0,000	0,000	0,000	0,000	0,000
5,000	1,000	-0,003	0,000	#NUM!	0,023	-32,600	-0,019	-10,500	0,000	0,000	177,204	98446,500
9,000	1,000	-0,001	0,000	#NUM!	0,076	-22,433	0,021	6,429	0,000	0,000	176,030	54330,167
15,000	1,000	-0,002	0,000	#NUM!	0,209	-13,611	0,025	4,714	0,000	0,000	172,209	31890,583
27,000	1,000	-0,002	0,000	#NUM!	0,694	-3,176	-0,003	-0,280	0,000	0,000	164,058	16878,440
47,000	1,000	-0,002	0,000	#NUM!	2,229	6,961	0,003	0,200	0,000	0,000	150,055	8868,511
81,000	1,000	-0,001	0,000	#NUM!	6,915	16,796	0,028	0,975	0,000	0,000	115,533	3962,051
100,000	1,000	-0,001	0,000	#NUM!	9,450	19,508	0,015	0,404	0,000	0,000	92,879	2579,959
142,000	1,000	-0,001	0,000	#NUM!	11,206	20,989	0,014	0,279	0,000	0,000	56,439	1104,057
248,000	1,000	-0,001	0,000	#NUM!	10,473	20,401	0,042	0,476	0,000	0,000	26,423	295,959
433,000	1,000	-0,002	0,000	#NUM!	9,967	19,971	0,041	0,260	0,000	0,000	13,979	89,680
600,000	1,000	-0,002	0,000	#NUM!	9,839	19,859	0,072	0,333	0,000	0,000	9,855	45,625
757,000	1,000	-0,002	0,000	#NUM!	9,786	19,813	0,056	0,207	0,000	0,000	7,664	28,125
900,000	1,000	-0,002	0,000	#NUM!	9,760	19,789	0,064	0,198	0,000	0,000	6,357	19,620
1322,000	1,000	-0,002	0,000	#NUM!	9,727	19,759	0,081	0,170	0,000	0,000	4,166	8,755
2308,000	1,000	-0,004	0,000	#NUM!	9,709	19,743	0,152	0,183	0,000	0,000	2,071	2,493
4032,000	0,999	-0,009	0,000	#NUM!	9,708	19,742	0,279	0,192	0,000	0,000	0,615	0,424
7043,000	0,997	-0,026	0,000	#NUM!	9,718	19,751	0,446	0,176	0,000	0,000	0,714	0,282
12302,000	0,993	-0,059	0,000	#NUM!	9,744	19,775	0,596	0,135	0,000	0,000	2,330	0,526
21487,000	0,987	-0,112	0,000	#NUM!	9,772	19,800	0,729	0,094	0,000	0,000	4,887	0,632
37531,000	0,982	-0,160	0,000	#NUM!	9,749	19,779	0,633	0,047	0,000	0,000	8,914	0,660
65555,000	0,978	-0,191	0,000	#NUM!	6,861	16,727	0,432	0,018	0,000	0,000	61,593	2,610
114503,000	0,976	-0,214	0,000	#NUM!	3,644	11,232	0,297	0,007	0,000	0,000	117,789	2,857
200000,000	0,972	-0,250	0,000	#NUM!	2,060	6,279	0,253	0,004	0,000	0,000	165,365	2,297
					81 < fc < 100 Hz	37531 < fc < 65555 Hz						
	0,995	-0,046	roken channel		9,728	19,906			roken channel			

Filterbox 1-Board 3-Channel 4

FILTERBOX	1		BOARD		3		CHANNEL		4			
FREQUENCY	RAW GAIN	RAW GAIN	LP GAIN	LP GAIN	HP GAIN	HP GAIN	RAW PHASE	RAW PHASE	LP PHASE	LP PHASE	HP PHASE	HP PHASE
[Hz]	[-]	[dB]	[-]	[dB]	[-]	[dB]	[deg]	[µs]	[deg]	[µs]	[deg]	[µs]
0,100	1,122	0,999	1,123	1,004	1,004	0,035	0,000	0,000	0,000	0,000	0,000	0,000
5,000	1,000	-0,002	0,974	-0,233	0,024	-32,576	0,024	13,333	-0,530	-294,667	179,087	99492,500
9,000	1,000	-0,003	0,973	-0,234	0,075	-22,551	-0,002	-0,571	-0,682	-210,571	175,801	54259,500
15,000	1,000	-0,001	0,974	-0,232	0,206	-13,706	0,021	3,846	-1,285	-237,923	174,669	32346,083
27,000	1,000	-0,001	0,974	-0,229	0,687	-3,264	0,012	1,231	-2,047	-210,577	164,309	16904,167
47,000	1,000	-0,001	0,975	-0,217	2,205	6,867	0,002	0,089	-3,589	-212,111	150,262	8880,756
81,000	1,000	-0,002	0,979	-0,185	6,859	16,725	0,016	0,544	-6,203	-212,709	116,251	3986,654
100,000	1,000	-0,002	0,982	-0,160	9,423	19,483	0,002	0,061	-7,664	-212,878	93,785	2605,143
142,000	1,000	-0,001	0,990	-0,086	11,263	21,033	0,012	0,229	-10,985	-214,893	57,060	1116,194
248,000	1,000	-0,001	1,024	0,204	10,538	20,455	0,024	0,268	-20,135	-225,522	26,680	298,833
433,000	1,000	-0,001	1,103	0,852	10,023	20,020	0,052	0,332	-40,362	-258,928	14,074	90,285
600,000	1,000	-0,002	1,112	0,925	9,893	19,906	0,081	0,377	-64,981	-300,839	9,910	45,880
757,000	1,000	-0,002	0,972	-0,245	9,839	19,859	0,059	0,216	-90,191	-330,951	7,739	28,399
900,000	1,000	-0,002	0,771	-2,261	9,813	19,836	0,063	0,194	-109,474	-337,883	6,424	19,827
1322,000	1,000	-0,002	0,359	-8,897	9,778	19,805	0,091	0,191	-139,826	-293,802	4,209	8,844
2308,000	1,000	-0,004	0,109	-19,260	9,760	19,789	0,143	0,172	-161,181	-193,989	2,097	2,523
4032,000	0,999	-0,009	0,034	-29,303	9,759	19,788	0,276	0,190	-177,411	-122,224	0,629	0,433
7043,000	0,997	-0,026	0,014	-37,356	9,768	19,797	0,443	0,175	-216,032	-85,203	0,676	0,267
12302,000	0,993	-0,059	0,016	-35,811	9,794	19,819	0,599	0,135	-262,743	-59,327	2,269	0,512
21487,000	0,987	-0,112	0,028	-30,937	9,822	19,844	0,724	0,094	-276,199	-35,706	4,800	0,620
37531,000	0,982	-0,160	0,048	-26,431	9,763	19,792	0,630	0,047	-284,388	-21,048	9,087	0,673
65555,000	0,978	-0,191	0,073	-22,769	6,685	16,502	0,436	0,018	-292,697	-12,403	62,657	2,655
114503,000	0,976	-0,214	0,086	-21,267	3,559	11,026	0,287	0,007	-42,562	-1,033	118,810	2,882
200000,000	0,972	-0,251	0,114	-18,855	2,009	6,058	0,264	0,004	-9,066	-0,126	186,589	2,592
			900 < fc < 1000 Hz		81 < fc < 100 Hz	37531 < fc < 65555 Hz						
	0,995	-0,046	0,983	-0,078	9,782	19,945						

Filterbox 1-Board 4 -Channel 1

FILTERBOX	1		BOARD		4		CHANNEL		1			
FREQUENCY	RAW GAIN	RAW GAIN	LP GAIN	LP GAIN	HP GAIN	HP GAIN	RAW PHASE	RAW PHASE	LP PHASE	LP PHASE	HP PHASE	HP PHASE
[Hz]	[-]	[dB]	[-]	[dB]	[-]	[dB]	[deg]	[µs]	[deg]	[µs]	[deg]	[µs]
0,100	1,122	1,001	1,123	1,004	1,004	0,031	0,000	0,000	0,000	0,000	0,000	0,000
5,000	1,000	-0,002	0,972	-0,244	0,024	-32,540	-0,002	-1,333	-0,397	-220,667	177,995	98886,000
9,000	1,000	-0,002	0,972	-0,244	0,075	-22,463	0,011	3,250	-0,657	-202,875	175,890	54287,167
15,000	1,000	-0,001	0,973	-0,242	0,207	-13,668	-0,013	-2,461	-1,120	-207,461	173,631	32153,846
27,000	1,000	-0,001	0,973	-0,239	0,689	-3,236	0,012	1,280	-2,043	-210,160	164,298	16903,125
47,000	1,000	-0,002	0,974	-0,228	2,211	6,892	-0,002	-0,111	-3,648	-215,622	150,224	8878,467
81,000	1,000	-0,002	0,978	-0,195	6,898	16,774	0,020	0,684	-6,202	-212,684	116,687	4001,603
100,000	1,000	-0,001	0,981	-0,169	9,506	19,560	0,010	0,286	-7,693	-213,684	94,231	2617,541
142,000	1,000	-0,001	0,989	-0,096	11,406	21,142	0,007	0,143	-11,002	-215,214	57,333	1121,536
248,000	1,000	-0,002	1,022	0,192	10,666	20,560	0,028	0,313	-20,156	-225,756	26,744	299,553
433,000	1,000	-0,001	1,101	0,835	10,138	20,119	0,060	0,383	-40,374	-259,007	14,096	90,429
600,000	1,000	-0,002	1,110	0,906	10,005	20,004	0,075	0,346	-64,900	-300,462	9,926	45,953
757,000	1,000	-0,002	0,971	-0,258	9,950	19,956	0,051	0,187	-90,055	-330,454	7,725	28,347
900,000	1,000	-0,002	0,770	-2,265	9,923	19,933	0,057	0,177	-109,296	-337,334	6,411	19,786
1322,000	1,000	-0,002	0,360	-8,883	9,887	19,901	0,080	0,167	-139,635	-293,400	4,206	8,837
2308,000	1,000	-0,004	0,109	-19,225	9,868	19,885	0,136	0,164	-160,575	-193,258	2,072	2,494
4032,000	0,999	-0,009	0,034	-29,265	9,867	19,884	0,282	0,194	-173,868	-119,784	0,569	0,392
7043,000	0,997	-0,025	0,012	-38,411	9,877	19,892	0,453	0,179	-200,160	-78,944	0,790	0,312
12302,000	0,993	-0,059	0,010	-39,897	9,903	19,915	0,605	0,137	-252,468	-57,007	2,472	0,558
21487,000	0,987	-0,112	0,017	-35,434	9,932	19,941	0,729	0,094	-273,828	-35,400	5,156	0,667
37531,000	0,982	-0,160	0,029	-30,751	9,899	19,912	0,636	0,047	-282,946	-20,942	9,650	0,714
65555,000	0,978	-0,191	0,046	-26,718	6,828	16,686	0,435	0,018	-291,037	-12,332	63,597	2,695
114503,000	0,976	-0,214	0,068	-23,310	3,633	11,206	0,290	0,007	-48,663	-1,181	120,170	2,915
200000,000	0,972	-0,249	0,094	-20,564	1,858	5,383	0,000	0,000	-11,948	-0,166	158,436	2,201
			900 < fc < 1000 Hz		81<fc<100 Hz	37531 < fc <65555Hz						
	0,995	-0,046	0,993	-0,089	9,880	20,043						

Filterbox 1-Board 4 -Channel 2

FILTERBOX	1		BOARD		4		CHANNEL		2			
FREQUENCY	RAW GAIN	RAW GAIN	LP GAIN	LP GAIN	HP GAIN	HP GAIN	RAW PHASE	RAW PHASE	LP PHASE	LP PHASE	HP PHASE	HP PHASE
[Hz]	[-]	[dB]	[-]	[dB]	[-]	[dB]	[deg]	[µs]	[deg]	[µs]	[deg]	[µs]
0,100	1,122	1,000	1,122	1,000	1,003	0,029	0,000	0,000	0,000	0,000	0,000	0,000
5,000	1,000	-0,003	0,967	-0,289	0,023	-32,737	0,025	13,667	-0,068	-38,000	176,315	97952,500
9,000	1,000	-0,002	0,967	-0,288	0,074	-22,561	0,006	1,714	-0,695	-214,571	175,739	54240,286
15,000	1,000	-0,002	0,968	-0,286	0,206	-13,712	-0,014	-2,615	-1,041	-192,692	169,166	31327,077
27,000	1,000	-0,001	0,968	-0,283	0,685	-3,288	-0,002	-0,231	-2,052	-211,115	164,312	16904,542
47,000	1,000	-0,001	0,969	-0,275	2,194	6,824	-0,002	-0,089	-3,613	-213,511	150,122	8872,444
81,000	1,000	-0,001	0,973	-0,239	6,820	16,676	-0,010	-0,354	-6,185	-212,089	116,628	3999,582
100,000	1,000	-0,001	0,976	-0,215	9,392	19,455	0,012	0,327	-7,704	-214,000	94,341	2620,577
142,000	1,000	-0,001	0,984	-0,141	11,310	21,069	0,010	0,200	-11,048	-216,129	57,634	1127,429
248,000	1,000	-0,001	1,017	0,143	10,622	20,524	0,035	0,394	-20,243	-226,732	26,979	302,179
433,000	1,000	-0,001	1,093	0,775	10,107	20,093	0,057	0,364	-40,504	-259,840	14,245	91,383
600,000	1,000	-0,001	1,100	0,831	9,976	19,979	0,078	0,360	-64,982	-300,841	10,019	46,385
757,000	1,000	-0,002	0,962	-0,339	9,922	19,932	0,062	0,229	-90,027	-330,349	7,808	28,650
900,000	1,000	-0,002	0,764	-2,341	9,896	19,909	0,053	0,164	-109,180	-336,975	6,503	20,071
1322,000	1,000	-0,002	0,357	-8,940	9,861	19,879	0,078	0,164	-139,494	-293,103	4,268	8,967
2308,000	1,000	-0,004	0,109	-19,268	9,843	19,862	0,144	0,173	-160,423	-193,076	2,125	2,557
4032,000	0,999	-0,009	0,034	-29,295	9,842	19,861	0,282	0,195	-173,866	-119,782	0,647	0,446
7043,000	0,997	-0,026	0,012	-38,424	9,852	19,870	0,456	0,180	-201,057	-79,297	0,671	0,265
12302,000	0,993	-0,059	0,010	-39,951	9,877	19,893	0,594	0,134	-250,382	-56,536	2,256	0,510
21487,000	0,987	-0,112	0,017	-35,421	9,908	19,919	0,725	0,094	-271,621	-35,114	4,801	0,621
37531,000	0,982	-0,160	0,029	-30,644	9,895	19,908	0,638	0,047	-278,050	-20,579	9,037	0,669
65555,000	0,978	-0,191	0,049	-26,157	6,843	16,704	0,435	0,018	-285,897	-12,114	62,508	2,649
114503,000	0,976	-0,214	0,078	-22,108	3,645	11,234	0,292	0,007	-63,736	-1,546	242,542	5,884
200000,000	0,972	-0,249	0,137	-17,275	2,077	6,350	0,271	0,004	-308,567	-4,286	164,567	2,286
			900 < fc < 1000 Hz		81<fc<100 Hz	37531 < fc <65555Hz						
	0,995	-0,046	0,976	-0,139	9,868	20,011						

Filterbox 1-Board 4 -Channel 3

FILTERBOX	1		BOARD		4		CHANNEL		3			
FREQUENCY	RAW GAIN	RAW GAIN	LP GAIN	LP GAIN	HP GAIN	HP GAIN	RAW PHASE	RAW PHASE	LP PHASE	LP PHASE	HP PHASE	HP PHASE
[Hz]	[-]	[dB]	[-]	[dB]	[-]	[dB]	[deg]	[µs]	[deg]	[µs]	[deg]	[µs]
0,100	1,001	0,011	0,999	-0,007	0,034	-29,457	0,000	0,000	0,000	0,000	0,000	0,000
5,000	1,000	-0,001	0,964	-0,320	0,023	-32,698	-0,008	-4,333	-0,632	-351,000	176,221	97900,667
9,000	1,000	0,000	0,964	-0,320	0,075	-22,498	0,044	13,714	-0,656	-202,429	175,632	54207,333
15,000	1,000	-0,002	0,964	-0,319	0,208	-13,649	-0,001	-0,154	-1,284	-237,692	173,801	32185,461
27,000	1,000	-0,001	0,964	-0,315	0,690	-3,220	-0,010	-1,080	-2,009	-206,640	164,364	16909,920
47,000	1,000	-0,002	0,965	-0,307	2,215	6,906	0,007	0,422	-3,630	-214,511	150,479	8893,556
81,000	1,000	-0,002	0,969	-0,271	6,916	16,797	0,016	0,557	-6,175	-211,759	116,568	3997,544
142,000	1,000	-0,001	0,980	-0,175	11,404	21,141	0,003	0,050	-10,954	-214,271	57,177	1118,479
248,000	1,000	-0,001	1,013	0,108	10,654	20,550	0,031	0,350	-20,073	-224,837	26,662	298,638
433,000	1,000	-0,001	1,089	0,741	10,126	20,109	0,068	0,436	-40,131	-257,450	14,054	90,160
600,000	1,000	-0,002	1,099	0,821	9,992	19,993	0,082	0,378	-64,378	-298,047	9,900	45,834
757,000	1,000	-0,002	0,965	-0,306	9,938	19,946	0,051	0,187	-89,375	-327,958	7,714	28,307
900,000	1,000	-0,002	0,769	-2,276	9,910	19,922	0,059	0,183	-108,599	-335,182	6,407	19,776
1322,000	1,000	-0,002	0,361	-8,852	9,875	19,891	0,091	0,192	-139,210	-292,508	4,201	8,828
2308,000	1,000	-0,004	0,110	-19,180	9,857	19,875	0,148	0,178	-160,245	-192,862	2,081	2,505
4032,000	0,999	-0,009	0,035	-29,210	9,855	19,873	0,286	0,197	-172,847	-119,080	0,600	0,413
7043,000	0,997	-0,026	0,012	-38,579	9,865	19,882	0,447	0,176	-163,512	-64,489	0,730	0,288
12302,000	0,993	-0,059	0,008	-41,573	9,891	19,905	0,601	0,136	-248,111	-56,023	2,351	0,531
21487,000	0,987	-0,112	0,014	-37,280	9,918	19,929	0,731	0,094	-273,335	-35,336	4,946	0,639
37531,000	0,982	-0,160	0,024	-32,387	9,849	19,868	0,646	0,048	-283,451	-20,979	9,160	0,678
65555,000	0,978	-0,191	0,041	-27,696	6,810	16,663	0,436	0,018	-287,780	-12,194	62,233	2,637
114503,000	0,976	-0,214	0,075	-22,557	3,622	11,179	0,293	0,007	-305,172	-7,403	117,860	2,859
200000,000	0,972	-0,248	0,098	-20,151	2,043	6,206	0,270	0,004	-17,109	-0,238	203,275	2,823
			900 < fc < 1000 Hz		81 < fc < 142 Hz	37531 < fc <65555Hz						
	0,995	-0,045	0,976	-0,227	9,882	20,068						

Filterbox 1-Board 4 -Channel 4

FILTERBOX	1		BOARD		4		CHANNEL		4			
FREQUENCY	RAW GAIN	RAW GAIN	LP GAIN	LP GAIN	HP GAIN	HP GAIN	RAW PHASE	RAW PHASE	LP PHASE	LP PHASE	HP PHASE	HP PHASE
[Hz]	[-]	[dB]	[-]	[dB]	[-]	[dB]	[deg]	[µs]	[deg]	[µs]	[deg]	[µs]
5,000	1,000	-0,001	0,966	-0,305	0,023	-32,598	0,011	6,333	-0,051	-28,333	177,838	98798,667
9,000	1,000	-0,003	0,965	-0,306	0,075	-22,464	-0,006	-2,000	-0,673	-207,571	175,832	54269,000
15,000	1,000	-0,002	0,966	-0,303	0,209	-13,618	-0,007	-1,231	-0,897	-166,154	170,185	31515,750
27,000	1,000	-0,002	0,966	-0,299	0,691	-3,214	0,009	0,960	-1,993	-205,080	164,290	16902,240
47,000	1,000	-0,001	0,967	-0,289	2,214	6,904	-0,002	-0,089	-3,352	-198,111	150,380	8887,711
81,000	1,000	-0,001	0,971	-0,254	6,890	16,765	-0,003	-0,089	-6,067	-208,051	116,141	3982,872
100,000	1,000	-0,001	0,974	-0,229	9,457	19,515	0,012	0,347	-7,542	-209,510	93,669	2601,908
142,000	1,000	-0,001	0,982	-0,153	11,299	21,061	0,001	0,021	-10,837	-212,000	57,030	1115,614
248,000	1,000	-0,001	1,016	0,142	10,578	20,488	0,044	0,488	-19,870	-222,553	26,665	298,663
433,000	1,000	-0,001	1,098	0,815	10,064	20,055	0,053	0,341	-39,899	-255,958	14,085	90,357
600,000	1,000	-0,002	1,114	0,935	9,933	19,941	0,073	0,338	-64,427	-298,274	9,919	45,923
757,000	1,000	-0,002	0,978	-0,196	9,880	19,895	0,049	0,181	-89,785	-329,461	7,732	28,371
900,000	1,000	-0,002	0,776	-2,204	9,853	19,871	0,060	0,186	-109,250	-337,193	6,425	19,830
1322,000	1,000	-0,002	0,360	-8,867	9,818	19,841	0,083	0,174	-139,948	-294,057	4,204	8,834
2308,000	1,000	-0,004	0,109	-19,257	9,800	19,824	0,146	0,175	-161,177	-193,984	2,082	2,506
4032,000	0,999	-0,009	0,034	-29,310	9,799	19,823	0,280	0,193	-177,161	-122,052	0,607	0,418
7043,000	0,997	-0,025	0,013	-37,475	9,809	19,832	0,449	0,177	-214,554	-84,621	0,723	0,285
12302,000	0,993	-0,058	0,016	-36,193	9,834	19,855	0,605	0,137	-262,351	-59,239	2,357	0,532
21487,000	0,987	-0,112	0,027	-31,318	9,863	19,880	0,727	0,094	-276,318	-35,722	4,946	0,639
37531,000	0,982	-0,160	0,046	-26,814	9,827	19,848	0,641	0,047	-284,761	-21,076	9,469	0,701
65555,000	0,978	-0,191	0,070	-23,120	6,729	16,559	0,443	0,019	-292,804	-12,407	63,312	2,683
114503,000	0,976	-0,214	0,084	-21,517	3,577	11,070	0,308	0,007	-41,457	-1,006	119,857	2,908
200000,000	0,972	-0,249	0,111	-19,102	2,027	6,136	0,307	0,004	-3,877	-0,054	161,210	2,239
			900 < fc < 1000 Hz		81<fc<100 Hz	37531 < fc <65555Hz						
	0,995	-0,045	0,975	-0,204	9,819	19,981						

Filterbox 2 -Board 1 -Channel 1

FILTERBOX	2		BOARD		1		CHANNEL		1			
FREQUENCY	RAW GAIN	RAW GAIN	LP GAIN	LP GAIN	HP GAIN	HP GAIN	RAW PHASE	RAW PHASE	LP PHASE	LP PHASE	HP PHASE	HP PHASE
[Hz]	[-]	[dB]	[-]	[dB]	[-]	[dB]	[deg]	[µs]	[deg]	[µs]	[deg]	[µs]
0,100	1,116	0,956	1,109	0,901	0,962	-0,334	0,000	0,000	0,000	0,000	0,000	0,000
5,000	0,933	-0,603	0,961	-0,346	0,045	-27,023	-0,001	-0,333	-0,002	-1,333	161,286	89603,500
9,000	0,933	-0,604	0,964	-0,314	0,092	-20,756	0,004	1,143	-0,367	-113,286	168,494	52004,429
15,000	0,933	-0,606	0,967	-0,294	0,228	-12,859	0,000	0,000	-0,842	-155,846	169,054	31306,385
27,000	0,932	-0,608	0,969	-0,277	0,732	-2,710	0,009	0,885	-1,924	-197,962	163,342	16804,750
47,000	0,932	-0,608	0,970	-0,261	2,339	7,379	0,006	0,378	-3,469	-205,023	149,246	8820,689
81,000	0,932	-0,610	0,974	-0,228	7,186	17,129	0,046	1,582	-6,244	-214,114	114,256	3918,228
100,000	0,932	-0,611	0,977	-0,202	9,743	19,774	0,055	1,531	-7,679	-213,296	91,646	2545,735
142,000	0,932	-0,612	0,986	-0,126	11,477	21,196	0,065	1,271	-11,022	-215,614	55,676	1089,114
248,000	0,932	-0,613	1,019	0,166	10,760	20,636	0,063	0,707	-20,221	-226,492	25,890	289,992
433,000	0,932	-0,615	1,100	0,827	10,260	20,223	0,061	0,394	-40,513	-259,896	13,151	84,367
600,000	0,931	-0,616	1,114	0,938	10,132	20,114	0,072	0,331	-65,186	-301,789	8,714	40,341
757,000	0,931	-0,618	0,979	-0,184	10,079	20,068	0,053	0,193	-90,634	-332,577	6,254	22,948
900,000	0,931	-0,620	0,779	-2,173	10,051	20,045	0,049	0,151	-110,147	-339,959	4,699	14,504
1322,000	0,931	-0,623	0,363	-8,803	10,012	20,010	0,126	0,265	-141,681	-297,700	1,680	3,530
2308,000	0,930	-0,627	0,110	-19,159	9,973	19,977	0,215	0,259	-164,724	-198,252	2,280	2,745
4032,000	0,930	-0,635	0,035	-29,186	9,911	19,923	0,367	0,253	-174,928	-120,513	6,970	4,802
7043,000	0,928	-0,653	0,014	-37,011	9,745	19,776	0,459	0,181	-232,495	-91,697	13,739	5,419
12302,000	0,924	-0,690	0,018	-35,081	9,289	19,359	0,703	0,159	-291,705	-65,867	24,265	5,479
21487,000	0,918	-0,746	0,026	-31,572	8,201	18,278	0,875	0,113	-325,336	-42,058	39,983	5,169
37531,000	0,912	-0,796	0,030	-30,581	5,901	15,418	0,790	0,058	-9,234	-0,683	63,584	4,706
65555,000	0,909	-0,828	0,013	-37,870	2,323	7,322	0,746	0,032	-78,689	-3,334	122,856	5,206
114503,000	0,907	-0,849	0,002	-53,837	0,809	-1,845	0,831	0,020	-4023203,067	-97600,622	169,281	4,107
200000,000	0,910	-0,815	0,006	-43,746	0,294	-10,629	2,496	0,035	-290,818	-4,039	141,504	1,965
			900 < f c < 1000 Hz		100<fc < 142 Hz	21487< fc < 37531 Hz						
	0,927	-0,661	0,990	-0,113	9,987	19,967						

Filterbox 2 -Board 1 -Channel 2

FILTERBOX	2		BOARD		1		CHANNEL		2			
FREQUENCY	RAW GAIN	RAW GAIN	LP GAIN	LP GAIN	HP GAIN	HP GAIN	RAW PHASE	RAW PHASE	LP PHASE	LP PHASE	HP PHASE	HP PHASE
[Hz]	[-]	[dB]	[-]	[dB]	[-]	[dB]	[deg]	[µs]	[deg]	[µs]	[deg]	[µs]
0,100	1,120	0,982	1,111	0,916	0,959	-0,364	0,000	0,000	0,000	0,000	0,000	0,000
5,000	0,940	-0,540	0,961	-0,345	0,048	-26,289	0,028	15,500	-0,110	-61,000	163,094	90608,000
9,000	0,940	-0,540	0,965	-0,311	0,106	-19,518	-0,022	-6,714	-0,475	-146,714	169,793	52405,143
15,000	0,939	-0,542	0,967	-0,291	0,269	-11,404	0,015	2,769	-0,868	-160,769	169,722	31430,000
27,000	0,939	-0,544	0,969	-0,276	0,879	-1,116	0,015	1,560	-1,981	-203,800	164,285	16901,750
47,000	0,939	-0,545	0,971	-0,260	2,890	9,217	0,020	1,178	-3,496	-206,644	148,401	8770,750
81,000	0,939	-0,546	0,974	-0,227	9,072	19,154	0,042	1,443	-5,966	-204,608	107,485	3686,051
100,000	0,939	-0,547	0,977	-0,201	11,622	21,306	0,050	1,398	-7,726	-214,622	81,438	2262,153
142,000	0,939	-0,547	0,986	-0,126	12,147	21,690	0,047	0,914	-11,103	-217,193	46,437	908,400
248,000	0,939	-0,549	1,019	0,161	10,854	20,712	0,066	0,736	-20,288	-227,244	21,358	239,224
433,000	0,939	-0,550	1,097	0,803	10,303	20,260	0,098	0,626	-40,622	-260,596	10,763	69,046
600,000	0,938	-0,552	1,109	0,897	10,171	20,148	0,100	0,462	-65,095	-301,368	7,030	32,545
757,000	0,938	-0,553	0,975	-0,223	10,117	20,101	0,061	0,224	-90,417	-331,780	4,940	18,128
900,000	0,938	-0,554	0,777	-2,195	10,089	20,077	0,060	0,185	-109,755	-338,751	3,589	11,077
1322,000	0,938	-0,556	0,364	-8,784	10,050	20,043	0,117	0,245	-141,137	-296,556	0,928	1,951
2308,000	0,938	-0,560	0,111	-19,101	10,011	20,010	0,185	0,222	-163,710	-197,032	2,707	3,258
4032,000	0,937	-0,567	0,035	-29,073	9,950	19,956	0,346	0,239	-181,177	-124,819	7,196	4,958
7043,000	0,935	-0,586	0,013	-37,908	9,785	19,811	0,542	0,214	-218,851	-86,315	13,860	5,466
12302,000	0,931	-0,623	0,012	-38,098	9,331	19,399	0,699	0,158	-76,231	-17,213	24,329	5,493
21487,000	0,925	-0,678	0,019	-34,591	8,247	18,326	0,866	0,112	-39,301	-5,081	40,040	5,176
37531,000	0,920	-0,727	0,021	-33,582	5,963	15,509	0,806	0,060	-4,482	-0,332	63,791	4,721
65555,000	0,916	-0,759	0,008	-42,179	2,353	7,434	0,730	0,031	-64,646	-2,739	236,875	10,037
114503,000	0,914	-0,780	0,003	-49,878	0,817	-1,751	0,765	0,019	-1872972,204	-45437,242	168,397	4,085
200000,000	0,908	-0,837	0,008	-42,029	0,297	-10,535	2,102	0,029	-338,362	-4,699	93,638	1,301
			900 < f c < 1000 Hz		47<fc <81 Hz	21487< fc < 37531 Hz						
	0,933	-0,599	0,976	-0,120	10,025	20,071						

Filterbox 2 -Board 1 -Channel 3

FILTERBOX	2		BOARD		1		CHANNEL		3			
FREQUENCY	RAW GAIN	RAW GAIN	LP GAIN	LP GAIN	HP GAIN	HP GAIN	RAW PHASE	RAW PHASE	LP PHASE	LP PHASE	HP PHASE	HP PHASE
[Hz]	[-]	[dB]	[-]	[dB]	[-]	[dB]	[deg]	[µs]	[deg]	[µs]	[deg]	[µs]
0,100	1,128	1,045	1,113	0,929	0,968	-0,286	0,000	0,000	0,000	0,000	0,000	0,000
5,000	0,997	-0,028	0,967	-0,292	0,024	-32,267	0,025	14,000	-0,378	-210,000	174,918	97176,500
9,000	0,997	-0,028	0,967	-0,294	0,077	-22,224	-0,013	-4,143	-0,718	-221,571	174,656	53906,167
15,000	0,997	-0,027	0,967	-0,292	0,216	-13,293	0,013	2,385	-1,167	-216,077	171,623	31782,000
27,000	0,997	-0,026	0,967	-0,288	0,718	-2,875	-0,010	-1,080	-2,070	-212,920	164,313	16904,640
47,000	0,997	-0,026	0,969	-0,278	2,310	7,271	-0,005	-0,311	-3,592	-212,267	149,902	8859,444
81,000	0,997	-0,026	0,972	-0,246	7,184	17,127	0,017	0,570	-6,265	-214,835	115,124	3948,000
100,000	0,997	-0,026	0,975	-0,221	9,801	19,825	0,014	0,378	-7,784	-216,214	92,259	2562,755
142,000	0,997	-0,026	0,983	-0,148	11,554	21,255	0,007	0,142	-11,133	-217,787	55,702	1089,626
248,000	0,997	-0,026	1,016	0,134	10,762	20,638	0,054	0,606	-20,338	-227,801	25,691	287,752
433,000	0,997	-0,025	1,092	0,765	10,237	20,203	0,044	0,285	-40,614	-260,548	13,006	83,435
600,000	0,997	-0,026	1,102	0,846	10,104	20,090	0,078	0,360	-65,007	-300,960	8,604	39,833
757,000	0,997	-0,025	0,969	-0,275	10,049	20,042	0,064	0,236	-90,250	-331,170	6,167	22,628
900,000	0,997	-0,025	0,773	-2,241	10,021	20,018	0,066	0,205	-109,516	-338,012	4,607	14,220
1322,000	0,997	-0,026	0,362	-8,831	9,980	19,983	0,085	0,179	-140,925	-296,110	1,631	3,427
2308,000	0,997	-0,027	0,109	-19,218	9,941	19,948	0,139	0,168	-163,758	-197,090	2,343	2,820
4032,000	0,996	-0,031	0,034	-29,409	9,879	19,894	0,214	0,147	-176,962	-121,915	7,019	4,835
7043,000	0,995	-0,045	0,013	-37,846	9,713	19,747	0,385	0,152	-229,893	-90,670	13,799	5,443
12302,000	0,991	-0,078	0,016	-35,919	9,258	19,331	0,633	0,143	-290,217	-65,531	24,376	5,504
21487,000	0,985	-0,131	0,025	-32,020	8,173	18,248	0,736	0,095	-38,276	-4,948	40,139	5,189
37531,000	0,980	-0,179	0,029	-30,749	5,870	15,372	0,620	0,046	-2,213	-0,164	63,818	4,723
65555,000	0,976	-0,209	0,011	-38,825	2,309	7,267	0,612	0,026	-49,907	-2,115	236,761	10,032
114503,000	0,974	-0,229	0,006	-44,921	0,802	-1,919	0,480	0,012	-40,631	-0,986	168,858	4,096
200000,000	0,973	-0,239	0,011	-38,918	0,277	-11,144	0,891	0,012	-331,666	-4,606	135,653	1,884
			900 < f c < 1000 Hz		47<fc <81 Hz	37351 < fc < 65555 Hz						
	0,992	-0,067	0,990	-0,136	9,955	19,448						

Filterbox 2 -Board 1 -Channel 4

FILTERBOX	2		BOARD		1		CHANNEL		4			
FREQUENCY	RAW GAIN	RAW GAIN	LP GAIN	LP GAIN	HP GAIN	HP GAIN	RAW PHASE	RAW PHASE	LP PHASE	LP PHASE	HP PHASE	HP PHASE
[Hz]	[-]	[dB]	[-]	[dB]	[-]	[dB]	[deg]	[µs]	[deg]	[µs]	[deg]	[µs]
0,100	1,115	0,945	1,109	0,902	0,961	-0,342	0,000	0,000	0,000	0,000	0,000	0,000
5,000	0,936	-0,573	0,960	-0,359	0,043	-27,357	0,014	7,667	-0,047	-26,333	162,080	90044,667
9,000	0,936	-0,573	0,963	-0,329	0,090	-20,931	0,018	5,571	-0,424	-131,000	167,559	51715,667
15,000	0,936	-0,573	0,965	-0,308	0,226	-12,919	-0,007	-1,308	-0,859	-159,000	169,523	31393,077
27,000	0,936	-0,574	0,967	-0,293	0,731	-2,723	0,024	2,440	-1,885	-193,960	163,965	16868,792
47,000	0,936	-0,576	0,968	-0,278	2,341	7,388	0,008	0,444	-3,479	-205,622	149,868	8857,422
81,000	0,936	-0,577	0,973	-0,241	7,282	17,245	0,057	1,949	-6,157	-211,152	115,079	3946,468
100,000	0,936	-0,577	0,975	-0,219	9,931	19,940	0,062	1,735	-7,663	-212,867	92,177	2560,469
142,000	0,936	-0,578	0,984	-0,144	11,685	21,353	0,054	1,050	-11,024	-215,650	55,552	1086,707
248,000	0,936	-0,579	1,017	0,144	10,868	20,723	0,074	0,833	-20,193	-226,171	25,617	286,931
433,000	0,935	-0,581	1,096	0,794	10,334	20,286	0,098	0,627	-40,422	-259,313	12,948	83,065
600,000	0,935	-0,582	1,110	0,903	10,200	20,172	0,093	0,431	-64,924	-300,572	8,579	39,716
757,000	0,935	-0,583	0,977	-0,203	10,144	20,124	0,098	0,360	-90,242	-331,138	6,118	22,449
900,000	0,935	-0,584	0,779	-2,173	10,115	20,099	0,095	0,292	-109,747	-338,725	4,568	14,098
1322,000	0,935	-0,586	0,364	-8,781	10,074	20,064	0,127	0,267	-141,324	-296,950	1,581	3,321
2308,000	0,934	-0,590	0,110	-19,149	10,034	20,030	0,180	0,217	-164,425	-197,893	2,367	2,849
4032,000	0,934	-0,597	0,035	-29,201	9,972	19,975	0,335	0,231	-184,524	-127,125	7,073	4,873
7043,000	0,932	-0,615	0,014	-37,143	9,804	19,828	0,466	0,184	-232,142	-91,558	13,930	5,494
12302,000	0,928	-0,651	0,017	-35,182	9,345	19,411	0,723	0,163	-291,030	-65,714	24,581	5,550
21487,000	0,922	-0,707	0,026	-31,624	8,249	18,328	0,790	0,102	-36,528	-4,722	40,512	5,237
37531,000	0,917	-0,756	0,029	-30,825	5,885	15,395	0,784	0,058	-6,916	-0,512	65,343	4,836
65555,000	0,913	-0,786	0,011	-39,336	2,294	7,213	0,730	0,031	-56,695	-2,402	234,297	9,928
114503,000	0,911	-0,808	0,005	-46,022	0,798	-1,960	0,825	0,020	-1785,167	-43,307	164,894	4,000
200000,000	0,910	-0,820	0,009	-40,746	0,281	-11,036	1,943	0,027	-1,182	-0,016	123,234	1,712
			900 < f c < 1000 Hz		47<fc <81 Hz	37351 < fc < 65555 Hz						
	0,930	-0,627	0,975	-0,129	10,027	19,531						

Filterbox 2 -Board 2 -Channel 2

FILTERBOX	2		BOARD		2		CHANNEL		2			
FREQUENCY	RAW GAIN	RAW GAIN	LP GAIN	LP GAIN	HP GAIN	HP GAIN	RAW PHASE	RAW PHASE	LP PHASE	LP PHASE	HP PHASE	HP PHASE
[Hz]	[-]	[dB]	[-]	[dB]	[-]	[dB]	[deg]	[µs]	[deg]	[µs]	[deg]	[µs]
0,100	1,119	0,973	1,110	0,906	0,959	-0,367	0,000	0,000	0,000	0,000	0,000	0,000
5,000	0,941	-0,532	0,957	-0,385	0,043	-27,329	-0,007	-3,667	-0,007	-3,667	160,777	89320,333
9,000	0,941	-0,532	0,960	-0,354	0,090	-20,926	-0,020	-6,286	-0,370	-114,286	168,002	51852,429
15,000	0,940	-0,533	0,962	-0,332	0,226	-12,933	0,023	4,308	-0,912	-168,846	168,982	31292,917
27,000	0,940	-0,534	0,964	-0,318	0,728	-2,757	0,031	3,160	-1,897	-195,160	163,711	16842,720
47,000	0,940	-0,535	0,966	-0,303	2,328	7,339	0,003	0,200	-3,493	-206,467	149,758	8850,933
81,000	0,940	-0,536	0,969	-0,269	7,214	17,164	0,041	1,418	-6,205	-212,785	115,178	3949,848
100,000	0,940	-0,536	0,972	-0,244	9,842	19,861	0,054	1,490	-7,718	-214,388	92,427	2567,408
142,000	0,940	-0,537	0,981	-0,169	11,635	21,315	0,054	1,057	-11,124	-217,600	55,946	1094,407
248,000	0,940	-0,538	1,014	0,119	10,865	20,720	0,059	0,663	-20,363	-228,081	25,864	289,699
433,000	0,940	-0,540	1,092	0,764	10,340	20,290	0,071	0,452	-40,766	-261,522	13,106	84,079
600,000	0,940	-0,541	1,103	0,848	10,207	20,178	0,058	0,269	-65,417	-302,856	8,690	40,231
757,000	0,940	-0,542	0,967	-0,291	10,152	20,131	0,037	0,136	-90,716	-332,878	6,237	22,887
900,000	0,939	-0,543	0,769	-2,279	10,123	20,107	0,045	0,140	-110,097	-339,805	4,669	14,412
1322,000	0,939	-0,545	0,360	-8,879	10,083	20,072	0,145	0,305	-141,371	-297,049	1,640	3,446
2308,000	0,939	-0,549	0,110	-19,192	10,043	20,038	0,214	0,258	-163,838	-197,186	2,303	2,772
4032,000	0,938	-0,556	0,035	-29,121	9,982	19,984	0,354	0,244	-179,194	-123,453	6,975	4,805
7043,000	0,936	-0,574	0,013	-37,998	9,816	19,838	0,502	0,198	-217,403	-85,744	13,755	5,425
12302,000	0,932	-0,610	0,012	-38,394	9,360	19,426	0,691	0,156	-77,414	-17,480	24,281	5,483
21487,000	0,926	-0,665	0,018	-34,884	8,271	18,352	0,836	0,108	-39,651	-5,126	40,046	5,177
37531,000	0,921	-0,714	0,020	-33,949	5,951	15,492	0,816	0,060	-4,039	-0,299	63,994	4,736
65555,000	0,918	-0,746	0,007	-42,850	2,337	7,373	0,744	0,032	-62,204	-2,636	123,563	5,236
114503,000	0,915	-0,767	0,003	-49,234	0,810	-1,836	0,769	0,019	-7942,943	-192,691	167,755	4,070
200000,000	0,911	-0,807	0,007	-43,205	0,249	-12,069	0,000	0,000	-15,144	-0,210	105,689	1,468
			900 < f c < 1000 Hz		47<fc <81 Hz	37351 < fc < 65555 Hz						
	0,935	-0,587	0,972	-0,165	10,058	19,531						

Filterbox 2 -Board 2 -Channel 4

FILTERBOX	2		BOARD		2		CHANNEL		4			
FREQUENCY	RAW GAIN	RAW GAIN	LP GAIN	LP GAIN	HP GAIN	HP GAIN	RAW PHASE	RAW PHASE	LP PHASE	LP PHASE	HP PHASE	HP PHASE
[Hz]	[-]	[dB]	[-]	[dB]	[-]	[dB]	[deg]	[µs]	[deg]	[µs]	[deg]	[µs]
0,100	1,120	0,981	1,113	0,929	0,969	-0,276	0,000	0,000	0,000	0,000	0,000	0,000
5,000	0,940	-0,538	0,963	-0,331	0,043	-27,368	0,004	2,333	-0,029	-5760,000	159,347	88526,000
9,000	0,940	-0,539	0,966	-0,300	0,089	-20,965	-0,007	-2,143	-0,344	-38211,444	169,004	52161,714
15,000	0,940	-0,540	0,968	-0,280	0,224	-12,983	0,034	6,308	-0,947	-63138,467	169,238	31340,417
27,000	0,940	-0,542	0,970	-0,265	0,722	-2,828	0,043	4,400	-1,954	-72360,000	163,556	16826,708
47,000	0,939	-0,544	0,972	-0,250	2,304	7,250	0,024	1,400	-3,586	-76296,000	149,542	8838,182
81,000	0,939	-0,545	0,975	-0,218	7,105	17,031	0,033	1,137	-6,298	-77755,506	115,095	3947,013
100,000	0,939	-0,545	0,978	-0,193	9,685	19,722	0,048	1,347	-7,838	-78377,140	92,567	2571,309
142,000	0,939	-0,546	0,986	-0,122	11,504	21,217	0,046	0,900	-11,265	-79331,141	56,349	1102,293
248,000	0,939	-0,547	1,018	0,151	10,798	20,667	0,076	0,850	-20,643	-83236,097	26,140	292,785
433,000	0,939	-0,549	1,090	0,746	10,290	20,249	0,089	0,573	-41,170	-95080,092	13,246	84,974
600,000	0,939	-0,550	1,093	0,775	10,161	20,138	0,088	0,410	-55,531	-109219,063	8,784	40,666
757,000	0,939	-0,551	0,957	-0,378	10,107	20,092	0,059	0,216	-90,479	-119522,865	6,309	23,152
900,000	0,938	-0,552	0,764	-2,338	10,079	20,068	0,066	0,205	-109,522	-121691,626	4,716	14,555
1322,000	0,938	-0,554	0,360	-8,864	10,039	20,034	0,109	0,229	-140,755	-106471,570	1,682	3,535
2308,000	0,938	-0,558	0,110	-19,172	9,999	20,000	0,197	0,238	-163,956	-71038,074	2,301	2,769
4032,000	0,937	-0,565	0,035	-29,230	9,937	19,945	0,339	0,234	-175,847	-43612,883	7,026	4,840
7043,000	0,935	-0,583	0,014	-36,987	9,769	19,797	0,540	0,213	-230,270	-32694,852	13,843	5,460
12302,000	0,931	-0,619	0,018	-35,032	9,311	19,380	0,682	0,154	-69,925	-5684,020	24,447	5,520
21487,000	0,925	-0,674	0,027	-31,485	8,218	18,296	0,863	0,112	-37,217	-1732,055	40,286	5,208
37531,000	0,920	-0,723	0,030	-30,538	5,891	15,404	0,810	0,060	-5,831	-155,352	64,479	4,772
65555,000	0,917	-0,754	0,011	-39,072	2,310	7,271	0,762	0,032	-58,822	-897,291	124,208	5,263
114503,000	0,915	-0,776	0,005	-46,616	0,803	-1,906	0,781	0,019	-18,931	-165,334	167,664	4,067
200000,000	0,908	-0,841	0,009	-41,035	0,253	-11,941	0,000	0,000	-0,190	-0,950	92,019	1,278
	0,934	-0,597	0,989	-0,148	10,032	19,469						

Appendix B – Setup for probes setting

The probes have to be mounted in the turbine test rig with a correct value of angle and depth in the turbine channel. In order to set the correct depth and angle it has been designed the tool depicted in figure 2.5. The explanation is in the same paragraph. Moreover, an Excel file has been written in order to set the correct position and angle of the probe knowing the geometry of the transducer and of the metallic tool. The following image is referred to a schematic representation of this setup: the acronyms used to states some geometric element are here reported.

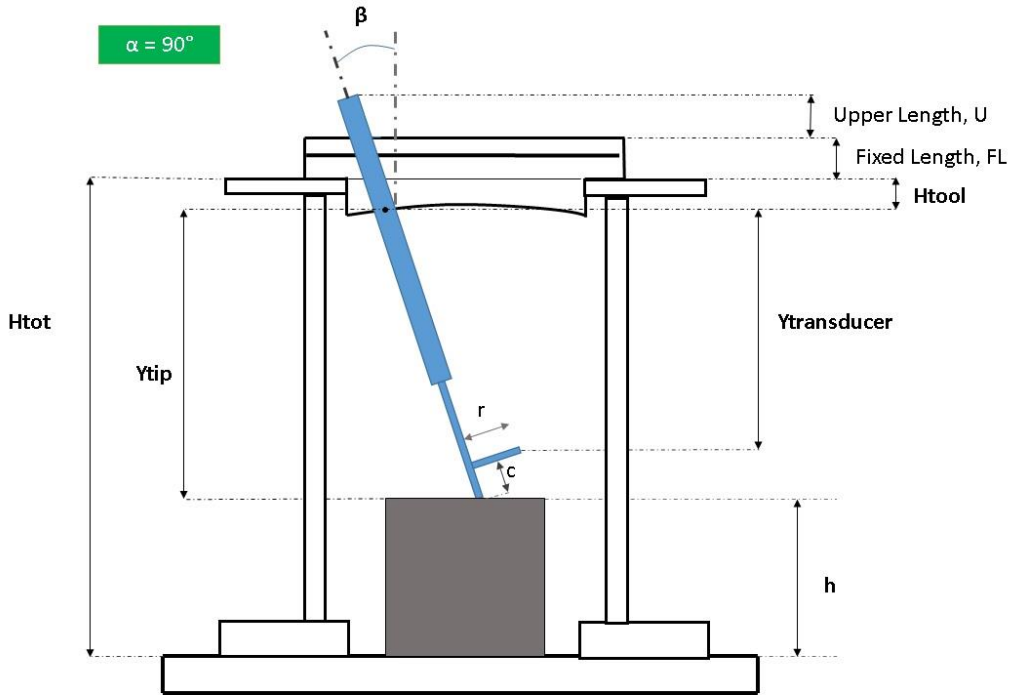

Figure 5.37: Setup for probes setting

It is possible to set the correct values of these parameters and reconstruct the geometry of a probe and obtain the correct setup.

Formula

$h = Htot - Htool - Ytip$

$U = l\,cos(\beta) - Ytip - Htool - FL$